UNCLASSIFIED

AD NUMBER
AD901196
LIMITATION CHANGES
TO: **Approved for public release; distribution is unlimited.**
FROM: **Distribution authorized to U.S. Gov't. agencies only; Test and Evaluation; JUL 1972. Other requests shall be referred to Air Force Armament Lab., Eglin AFB, FL.**
AUTHORITY
AFATL ltr 16 Dec 1975

THIS PAGE IS UNCLASSIFIED

AEDC-TR-72-95
AFATL-TR-72-120

cy.2

SEPARATION CHARACTERISTICS OF SEVERAL EXTERNAL STORES FROM THE A-7D AIRCRAFT AT MACH NUMBERS FROM 0.325 TO 0.95

Robert H. Roberts

ARO, Inc.

July 1972

This document has been approved for public release its distribution unlimited Per TAB 76-7 26 March, 1976

Distribution limited to U.S. Government agencies only; this report contains information on test and evaluation of military hardware; July 1972; other requests for this document must be referred to Air Force Armament Laboratory (DLGC), Eglin AFB, Florida 32542.

PROPULSION WIND TUNNEL FACILITY
ARNOLD ENGINEERING DEVELOPMENT CENTER
AIR FORCE SYSTEMS COMMAND
ARNOLD AIR FORCE STATION, TENNESSEE

NOTICES

SEPARATION CHARACTERISTICS OF SEVERAL EXTERNAL STORES FROM THE A-7D AIRCRAFT AT MACH NUMBERS FROM 0.325 to 0.95

Robert H. Roberts
ARO, Inc.

FOREWORD

The work reported herein was sponsored by the Air Force Armament Laboratory (AFATL/DLGC/Lt S. C. Braud), Air Force Systems Command (AFSC), under Program Element 27121F, System 337A.

The test results presented were obtained by ARO, Inc. (a subsidiary of Sverdrup & Parcel and Associates, Inc.), contract operator of the Arnold Engineering Development Center (AEDC), AFSC, Arnold Air Force Station, Tennessee, under Contract F40600-72-C-0003. The test was conducted from April 5 to 12, 1972, under ARO Project No. PC0230. The manuscript was submitted for publication on May 18, 1972.

This technical report has been reviewed and is approved.

GEORGE F. GAREY
Lt Colonel, USAF
Chief Air Force Test Director, PWT
Directorate of Test

FRANK J. PASSARELLO
Colonel, USAF
Acting Director of Test

ABSTRACT

Tests were conducted in the Aerodynamic Wind Tunnel (4T) using 0.05-scale models to investigate the separation characteristics of the SUU-25C/A and CBU-52B/B dispensers, MK-20 and BLU-52A/B bombs, and the 300-gal fuel tank when released from the Multiple Ejection Rack (MER), the Triple Ejection Rack (TER), and wing-pylon locations on the left and right wing of the A-7D aircraft. Captive trajectory data were obtained at Mach numbers from 0.325 to 0.95 at simulated pressure altitudes from 4000 to 7000 ft. The parent-aircraft angle of attack was varied from 2.0 to 10.6 deg, depending on Mach number, climb angle, and simulated altitude. At selected test conditions, parent climb (dive) angles of -50 and -70 deg. were simulated.

CONTENTS

NOMENCLATURE

BL	Aircraft buttock line from plane of symmetry, in., model scale
b	Store reference dimension, ft, full scale
C_ℓ	Store rolling-moment coefficient, rolling moment/q_∞Sb
C_{ℓ_p}	Store roll-damping derivative, $dC_\ell/d(pb/2V_\infty)$
C_m	Store pitching-moment coefficient, referenced to the store cg, pitching moment/q_∞Sb
C_{m_q}	Store pitch-damping derivative, $dC_m/d(qb/2V_\infty)$
C_n	Store yawing-moment coefficient, referenced to the store cg, yawing moment/q_∞Sb
C_{n_r}	Store yaw-damping derivative, $dC_n/d(rb/2V_\infty)$
FS	Aircraft fuselage station, in., model scale
F_Z	MER/TER ejector force, lb
F_{Z_1}	Pylon forward ejector force, lb
F_{Z_2}	Pylon aft ejector force, lb
H	Pressure altitude, ft
I_{xx}	Full-scale moment of inertia about the store X_B axis, slug-ft^2
I_{yy}	Full-scale moment of inertia about the store Y_B axis, slug-ft^2
I_{zz}	Full-scale moment of inertia about the store Z_B axis, slug-ft^2
M_∞	Free-stream Mach number
$\overline{m}$	Full-scale store mass, slugs
p	Store angular velocity about the X_B axis, radians/sec
p_∞	Free-stream static pressure, psfa
q	Store angular velocity about the Y_B axis, radians/sec
q_∞	Free-stream dynamic pressure, psf

r	Store angular velocity about the Z_B axis, radians/sec
S	Store reference area, ft^2, full scale
t	Real trajectory time from initiation of trajectory, sec
V_∞	Free-stream velocity, ft/sec
WL	Aircraft waterline from reference horizontal plane, in., model scale
X	Separation distance of the store cg parallel to the flight axis system X_F direction, ft, full scale measured from the prelaunch position
X_{cg}	Full-scale cg location, ft, from nose of store
X_L	Ejector piston location relative to the store cg, positive forward of store cg, ft, full scale
X_{L_1}	Forward ejector piston location relative to the store cg, positive forward of store cg, ft, full scale
X_{L_2}	Aft ejector piston location relative to the store cg, positive forward of store cg, ft, full scale
Y	Separation distance of the store cg parallel to the flight axis system Y_F direction, ft, full scale measured from the prelaunch position
Z	Separation distance of the store cg parallel to the flight-axis system Z_F direction, ft, full scale measured from the prelaunch position
ZE	Ejector stroke length, ft, full scale
α	Parent-aircraft model angle of attack relative to the free-stream velocity vector, deg
θ	Angle between the store longitudinal axis and its projection in the X_F-Y_F plane, positive when store nose is raised as seen by pilot, deg
$\bar{\theta}$	Simulated parent-aircraft climb angle, angle between the flight direction and the earth horizontal, deg, positive for increasing altitude
ψ	Angle between the projection of the store longitudinal axis in the X_F-Y_F plane and the X_F axis, positive when the store nose is to the right as seen by the pilot, deg
ϕ	Angle between the projection of the store lateral axis in the Y_F-Z_F plane and the Y_F axis, positive for clockwise rotation when looking upstream, deg

FLIGHT-AXIS SYSTEM COORDINATES

Directions

X_F — Parallel to the free-stream wind vector, positive direction is forward as seen by the pilot

Y_F — Perpendicular to the X_F and Z_F directions, positive direction is to the right as seen by the pilot

Z_F — In the aircraft plane of symmetry, perpendicular to the free-stream wind vector, positive direction is downward

The flight-axis system origin is coincident with the aircraft cg and remains fixed with respect to the parent aircraft during store separation. The X_F, Y_F, and Z_F coordinate axes do not rotate with respect to the initial flight direction and attitude.

STORE BODY-AXIS SYSTEM COORDINATES

Directions

X_B — Parallel to the store longitudinal axis, positive direction is upstream in the prelaunch position

Y_B — Perpendicular to the store longitudinal axis, and parallel to the flight-axis system X_F-Y_F plane when the store is at zero roll angle, positive direction is to the right looking upstream when the store is at zero yaw and roll angles

Z_B — Perpendicualr to both the X_B and Y_B axes, positive direction is downward as seen by the pilot when the store is at zero pitch and roll angles.

The store body-axis system origin is coincident with the store cg and moves with the store during separation from the parent airplane. The X_B, Y_B, and Z_B coordinate axes rotate with the store in pitch, yaw, and roll so that mass moments of inertia about the three axes are not time-varying quantities.

SECTION I
INTRODUCTION

The purpose of this investigation was to determine the separation characteristics of the SUU-25C/A and CBU-52B/B dispensers, MK-20 and BLU-52A/B bombs, and the 300-gal fuel tank when released from the Multiple Ejection Rack (MER), the Triple Ejection Rack (TER), and wing-pylon locations on the left and right wings of the A-7D aircraft. For these tests, the parent-aircraft model was mounted on the main tunnel support system, and the store models were mounted on the captive trajectory support (CTS) system. Captive-trajectory data were obtained at Mach numbers from 0.325 to 0.95 at simulated pressures altitudes from 4000 to 7000 ft. At selected test conditions, parent climb (dive) angles of -50 and -70 deg were simulated. The ejector forces used were constant values provided by the Air Force Armament Laboratory (AFATL/DLGC).

Separation trajectories were obtained for the 300-gal fuel tank configuration with six sets of mass properties. In addition to the completely full and empty tank loadings, four conditions were examined which correspond to partial loads, or ballasting, in increments of approximately 100 lb located near the nose of the tank. These partially loaded configurations are referred to herein as Cargo No. 1, Cargo No. 2, Cargo No. 3, and Cargo No. 4 in order of increasing weight.

SECTION II
APPARATUS

2.1 TEST FACILITY

The Aerodynamic Wind Tunnel (4T) is a closed-loop, continuous flow, variable density tunnel in which the Mach number can be varied from 0.1 to 1.3. At all Mach numbers, the stagnation pressure can be varied from 300 to 3700 psfa. The test section is 4 ft square and 12.5 ft long with perforated, variable porosity (0.5- to 10-percent open) walls. It is completely enclosed in a plenum chamber from which the air can be evacuated, allowing part of the tunnel airflow to be removed through the perforated walls of the test section.

For store separation testing, two separate and independent support systems are used to support the models. The parent-aircraft model is inverted in the test section and supported by an offset sting attached to the main pitch sector. The store model is supported by the CTS which extends down from the tunnel top wall and provides store movement (six degreees of freedom) independent of the parent-aircraft model. An isometric drawing of a typical store separation installation is shown in Fig. 1 (Appendix I).

Also shown in Fig. 1 is a block diagram of the computer control loop used during captive trajectory testing. The analog system and the digital computer work as an integrated unit and, utilizing required input information, control the store movement during a trajectory. Store positioning is accomplished by use of six individual d-c electric motors. Maximum translational travel of the CTS is ±15 in. from the tunnel centerline in the lateral and vertical directions and 36 in. in the axial direction. Maximum angular

displacements are ±45 deg in pitch and yaw and ±360 deg in roll. A more complete description of the test facility can be found in the Test Facilities Handbook.[1] A schematic showing the test section details and the location of the models in the tunnel is shown in Fig. 2.

2.2 TEST ARTICLES

The test articles were 0.05-scale models of the A-7D parent aircraft and the various stores. A sketch showing the basic dimensions of the A-7D parent model is shown in Fig. 3. Both the left and right wings of the A-7D were equipped for store separation. Details and dimensions of the pylons are shown in Fig. 4, the TER and MER in Figs. 5 and 6, and the store models in Figs. 7 through 13.

The A-7D parent model was geometrically similar to the full-scale airplane except for some modifications incident to the wind tunnel installation and CTS operation. Horizontal tail surfaces were removed because of interference with the CTS support. The parent model was inverted in the tunnel and attached by a 23-deg offset sting to the main sting-support system. The A-7D aircraft has three pylon stations on each wing. The mounting surfaces of all three pylons are inclined at a 3-deg nose-down angle with respect to the aircraft waterline. Figure 14 shows the numbering sequence of the TER and MER stations and the roll orientation of stores mounted on each of the launch positions, and Fig. 15 shows a typical tunnel installation photograph of the parent aircraft, store models, and the CTS.

2.3 INSTRUMENTATION

A six-component, internal strain-gage balance was used to obtain force and moment data on the store model. Translational and angular positions of the store model were obtained from the CTS analog outputs. A digital readout from the main pitch sector was used for setting angle of attack for the parent aircraft. The MER, TER, and pylons were instrumented with touch wires which aided in positioning the store model for launch. The system was also electrically connected to automatically stop the CTS and main pitch sector movement if the store model or sting support contacted the MER, TER, or the aircraft model surface.

SECTION III
TEST DESCRIPTION

3.1 TEST CONDITIONS

Separation trajectory data were obtained at Mach numbers from 0.325 to 0.95 at simulated pressure altitudes from 4000 to 7000 ft. Tunnel dynamic pressure ranged from 230 to 850 psf, and tunnel stagnation temperature was maintained near 100°F.

---

[1]Test Facilities Handbook (Ninth Edition). "Propulsion Wind Tunnel Facility, Vol. 4." Arnold Engineering Development Center, July 1971.

Tunnel conditions were held constant at the desired Mach number and stagnation pressure while data for each trajectory were obtained. The trajectories were terminated when the store or sting contacted the parent-aircraft model or when a CTS travel limit was reached.

3.2 TRAJECTORY DATA ACQUISITION

To obtain a trajectory, test conditions were established in the tunnel and the parent model was positioned at the desired angle of attack. The store model was then oriented to a position corresponding to the store carriage location. After the store was set at the desired initial position, operational control of the CTS was switched to the digital computer which controlled the store movement during the trajectory through commands to the CTS analog system (see block diagram, Fig. 1). Data from the wind tunnel, consisting of measured model forces and moments, wind tunnel operating conditions, and CTS rig positions, were input to the digital computer for use in the full-scale trajectory calculations.

The digital computer was programmed to solve the six-degree-of-freedom equations to calculate the angular and linear displacements of the store relative to the parent-aircraft pylon. In general, the program involves using the last two successive measured values of each static aerodynamic coefficient to predict the magnitude of the coefficients over the next time interval of the trajectory. These predicted values are used to calculate the new position and attitude of the store at the end of the time interval. The CTS is then commanded to move the store model to this new position and the aerodynamic loads are measured. If these new measurements agree with the predicted values, the process is continued over another time interval of the same magnitude. If the measured and predicted values do not agree within the desired precision, the calculation is repeated over a time interval one-half the previous value. This process is repeated until a complete trajectory has been obtained.

In applying the wind tunnel data to the calculations of the full-scale store trajectories, the measured forces and moments are reduced to coefficient form and then applied with proper full-scale store dimensions and flight dynamic pressure. Dynamic pressure was calculated using a flight velocity equal to the free-stream velocity component plus the components of store velocity relative to the aircraft, and a density corresponding to the simulated altitude.

The initial portion of each launch trajectory incorporated simulated ejector forces in addition to the measured aerodynamic forces acting on the store. The ejector forces for the stores are presented in Table I (Appendix II). The ejector force was considered to act perpendicular to the rack or pylon mounting surface. The locations of the applied ejector forces and other full-scale store parameters used in the trajectory calculations are listed in Table II.

3.3 CORRECTIONS

Balance, sting, and support deflections caused by the aerodynamic loads on the store models were accounted for in the data reduction program to calculate the true store-model angles. Corrections were also made for model weight tares to calculate the net aerodynamic forces on the store model.

3.4 PRECISION OF DATA

The trajectory data are subject to error from several sources including tunnel conditions, balance measurements, extrapolation tolerances allowed in the predicted coefficients, computer inputs, and CTS positioning control. Maximum error in the CTS position control was ±0.05 in. for the translational settings, ±0.15 deg for angular displacement settings in pitch and yaw, and ±1 deg for angular settings in roll. Extrapolation tolerances were ±0.10 for each of the aerodynamic coefficients. The maximum uncertainties in the full-scale position data caused by the balance precision limitations are given in Table III. Bias errors have been neglected.

The estimated uncertainty in setting Mach number was no greater than ±0.003, and the uncertainty in parent-model angle of attack was estimated to be ±0.1 deg.

SECTION IV
RESULTS AND DISCUSSION

Data taken during this test consisted of ejector-separated store trajectories of various stores from MER, TER, and pylon stations on the left and right wings of the A-7D aircraft. Table IV describes the A-7D load configurations for this test. The letters "L" or "R" following the configuration number denote store launches from the left or right wing of the aircraft, respectively. Data showing the linear and angular displacements of the store relative to the mate position on the racks or pylon are presented as functions of full-scale trajectory time in Figs. 16 through 33. Positive X, Y, and Z displacements (as seen by the pilot) are forward, to the right, and down, respectively. Positive changes in pitch, yaw, and roll (as seen by the pilot) are nose up, nose right, and clockwise, respectively. Termination of most trajectories was either the result of limitations imposed by the CTS system (such as sting-to-parent-aircraft contact or a store-support-system travel limit) or manual termination after the store had separated a specified distance from the aircraft.

Figures 16 through 21 present separation trajectory data for the SUU-25C/A dispenser from the outboard pylon. These data all exhibit an initial nose-down pitch motion and an outboard yaw motion. The only effect of an increase in Mach number is a slightly more rapid nose-down pitch. Ejector force number 1 caused the store to pitch nose down less rapidly than ejector force number 2. By comparing data for configuration 1L with configurations 2L or 2R, launches from the outboard pylon with an adjacent MER on the centerline pylon are seen to be almost identical to launches with an adjacent MER plus stores on the centerline pylon.

Separation trajectory data for the MK-20 Rockeye bomb are presented in Figs. 22 through 25. If a trajectory was of sufficient length to reach the position where the fins could be deployed, the open-fin configuration was used to obtain additional data. This continuation trajectory was initiated from the chosen store location along the original trajectory. The criterion for fin deployment was a clearance of at least 1 ft between the rack and the store center of gravity. The trajectories where fin deployment occurred are denoted by an asterisk in the figure heading next to the symbol, deployment occurring

at Z = 1.0 ft for all cases. These data show that the fin deployment had a significant effect on all of the angular motions, causing a reversal in direction of the pitch or yaw for many trajectories.

Figures 26 and 27 present separation trajectory data for the 300-gal fuel tank from the inboard pylon. The fuel tank displacements were only slightly affected by changes in Mach number and by the addition of adjacent stores on the centerline MER and outboard TER. In general, the pitch motion was favorably affected by ballasting, probably because of the change in ejector-induced pitch resulting from the change in center-of-gravity location.

Separation trajectories of the CBU-52B/B dispenser are presented in Figs. 28 through 30. These data show an initial nose-down pitch motion with an outboard yaw motion for configuration 18L (outboard pylon) and 18R (center pylon) launches, and an inboard yaw motion for configuration 20R (inboard pylon) launches. Ejector force number 9 caused the store to pitch nose down less rapidly than ejector force number 8. The store displacements are relatively unaffected by changes in Mach number.

Separation trajectories of the BLU-52A/B bomb are presented in Figs. 31 through 33. These data exhibit the same trends as the CBU-52B/B dispenser separation data. Ejector force number 11 caused a less rapid nose-down store pitch than ejector force number 10.

APPENDIXES
I. ILLUSTRATIONS
II. TABLES

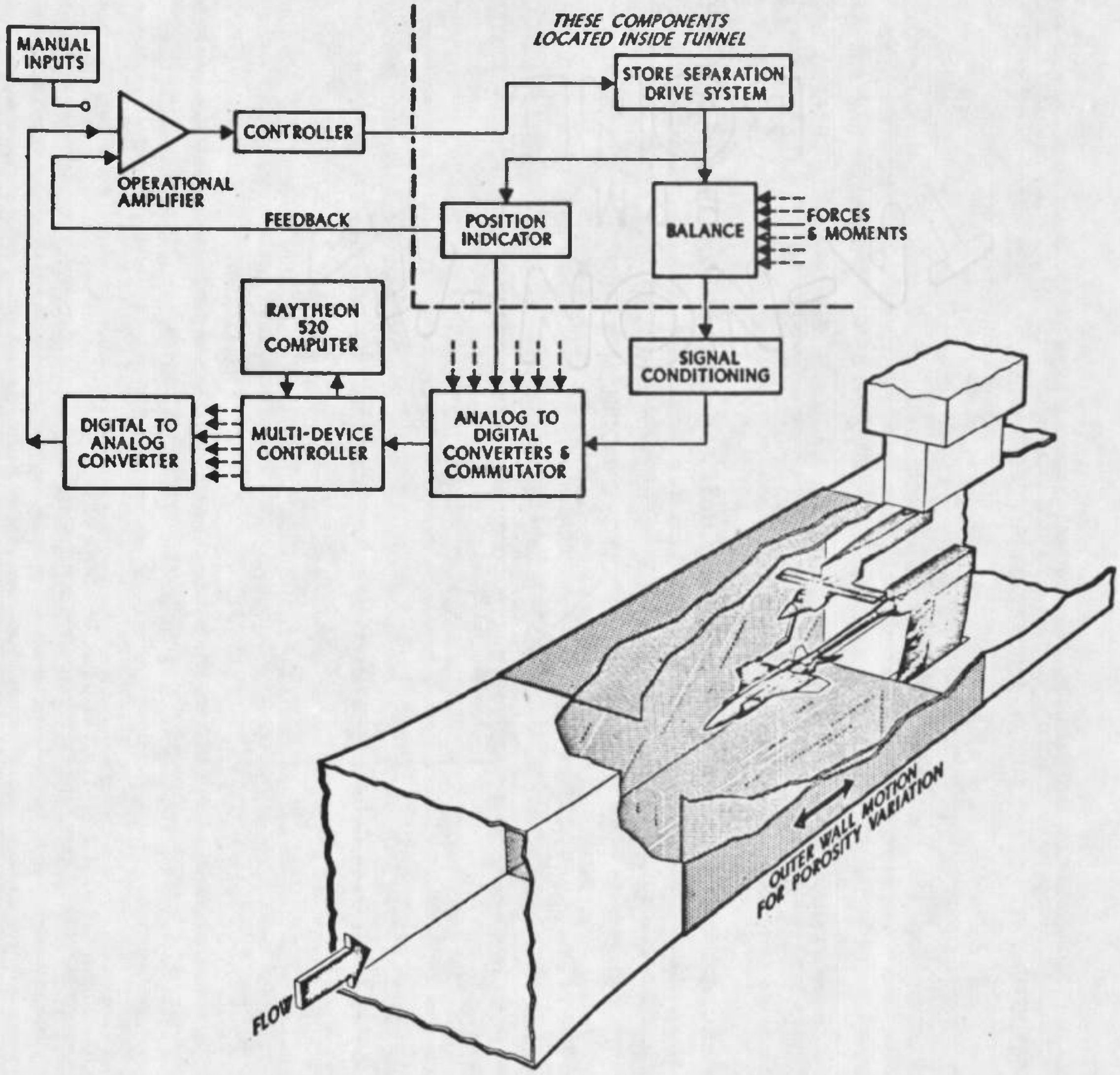

Fig. 1 Isometric Drawing of a Typical Store Separation Installation and a Block Diagram of the Computer Control Loop

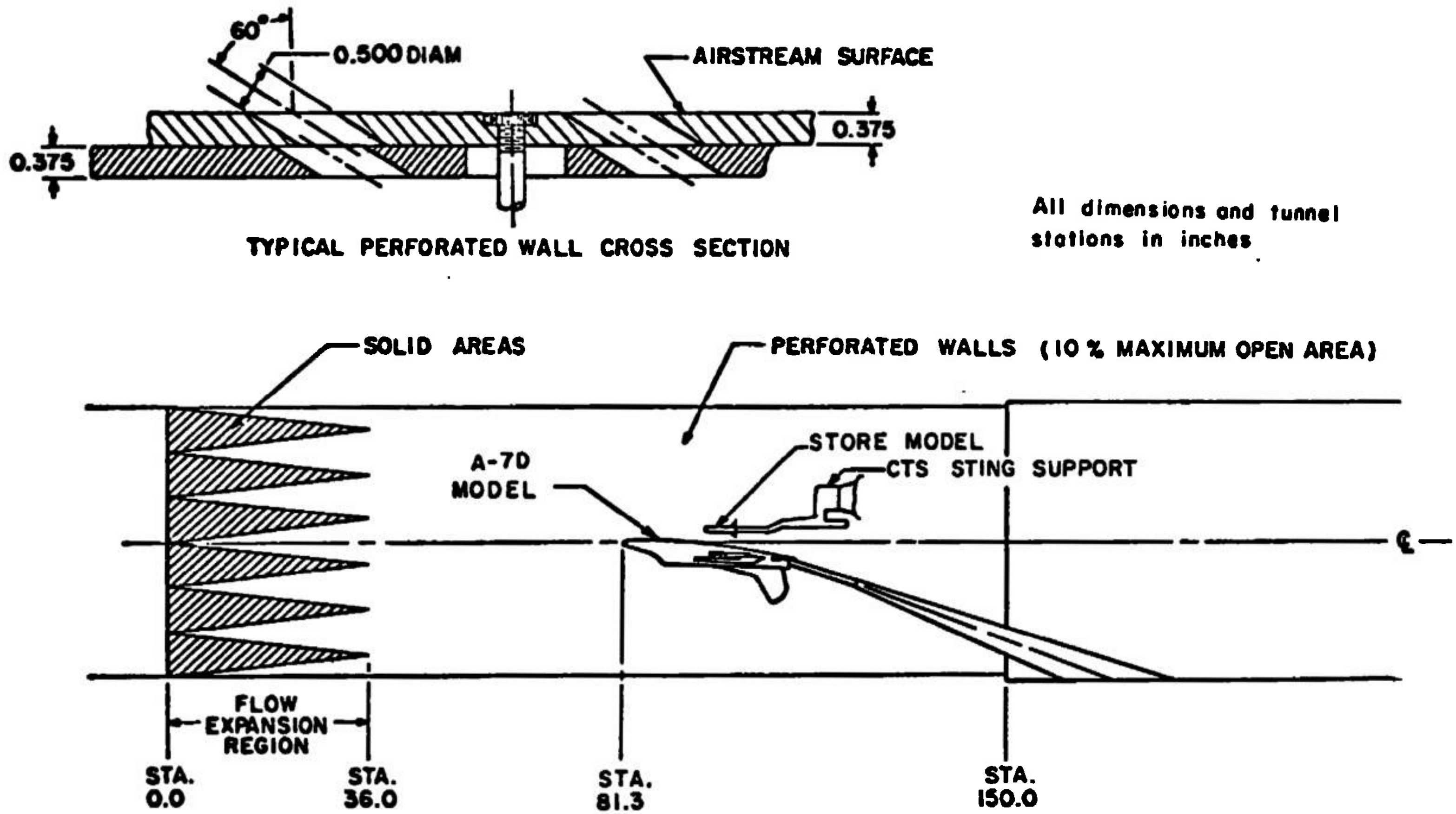

Fig. 2 Schematic of the Tunnel Test Section Showing Model Location

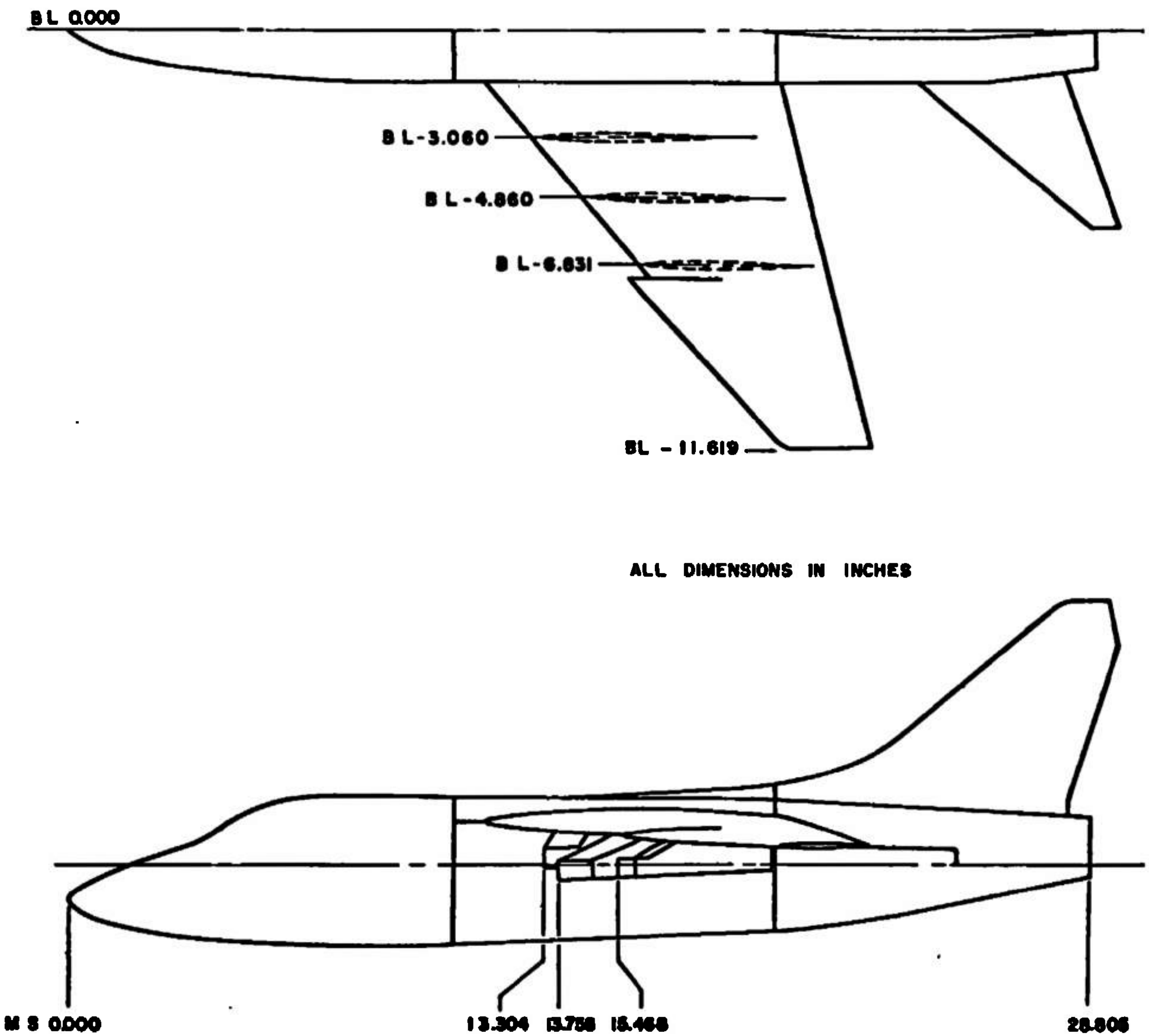

Fig. 3 Sketch of the A-7D Parent-Aircraft Model

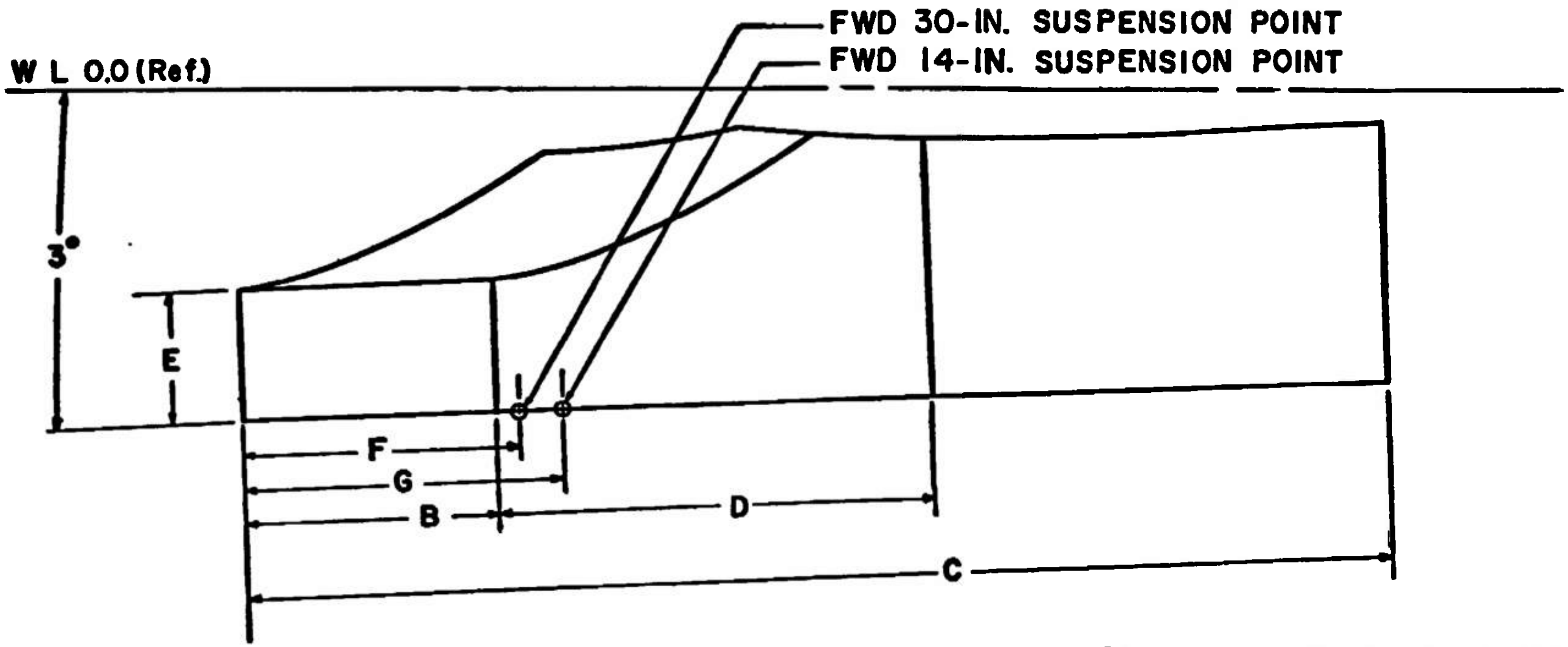

ALL DIMENSIONS IN INCHES

	INBOARD	CENTER	OUTBOARD
B	1.030	1.030	0.515
C	4.580	4.850	4.437
D	1.630	1.905	2.008
E	0.575	0.575	0.513
F	0.950	0.950	0.750
G	1.350	1.350	1.150

Fig. 4 Details and Dimensions of the A-7D Model Pylons

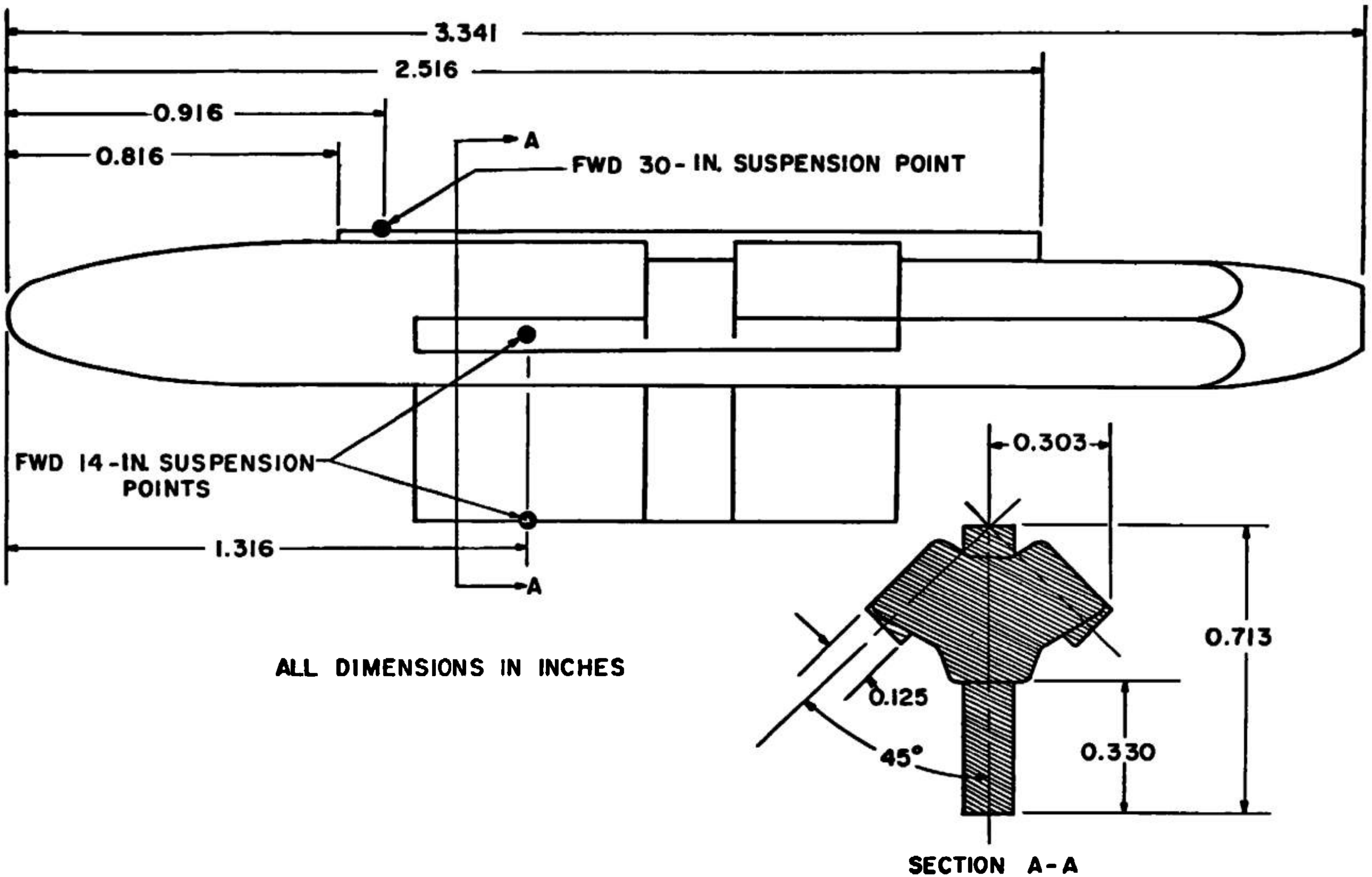

Fig. 5 Details and Dimensions of the TER Model

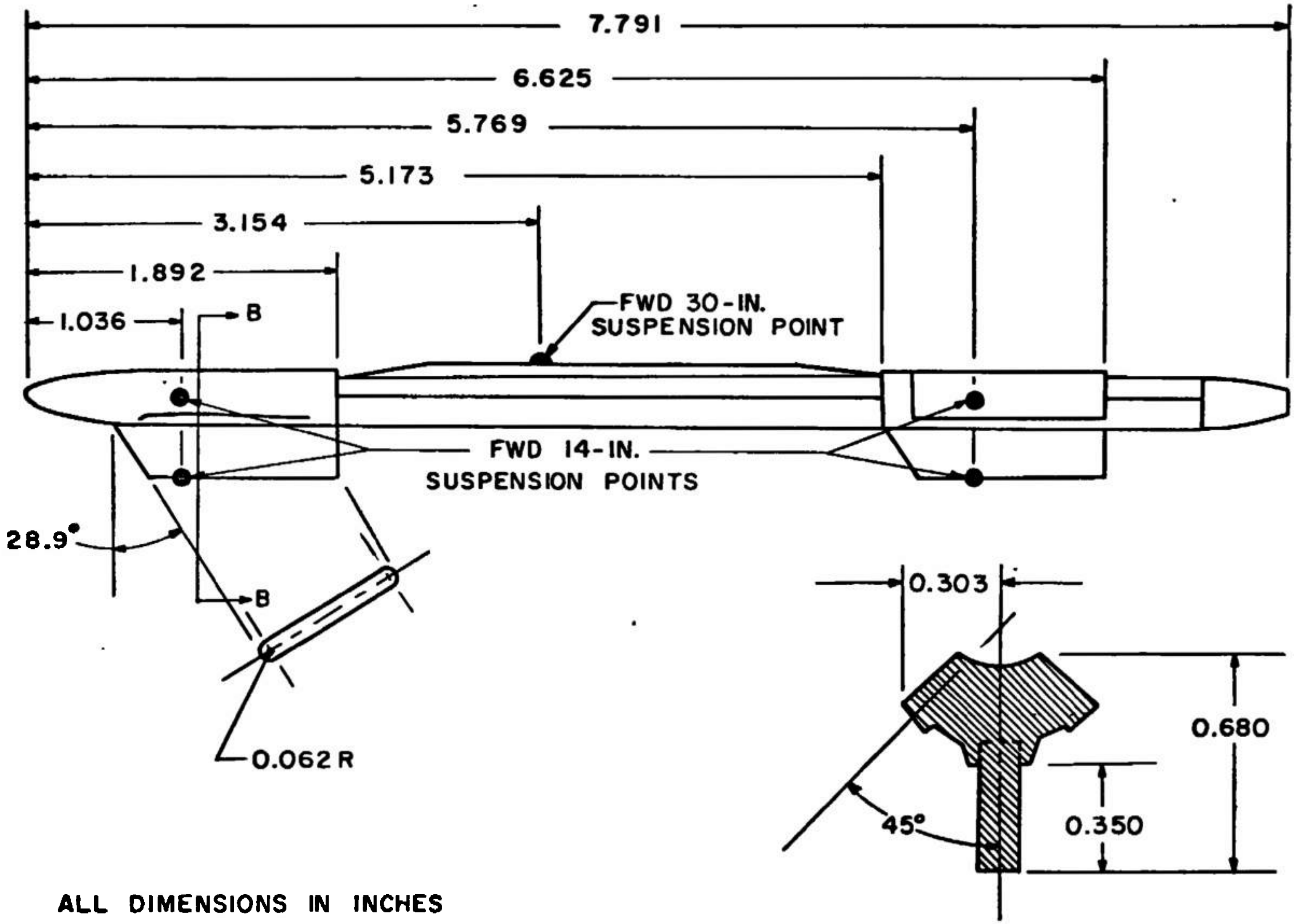

Fig. 6 Details and Dimensions of the MER Model

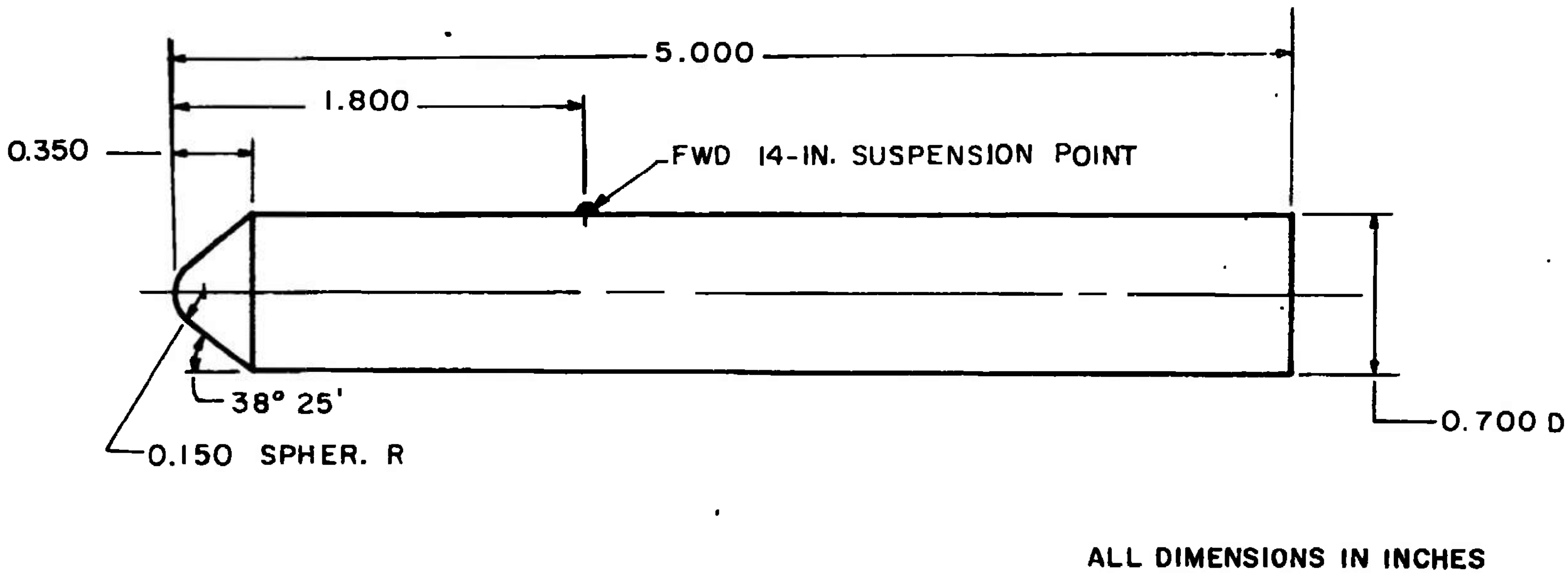

Fig. 7 Details and Dimensions of the SUU-25C/A Dispenser Model

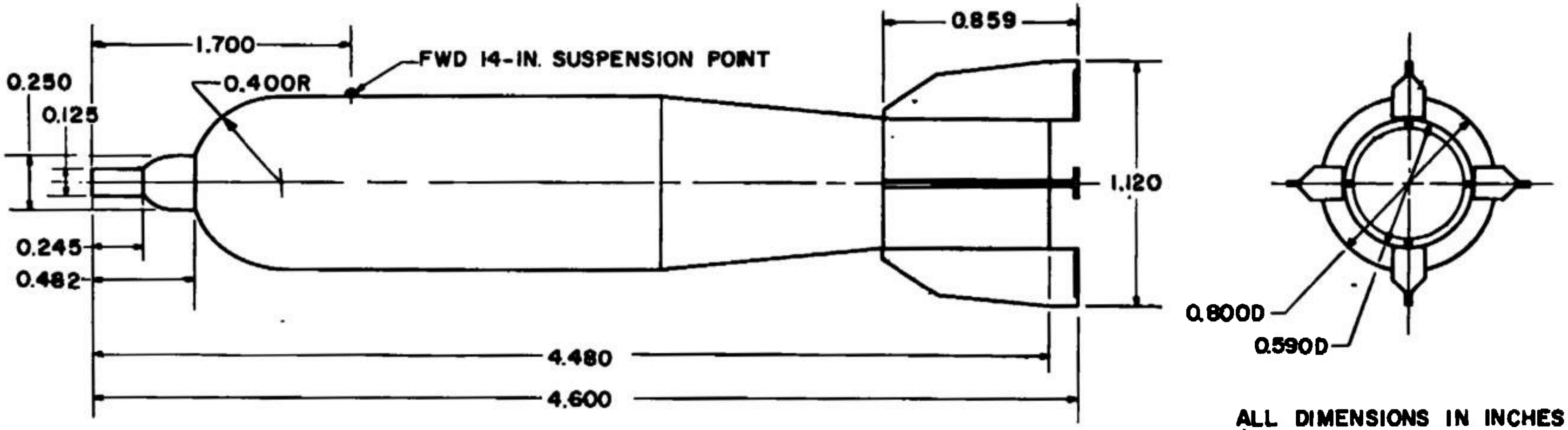

Fig. 8 Details and Dimensions of the CBU-52B/B Dispenser Model

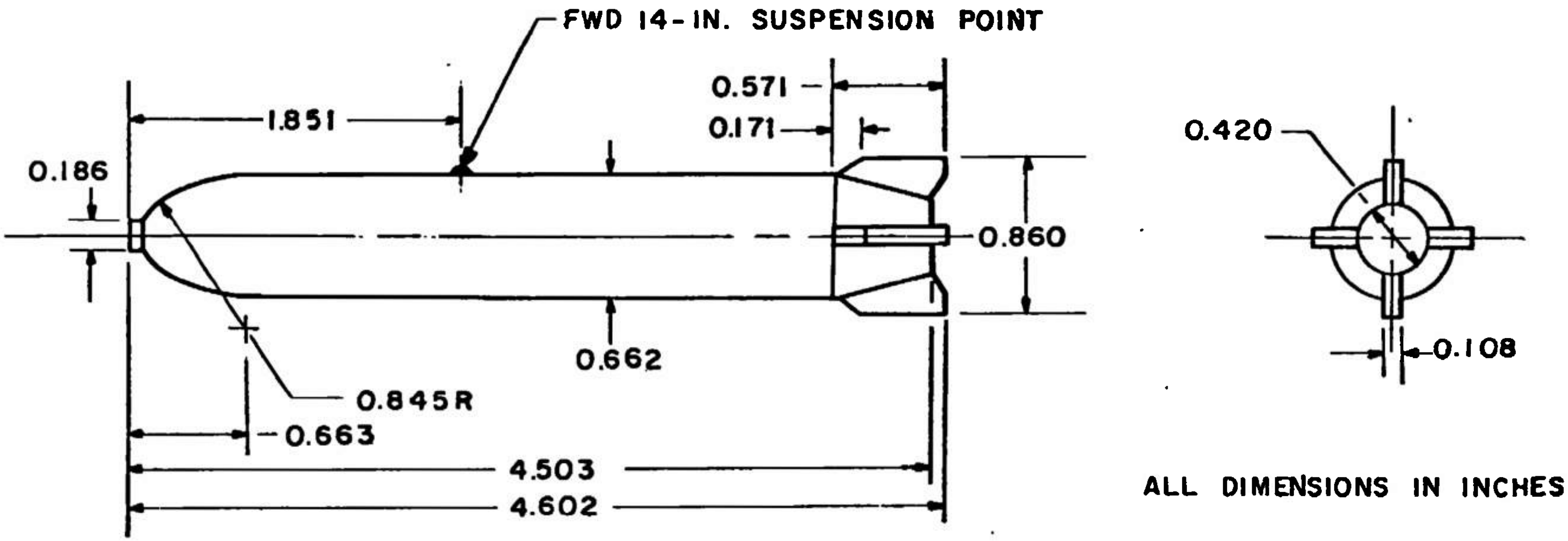

a. Fins Closed
Fig. 9 Details and Dimensions of the MK-20 Rockeye Bomb Model

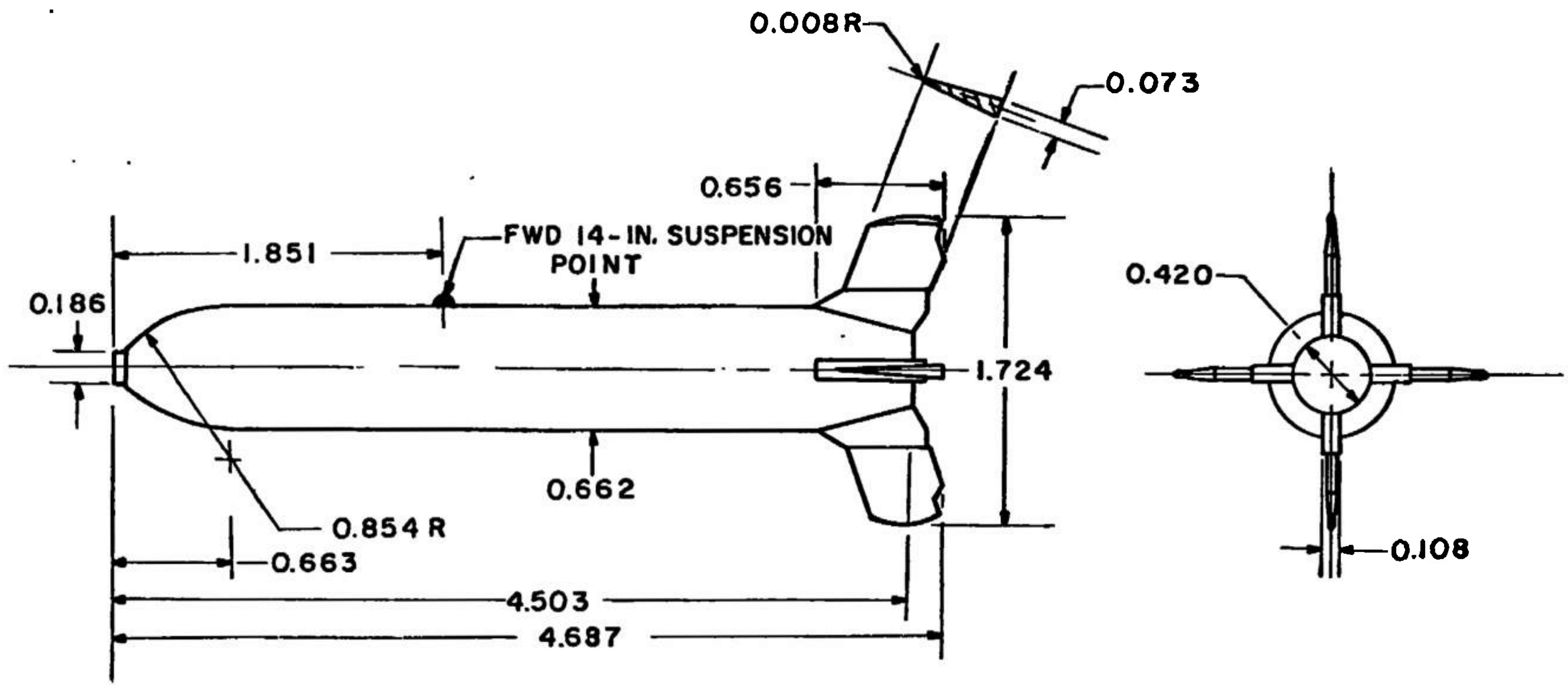

ALL DIMENSIONS IN INCHES

b. Fins Deployed
Fig. 9 Concluded

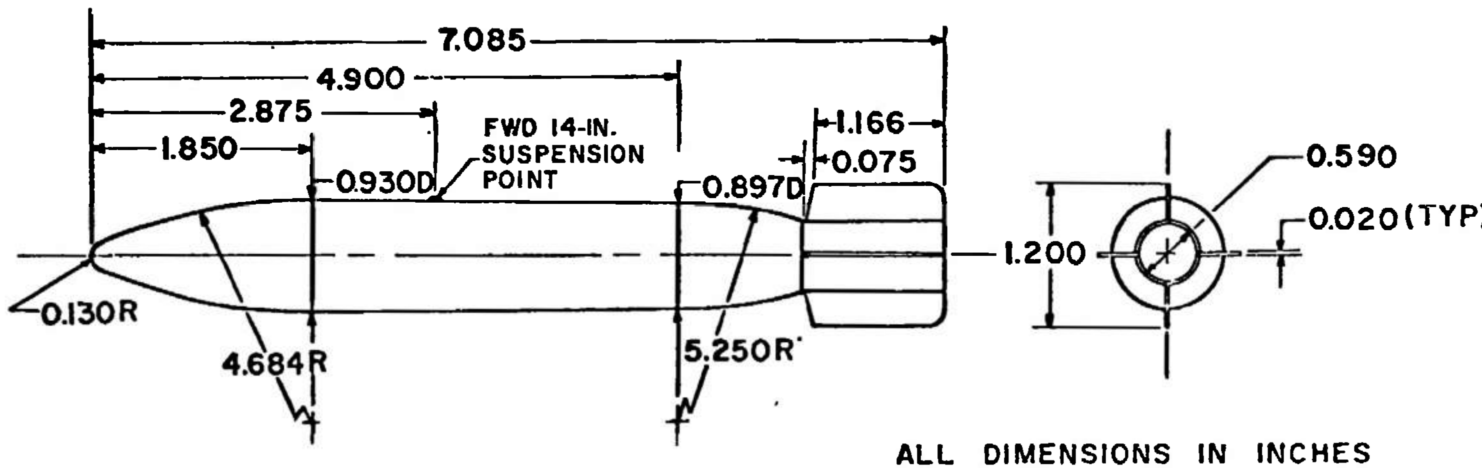

Fig. 10 Details and Dimensions of the BLU-52A/B Bomb Model

ORDINATES

MODEL STA "X"	RADIUS "R"	MODEL STA "X"	RADIUS "R"
0.000	0.0000	2.250	0.5531
0.060	0.0000	2.500	0.5777
0.100	0.0511	2.750	0.5888
0.150	0.0751		CONSTANT SLOPE
0.200	0.0981	3.450	0.6625
0.250	0.1203		CONSTANT DIAM
0.300	0.1415	6.638	0.6625
0.350	0.1619		CONSTANT SLOPE
0.400	0.1815	7.713	0.5680
0.450	0.2003	7.763	0.5637
0.500	0.2183	8.013	0.5409
0.550	0.2355	8.263	0.5162
0.600	0.2521	8.513	0.4899
0.650	0.2680	8.763	0.4820
0.700	0.2833	9.013	0.4327
0.750	0.2979	9.113	0.4206
0.800	0.3119		CONSTANT SLOPE
0.850	0.3253	10.900	0.1615
0.900	0.3383	10.950	0.1733
1.000	0.3625	11.000	0.1646
1.250	0.4153	11.100	0.1441
1.500	0.4587	11.200	0.1170
1.750	0.4950	11.300	0.0725
2.000	0.5260	11.350	0.0000

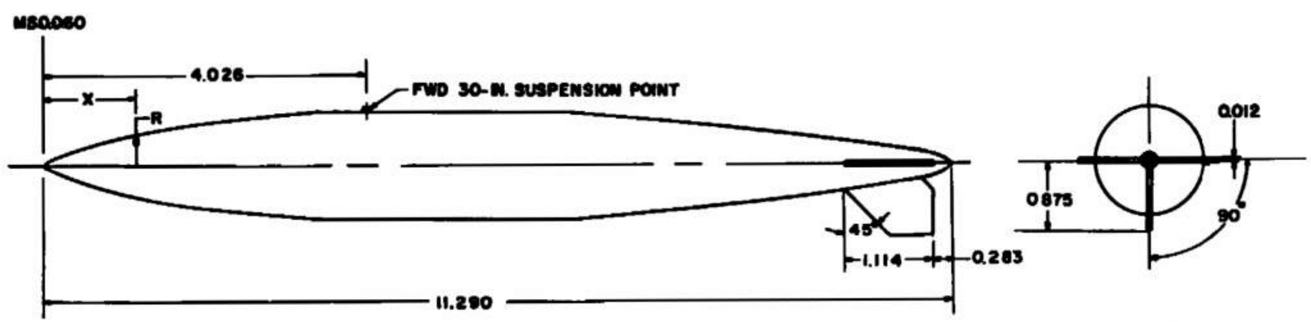

ALL DIMENSIONS AND MODEL STATIONS IN INCHES

Fig. 11 Details and Dimensions of the 300-gal Fuel Tank Model

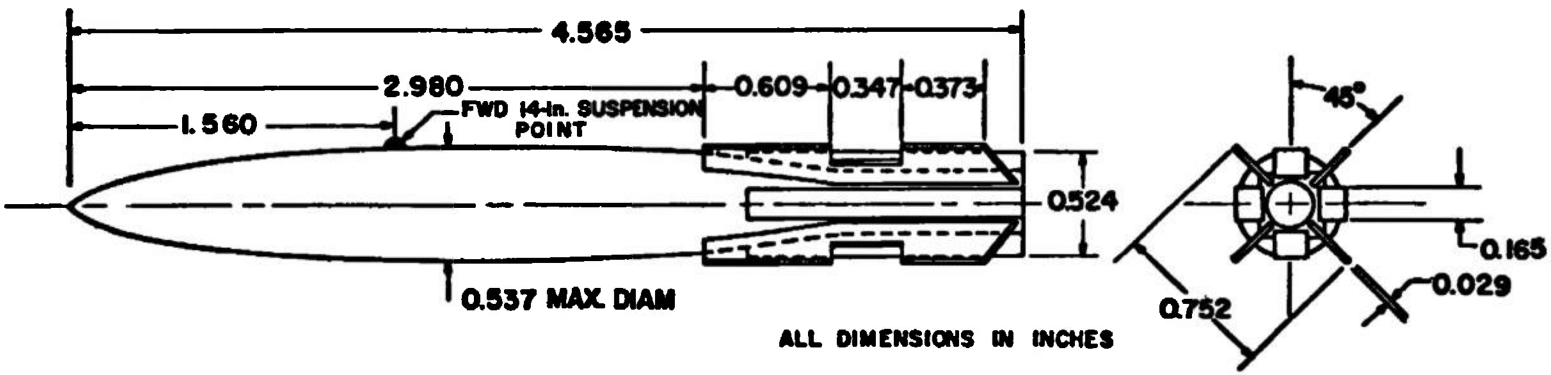

Fig. 12 Details and Dimensions of the MK-82 Snakeye Bomb Model

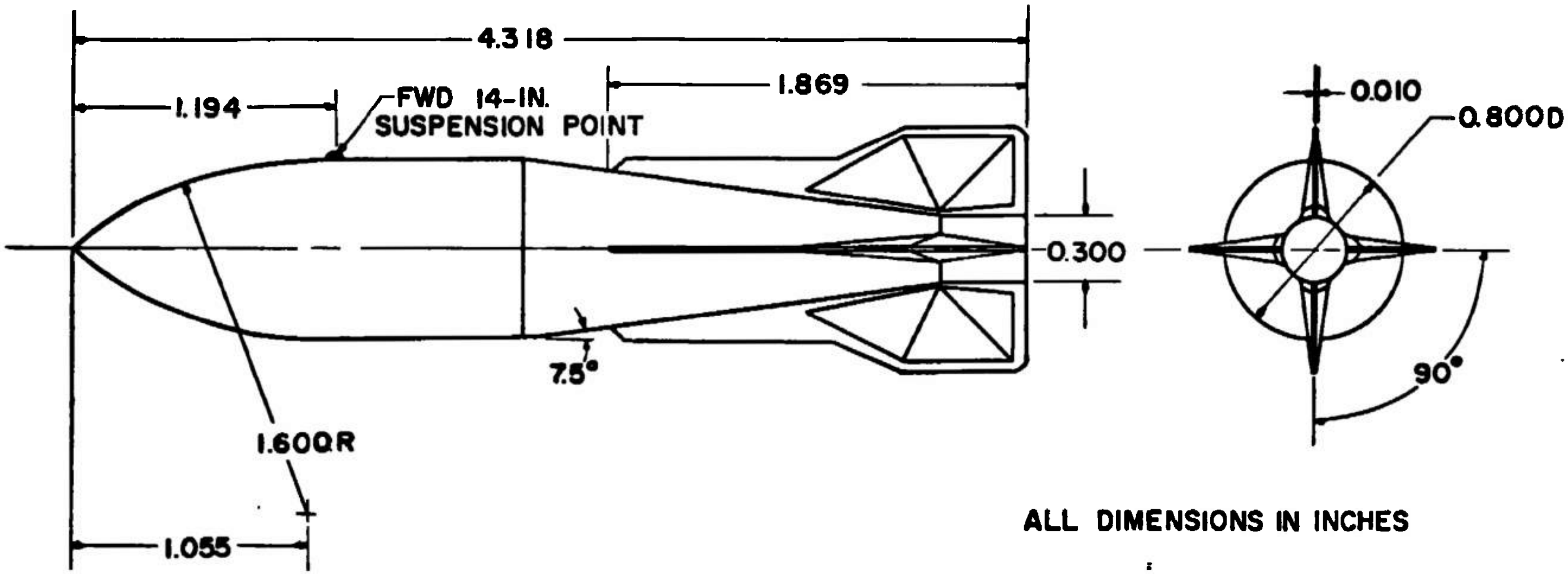

Fig. 13 Details and Dimensions of the M-117 Bomb Model with MAU-103A/B Fins

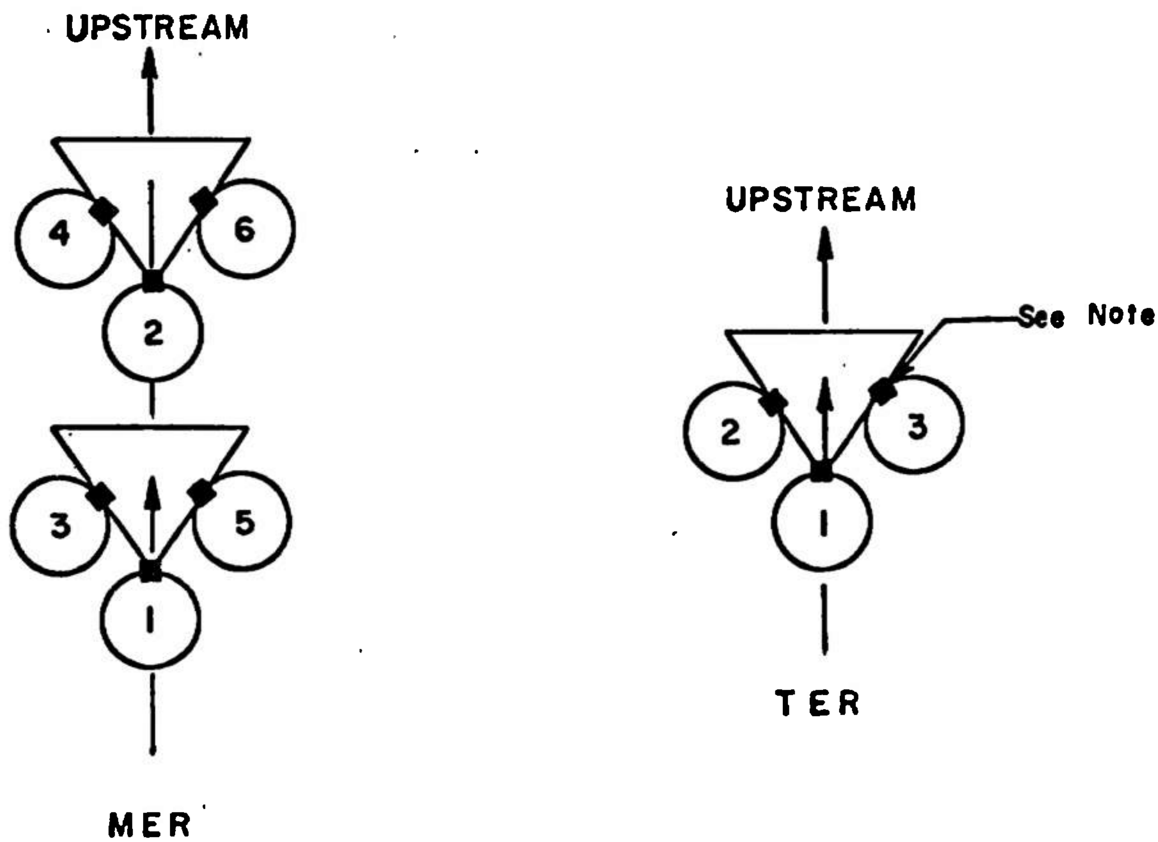

NOTE: The square indicates the orientation of the suspension lugs

TYPE RACK	STATION	ROLL ORIENTATION, deg
MER	1	0
	2	0
	3	45
	4	45
	5	-45
	6	-45
TER	1	0
	2	45
	3	-45

Fig. 14 Schematic of the TER and MER Store Stations and Orientations

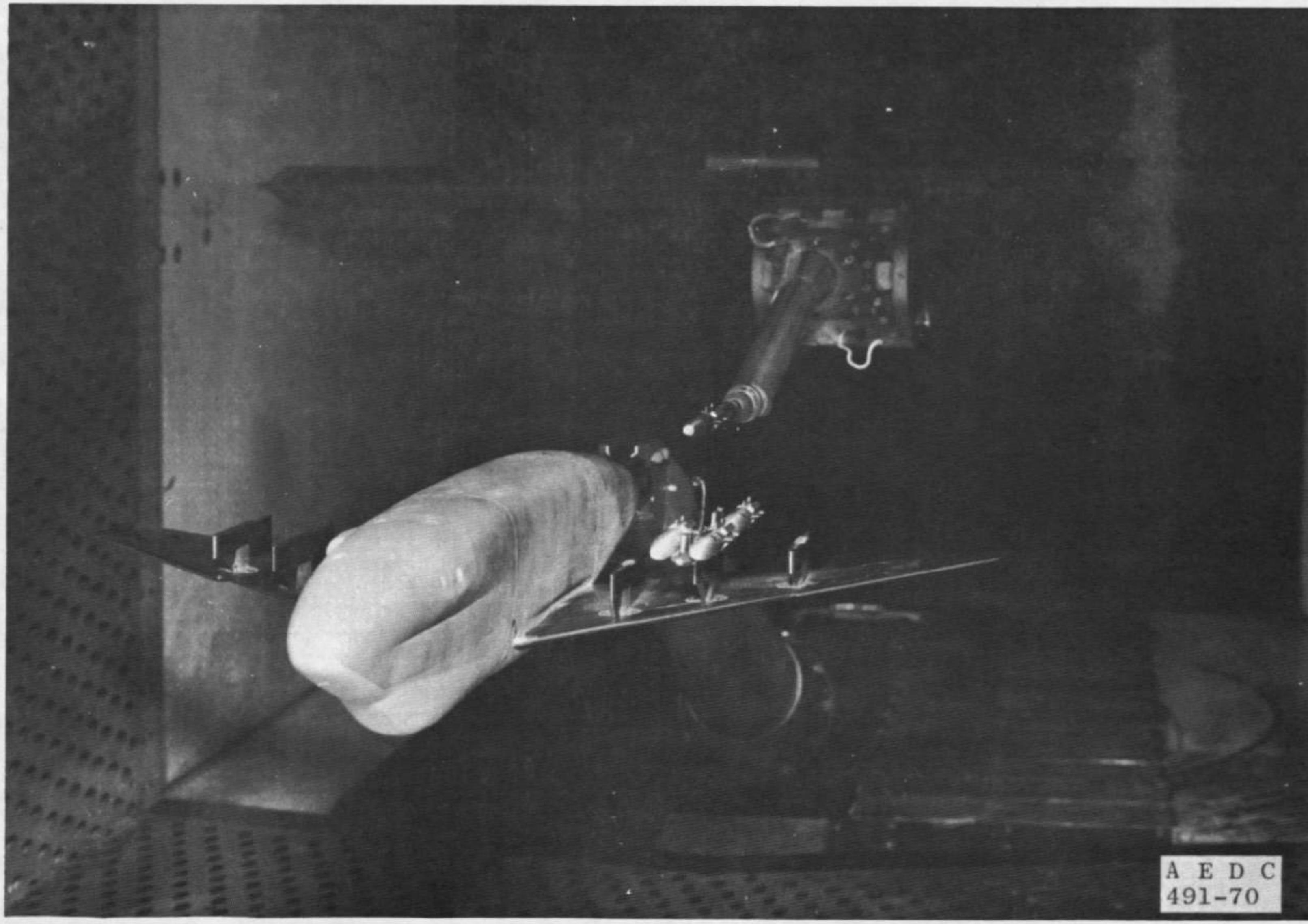

Fig. 15 Tunnel Installation Photograph Showing Parent Aircraft, Store, and Captive Trajectory Support

SYMBOL	CONF	M_∞	α	H	$\bar{\theta}$	EJECTOR FORCE
□	1L	0.325	10.6	4000	0	1
○	1L	0.325	10.6	4000	0	2

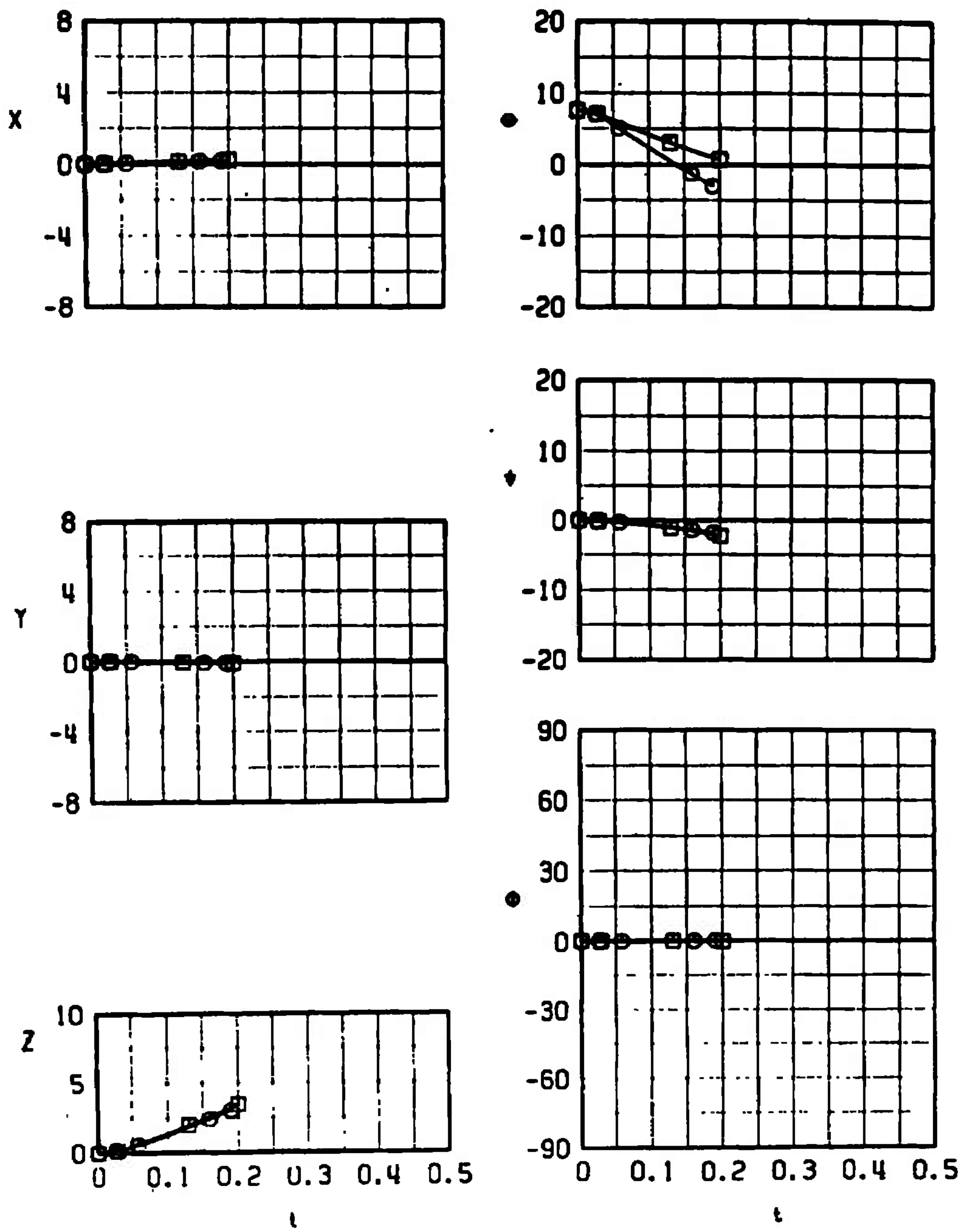

a. $M_\infty = 0.325$

Fig. 16 Separation Characteristics of the SUU-25C/A Dispenser (Empty) from the Outboard Pylon, Configuration 1L

SYMBOL	CONF	M_∞	α	H	$\bar{\theta}$	EJECTOR FORCE
□	1L	0.530	4.6	4000	0	1
○	1L	0.530	4.6	4000	0	2

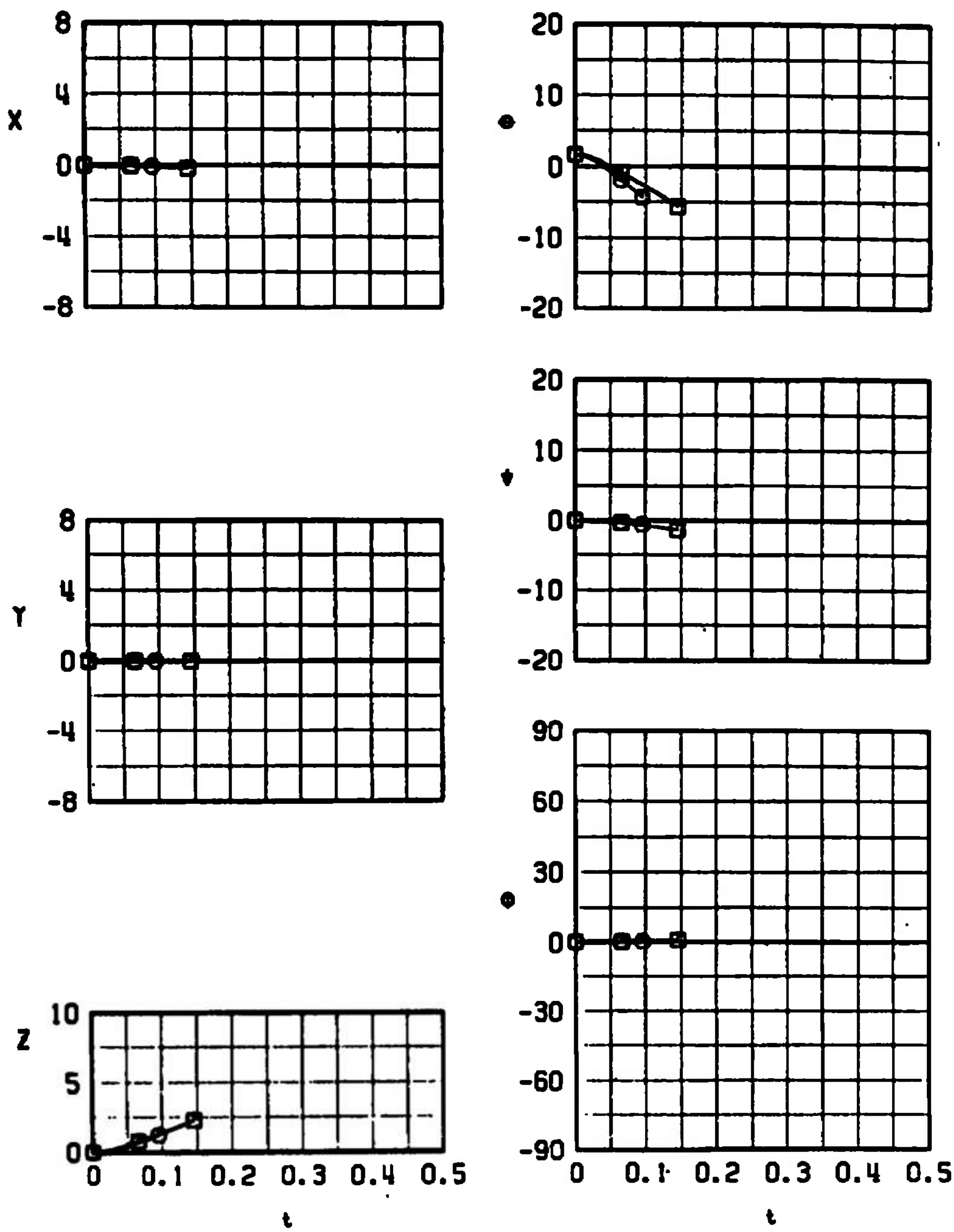

b. M_∞ = 0.530
Fig. 16 Continued

SYMBOL	CONF	M_∞	α	H	ψ	EJECTOR FORCE
□	1L	0.730	3.0	4000	0	1
○	1L	0.730	3.0	4000	0	2

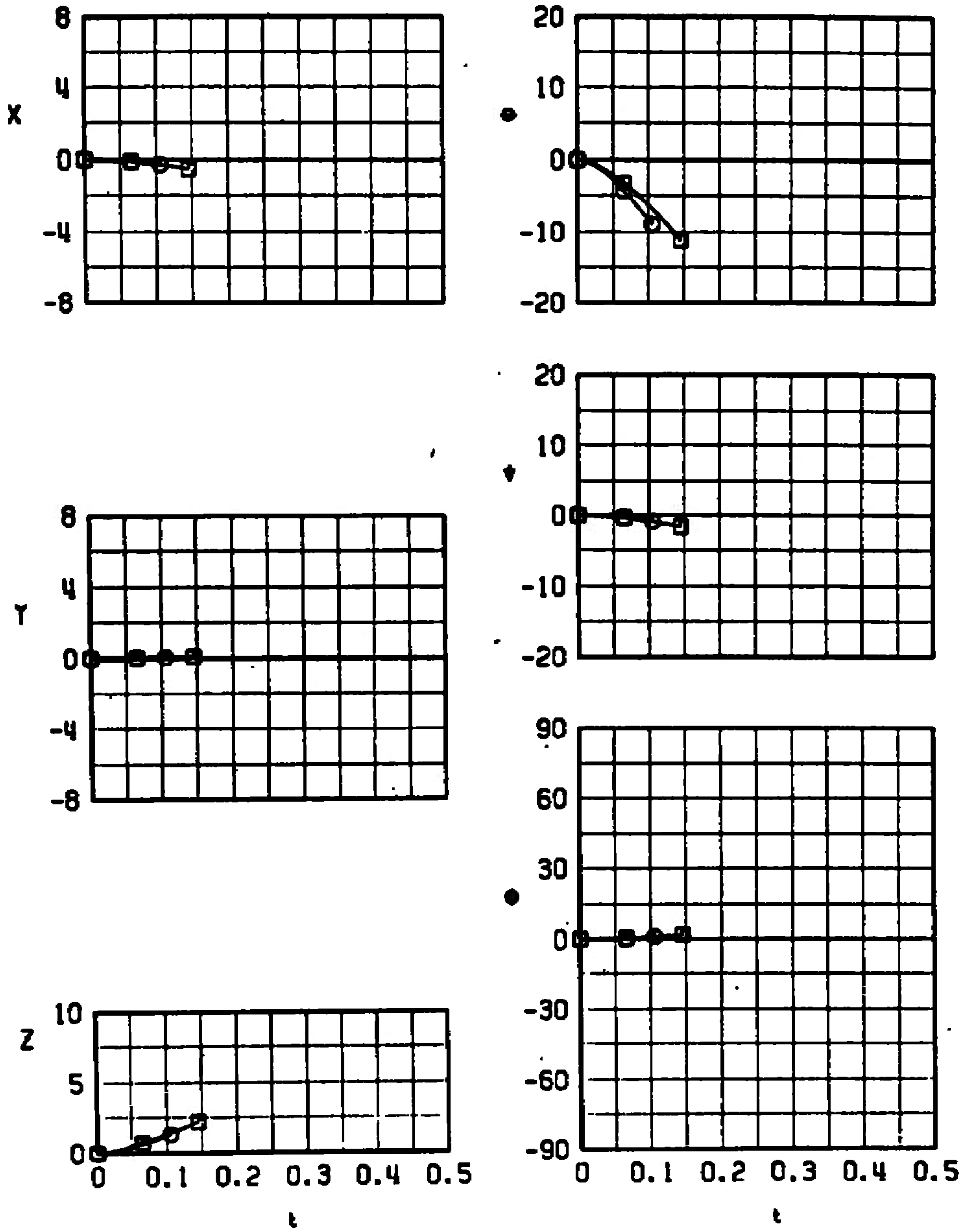

c. $M_\infty = 0.730$
Fig. 16 Continued

SYMBOL	CONF	M_∞	α	H	$\bar{\psi}$	EJECTOR FORCE
□	1L	0.814	2.8	4000	0	1
○	1L	0.814	2.8	4000	0	2

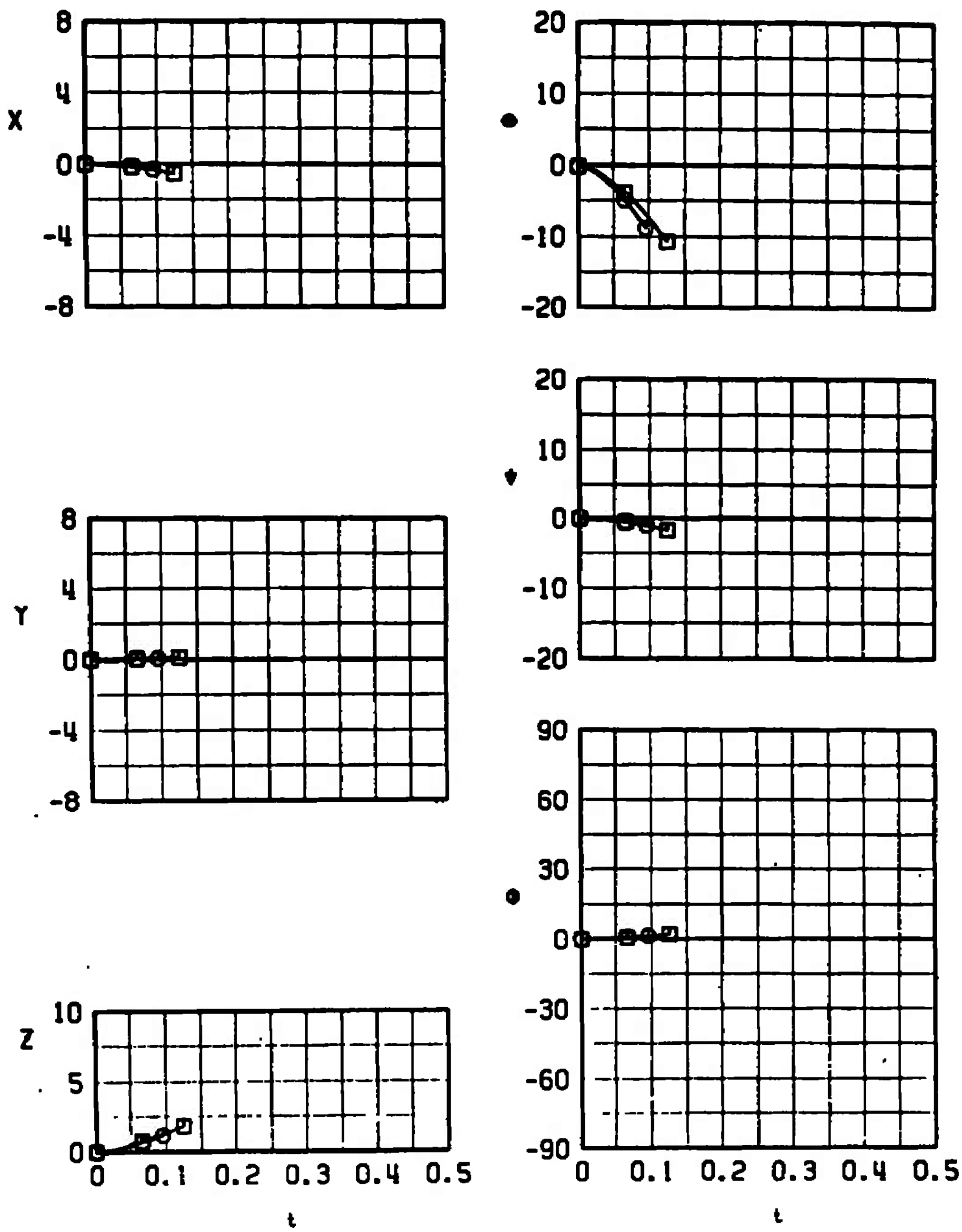

d. M_∞ = 0.814
Fig. 16 Concluded

SYMBOL	CONF	M_∞	α	H	$\bar{\theta}$	EJECTOR FORCE
□	2L	0.407	8.2	4000	0	1
○	2L	0.650	3.8	4000	0	1
△	2L	0.814	3.0	4000	0	1

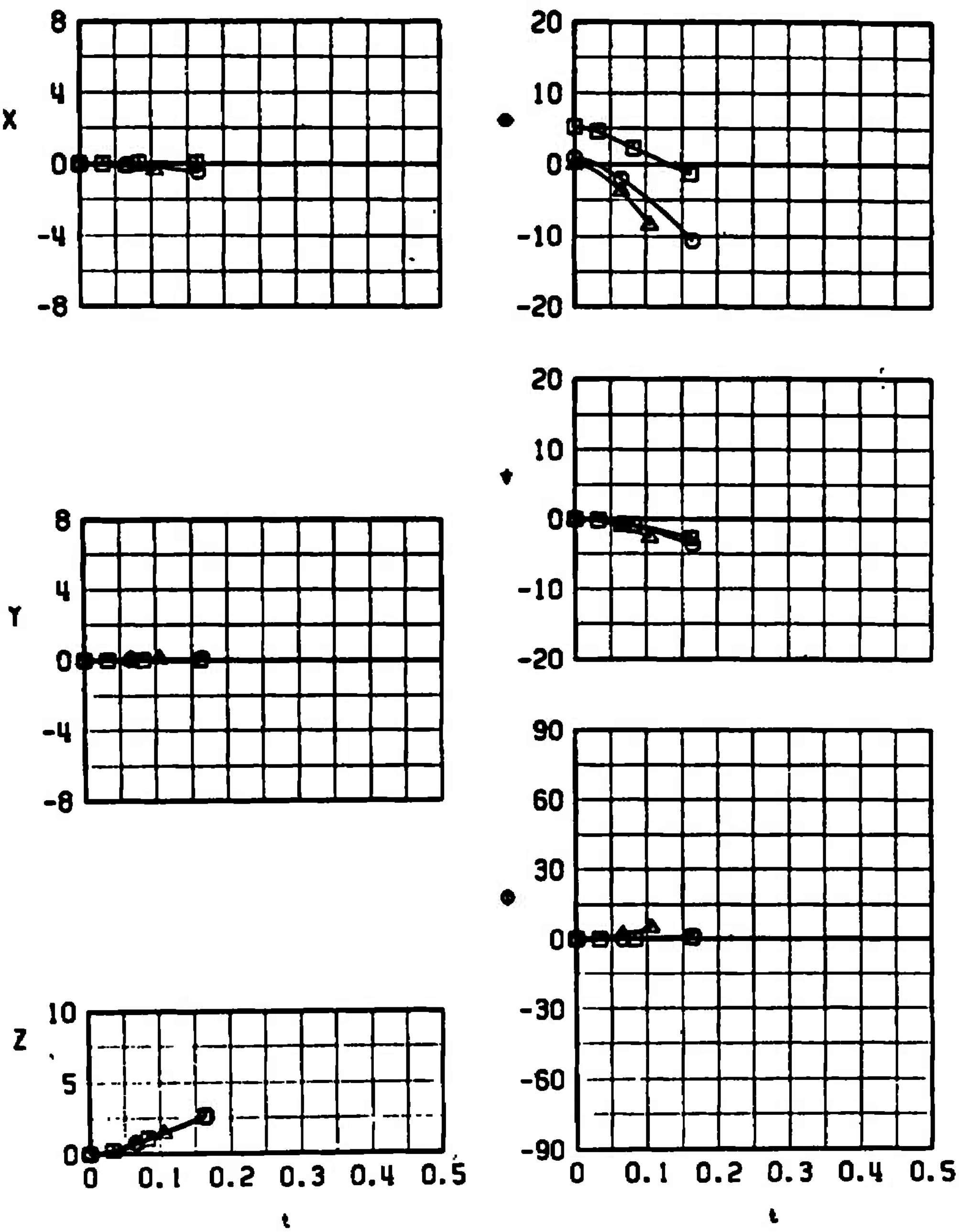

Fig. 17 Separation Characteristics of the SUU-25C/A Dispenser (Empty) from the Outboard Pylon, Configuration 2L

SYMBOL	CONF	M_∞	α	H	$\dot{\phi}$	EJECTOR FORCE
□	2R	0.407	8.2	4000	0	1
○	2R	0.650	3.8	4000	0	1
△	2R	0.814	3.0	4000	0	1

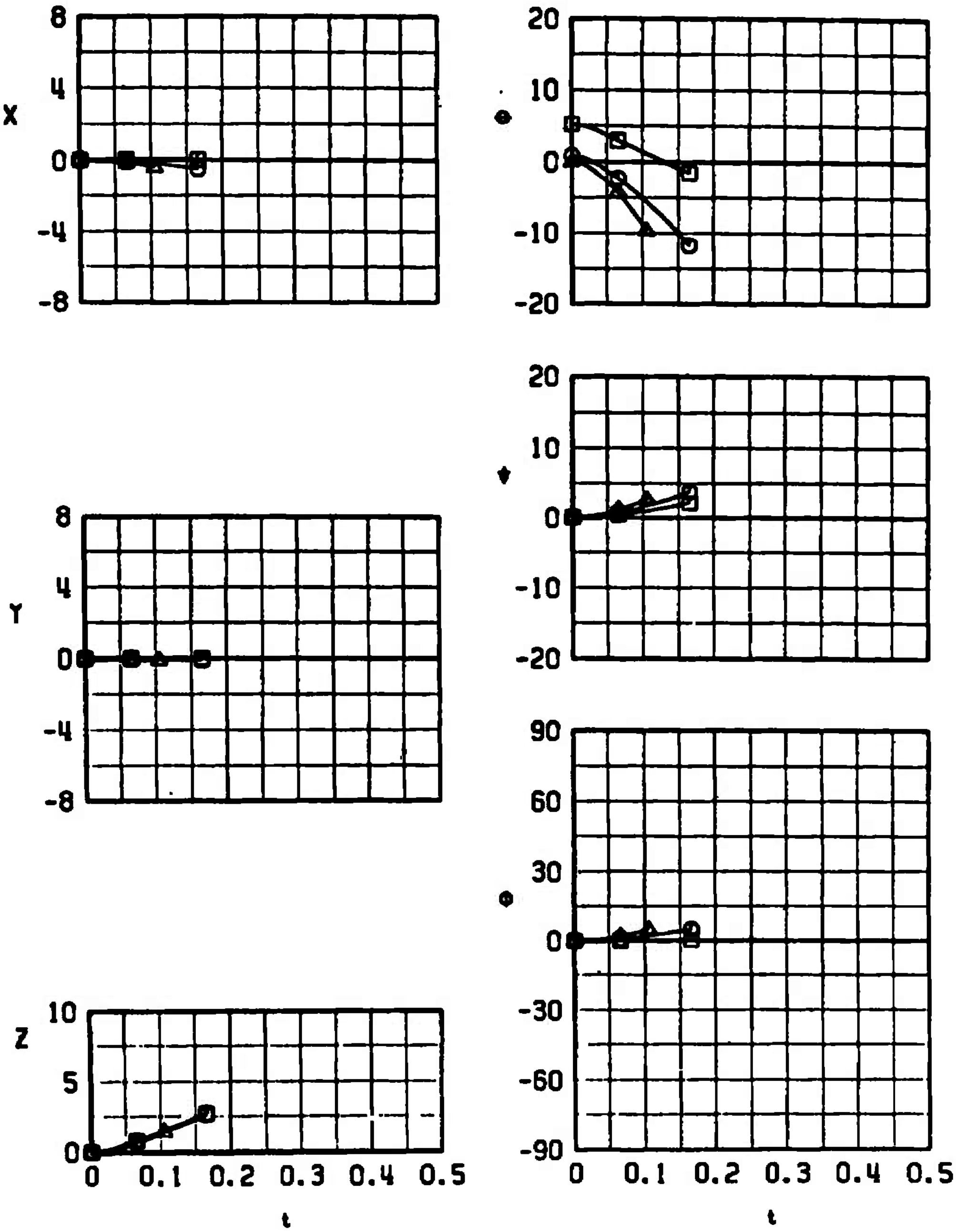

Fig. 18 Separation Characteristics of the SUU-25C/A Dispenser (Empty) from the Outboard Pylon, Configuration 2R

SYMBOL	CONF	M_∞	α	H	$\bar{\theta}$	EJECTOR FORCE
□	1L	0.325	10.6	4000	0	3
○	1L	0.325	10.6	4000	0	4

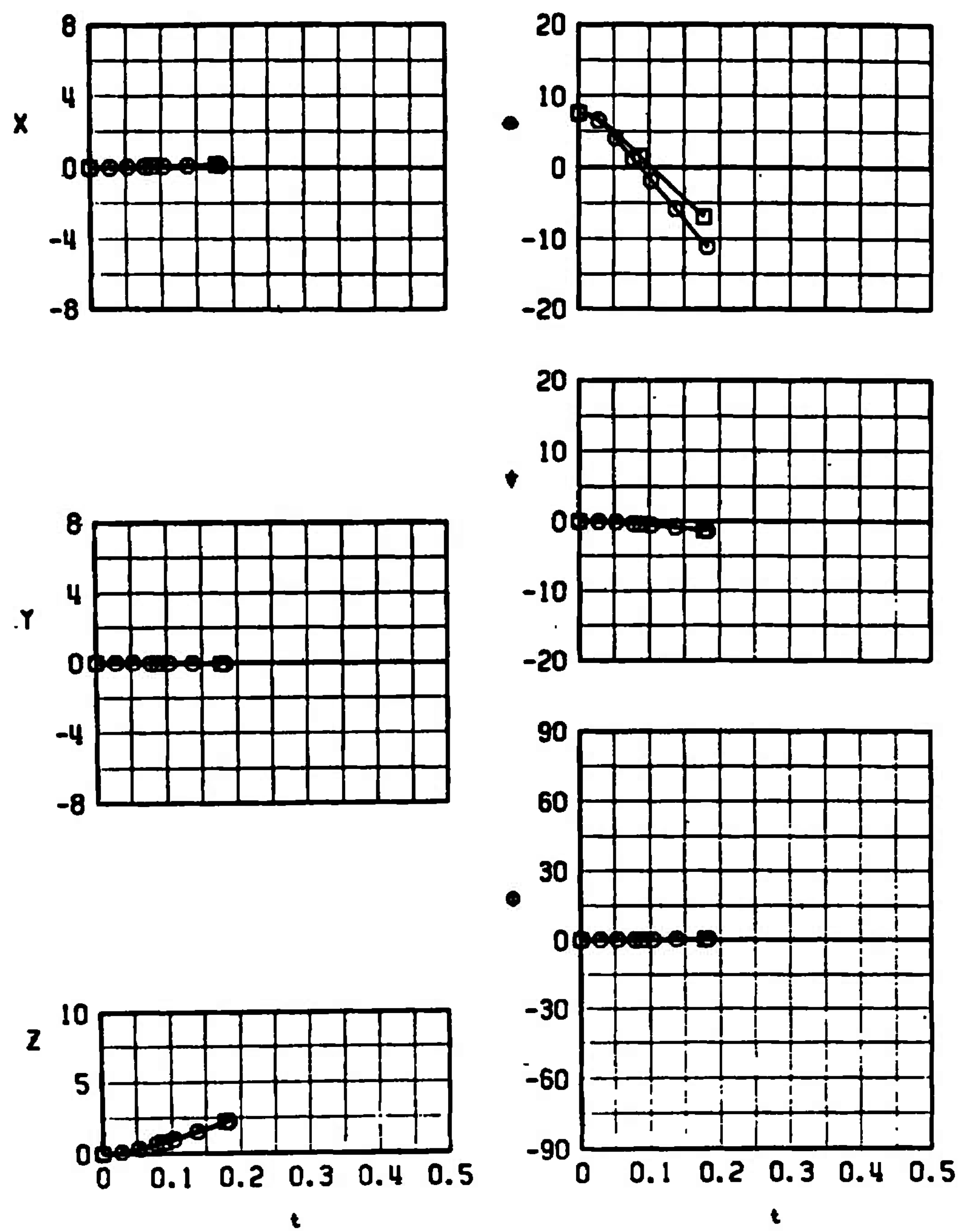

a. $M_\infty = 0.325$

Fig. 19 Separation Characteristics of the SUU-25C/A Dispenser (Full) from the Outboard Pylon, Configuration 1L

SYMBOL	CONF	M_∞	α	H	$\bar{\theta}$	EJECTOR FORCE
□	1L	0.530	4.6	4000	0	3
○	1L	0.530	4.6	4000	0	4

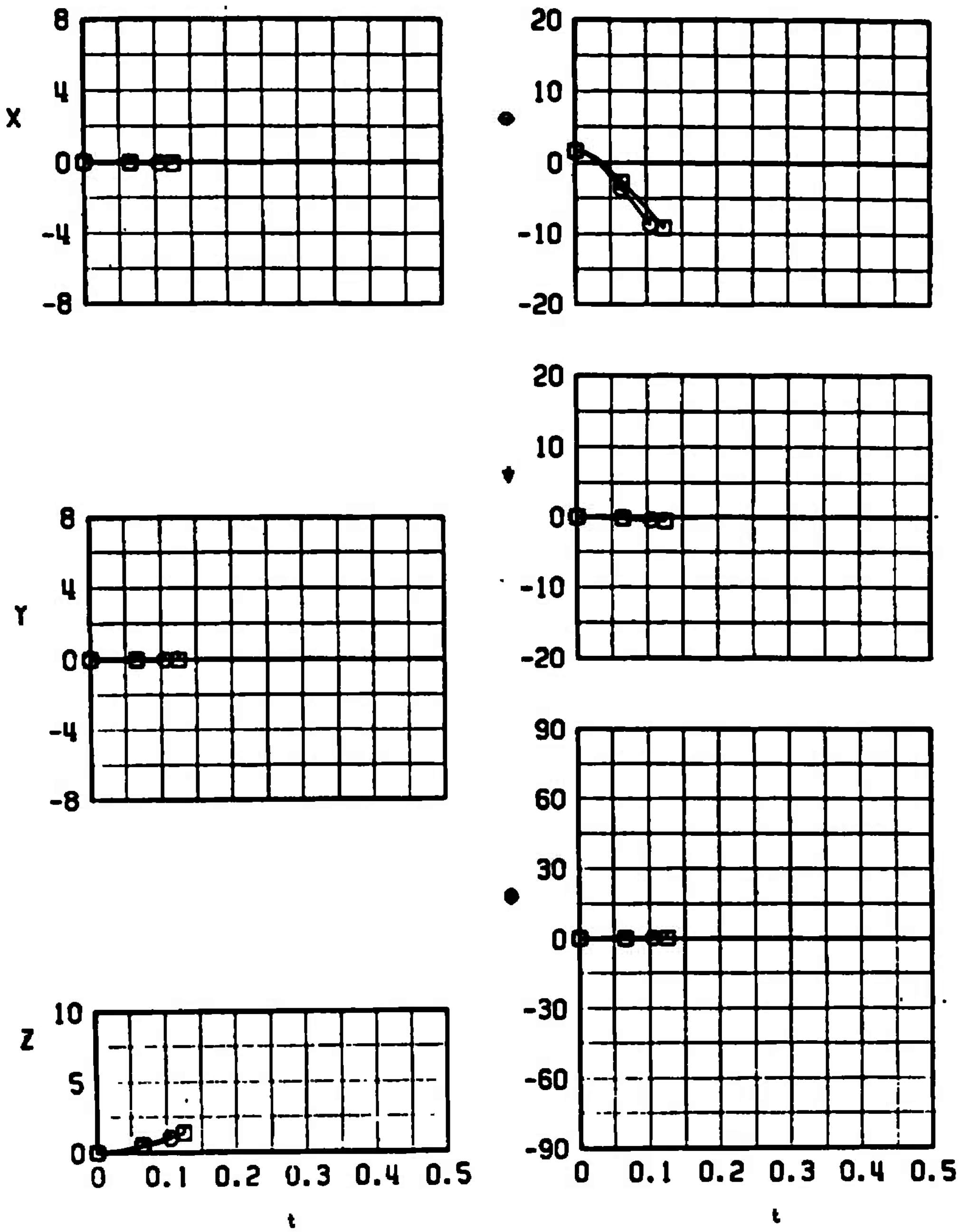

b. $M_\infty = 0.530$
Fig. 19 Continued

SYMBOL	CONF	M_∞	α	H	$\bar{\theta}$	EJECTOR FORCE
□	1L	0.730	3.0	4000	0	3
○	1L	0.730	3.0	4000	0	4

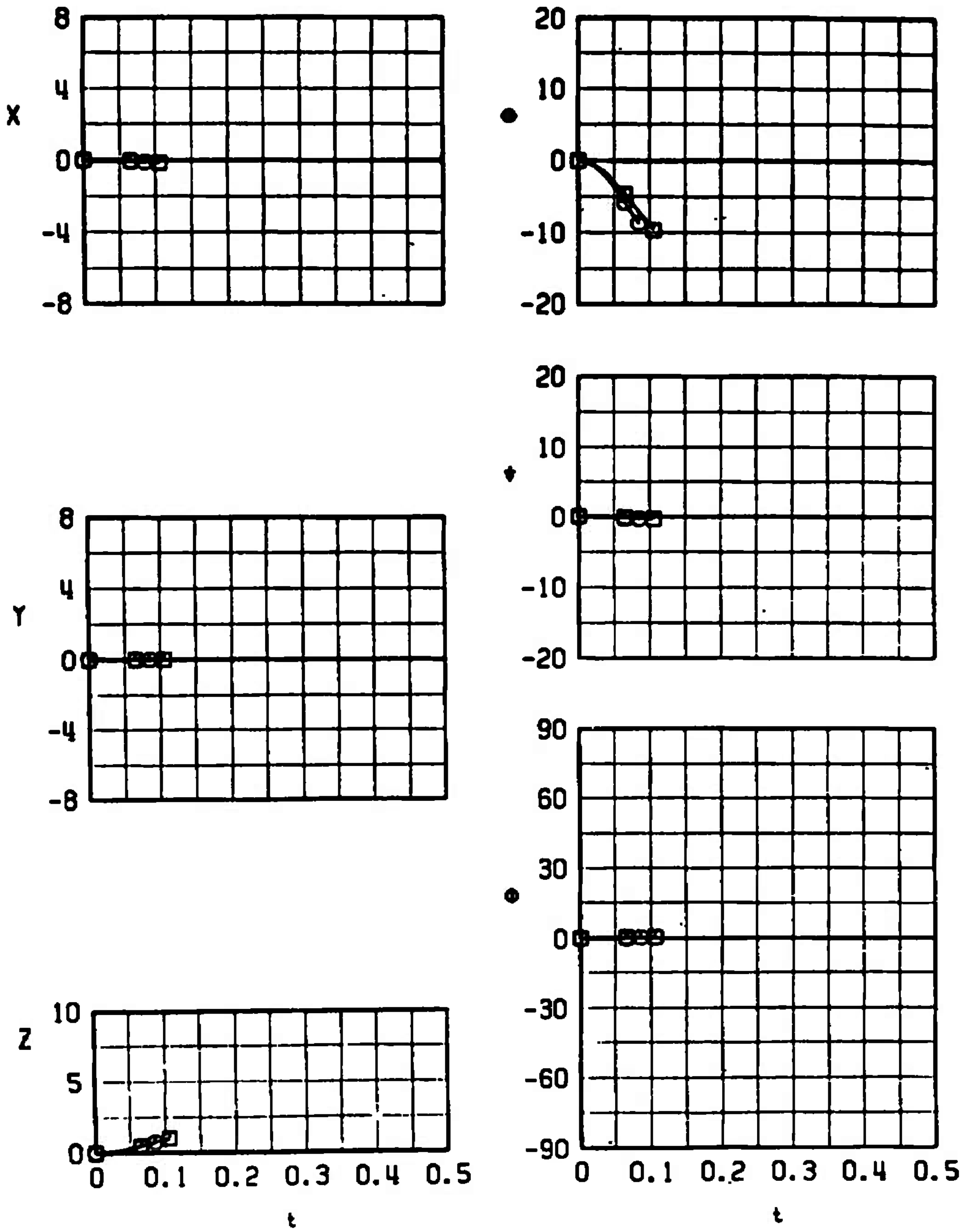

c. M_∞ = 0.730

Fig. 19 Continued

SYMBOL	CONF	M_∞	α	H	$\bar{\phi}$	EJECTOR FORCE
□	1L	0.814	2.8	4000	0	3
○	1L	0.814	2.8	4000	0	4

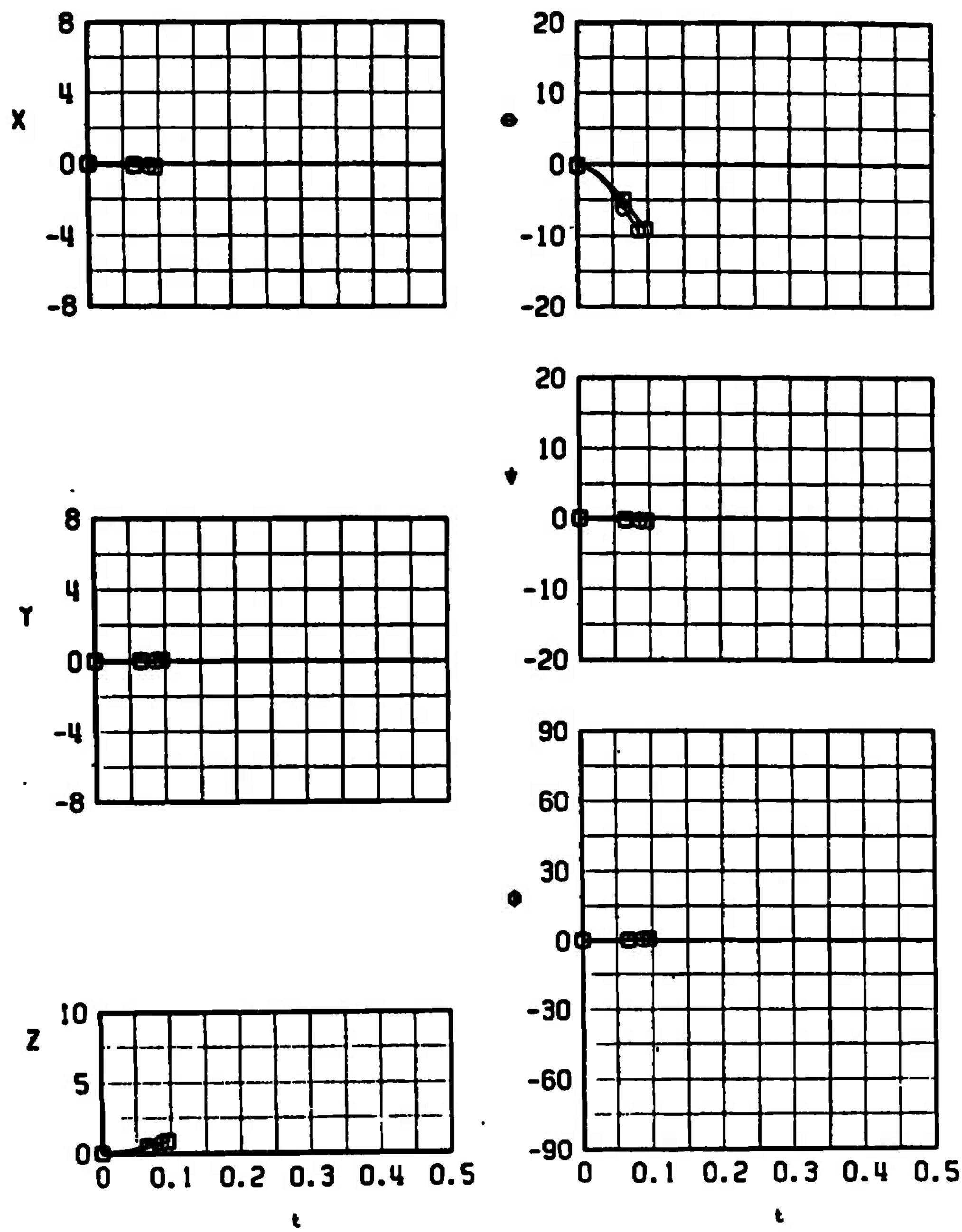

d. $M_\infty = 0.814$
Fig. 19 Concluded

SYMBOL	CONF	M_∞	α	H	$\bar{\delta}$	EJECTOR FORCE
□	2L	0.407	8.2	4000	0	3
○	2L	0.650	3.8	4000	0	3
△	2L	0.814	3.0	4000	0	3

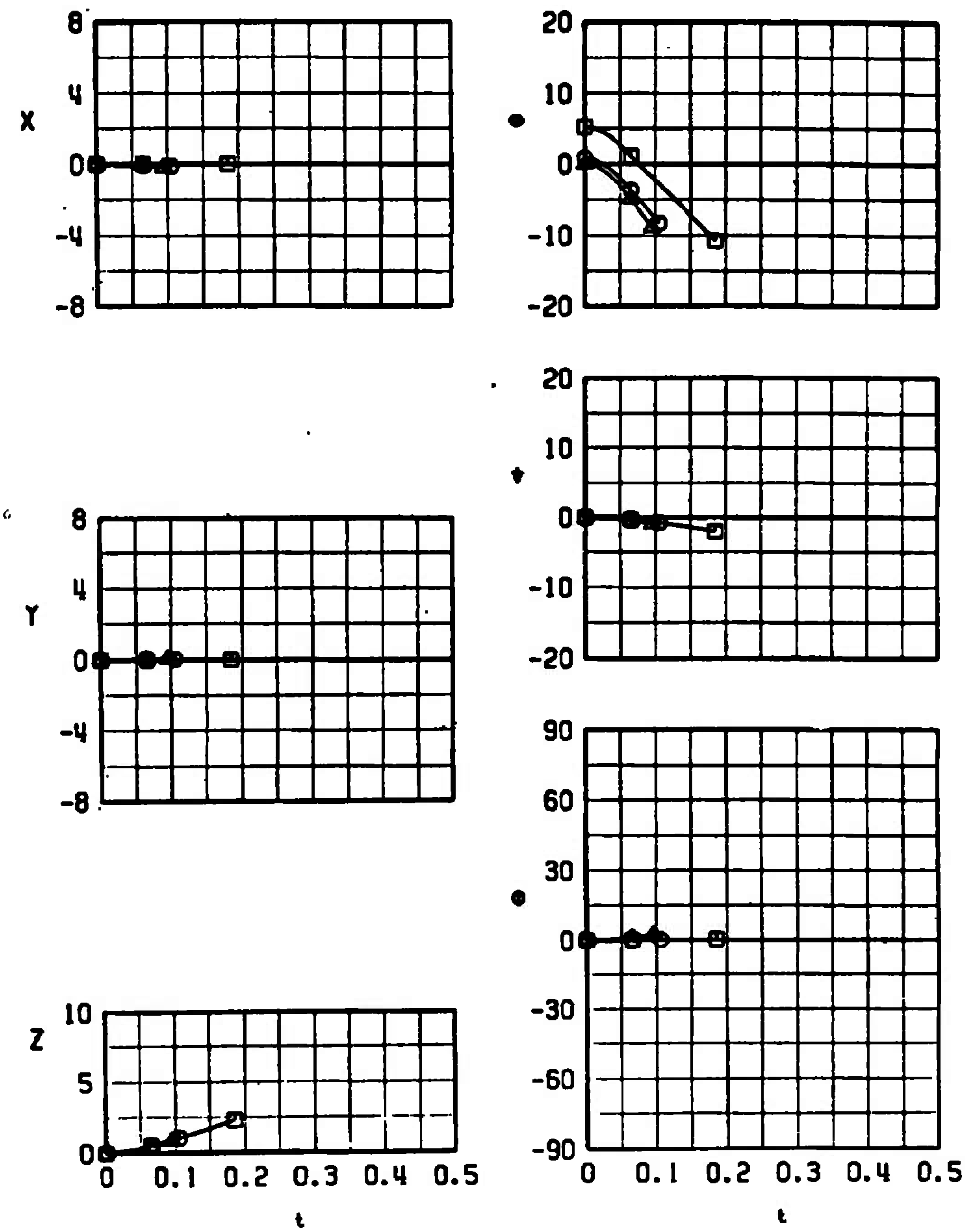

Fig. 20 Separation Characteristics of the SUU-25C/A Dispenser (Full) from the Outboard Pylon, Configuration 2L

SYMBOL	CONF	M_∞	α	H	γ	EJECTOR FORCE
□	2R	0.407	8.2	4000	0	3
○	2R	0.650	3.8	4000	0	3
△	2R	0.814	3.0	4000	0	3

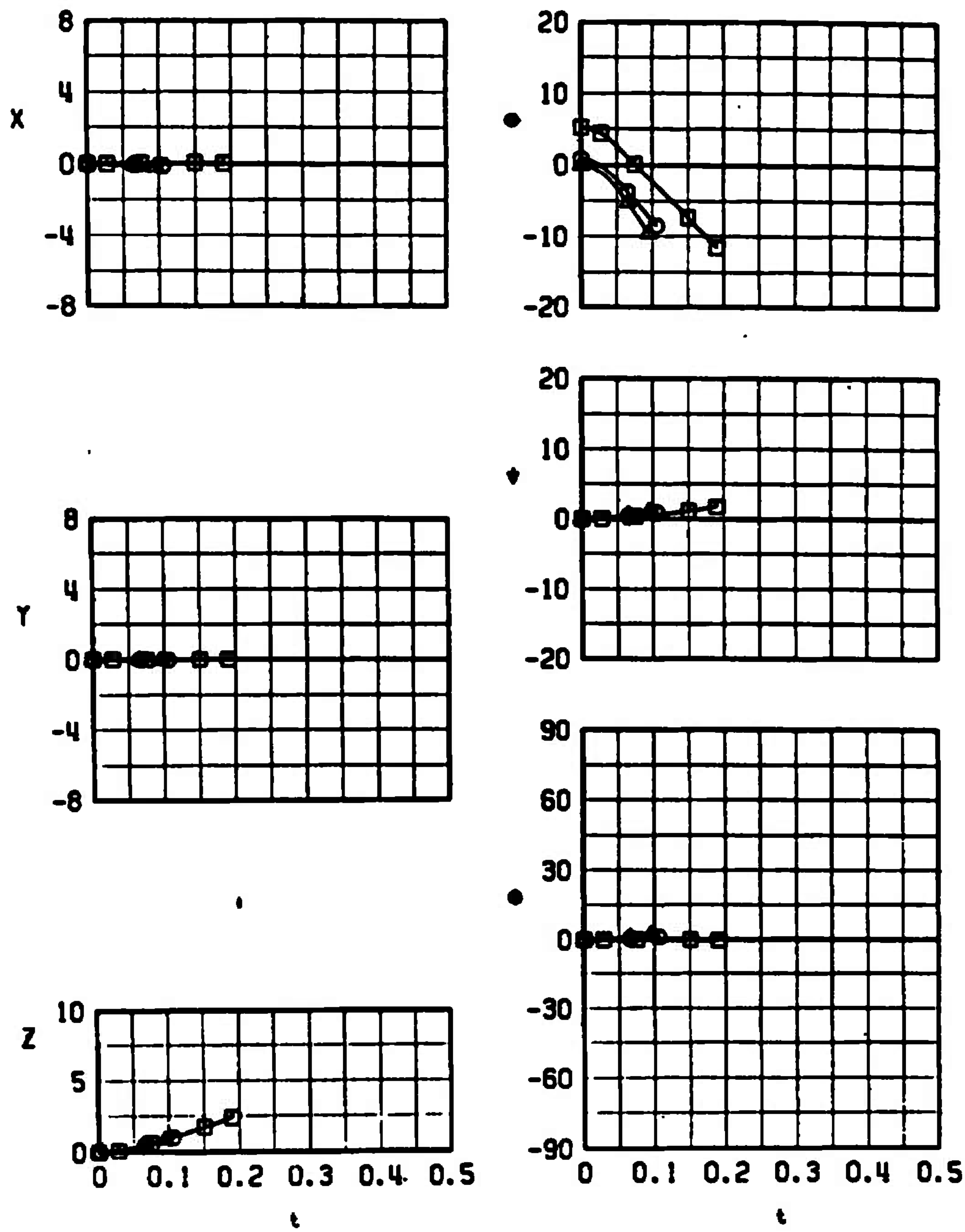

Fig. 21 Separation Characteristics of the SUU-25C/A Dispenser (Full) from the Outboard Pylon, Configuration 2R

SYMBOL	CONF	M_∞	α	H	$\dot{\theta}$	EJECTOR FORCE
□	3R	0.730	3.4	4000	0	5
○*	3R	0.780	2.2	7000	-70	5
◁*	3R	0.860	2.1	7000	-70	5
▽*	3R	0.950	2.0	7000	-70	5

*FINS DEPLOYED AT Z = 1.0 FT

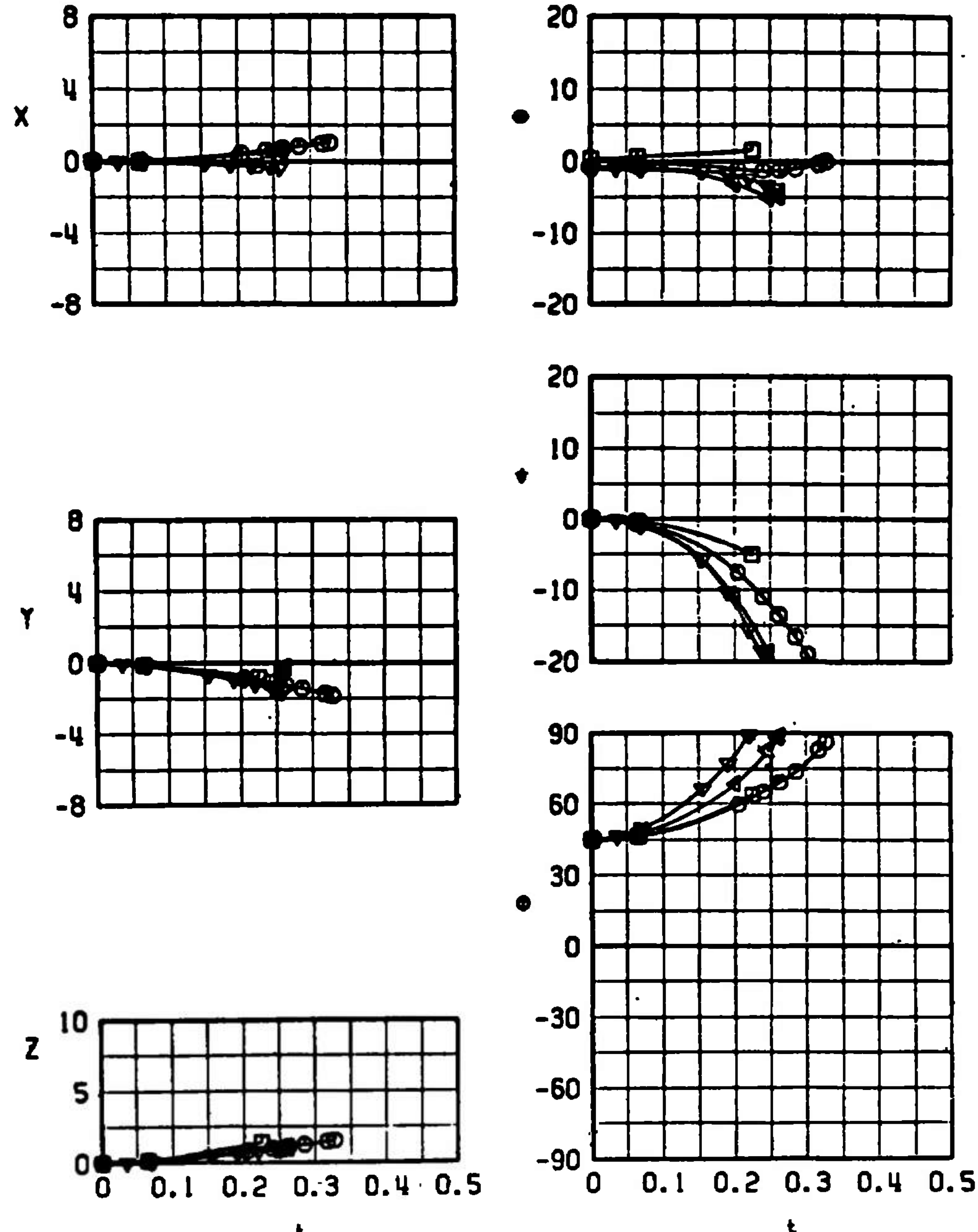

a. Configuration 3R

Fig. 22 Separation Characteristics of the MK-20 Rockeye Bomb from the MER on the Center Pylon Station; Inboard Pylon Empty and MER on the Outboard Pylon

SYMBOL	CONF	M_∞	α	H	$\bar{\theta}$	EJECTOR FORCE
◁*	4R	0.860	2.1	7000	-70	5
▽*	4R	0.950	2.0	7000	-70	5

*FINS DEPLOYED AT Z = 1.0 FT

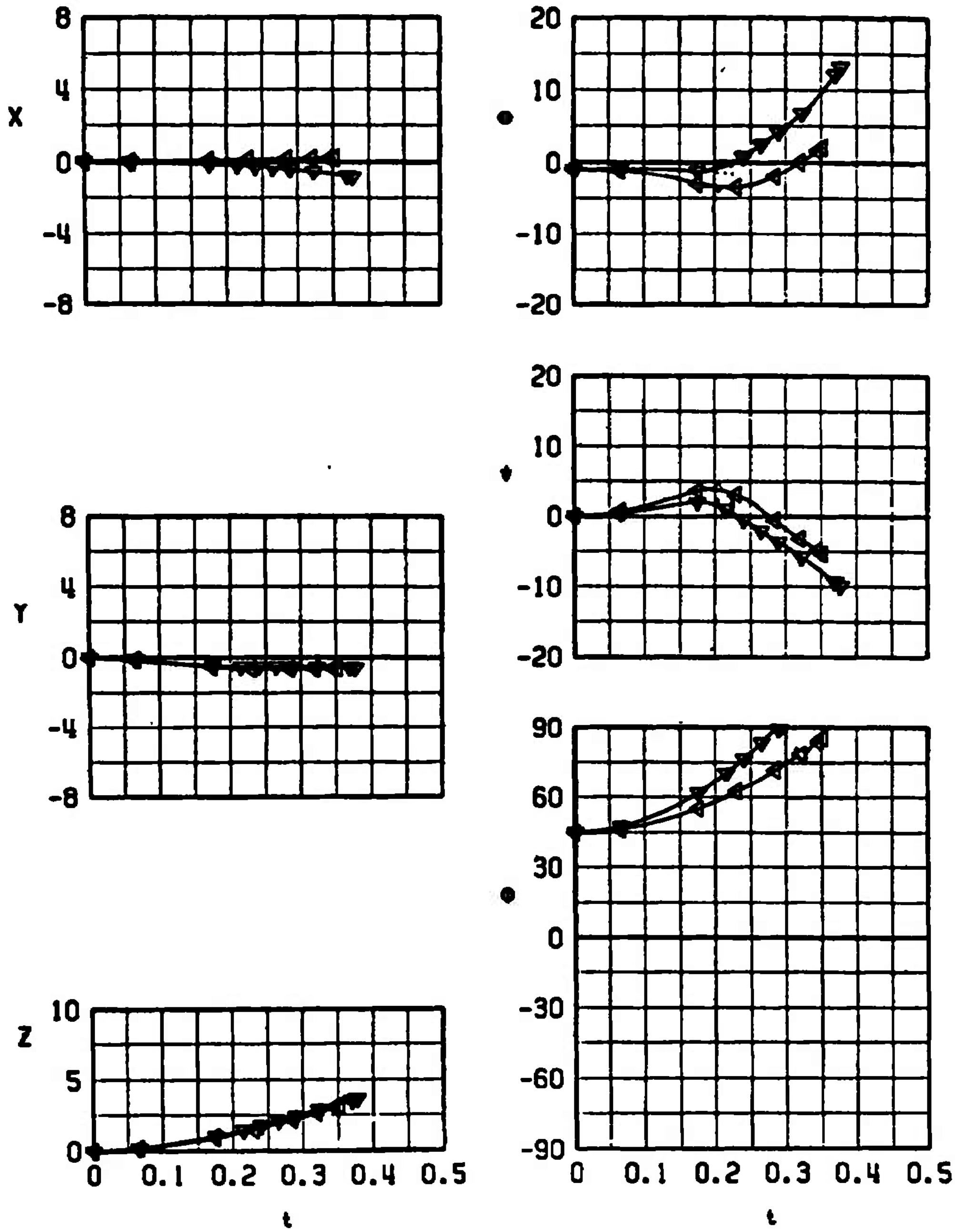

b. Configuration 4R
Fig. 22 Continued

SYMBOL	CONF	M_∞	α	H	$\bar{\phi}$	EJECTOR FORCE
□	5R	0.730	3.4	4000	0	5
○	5R	0.780	2.2	7000	-70	5
◁	5R	0.860	2.1	7000	-70	5
▽	5R	0.950	2.0	7000	-70	5

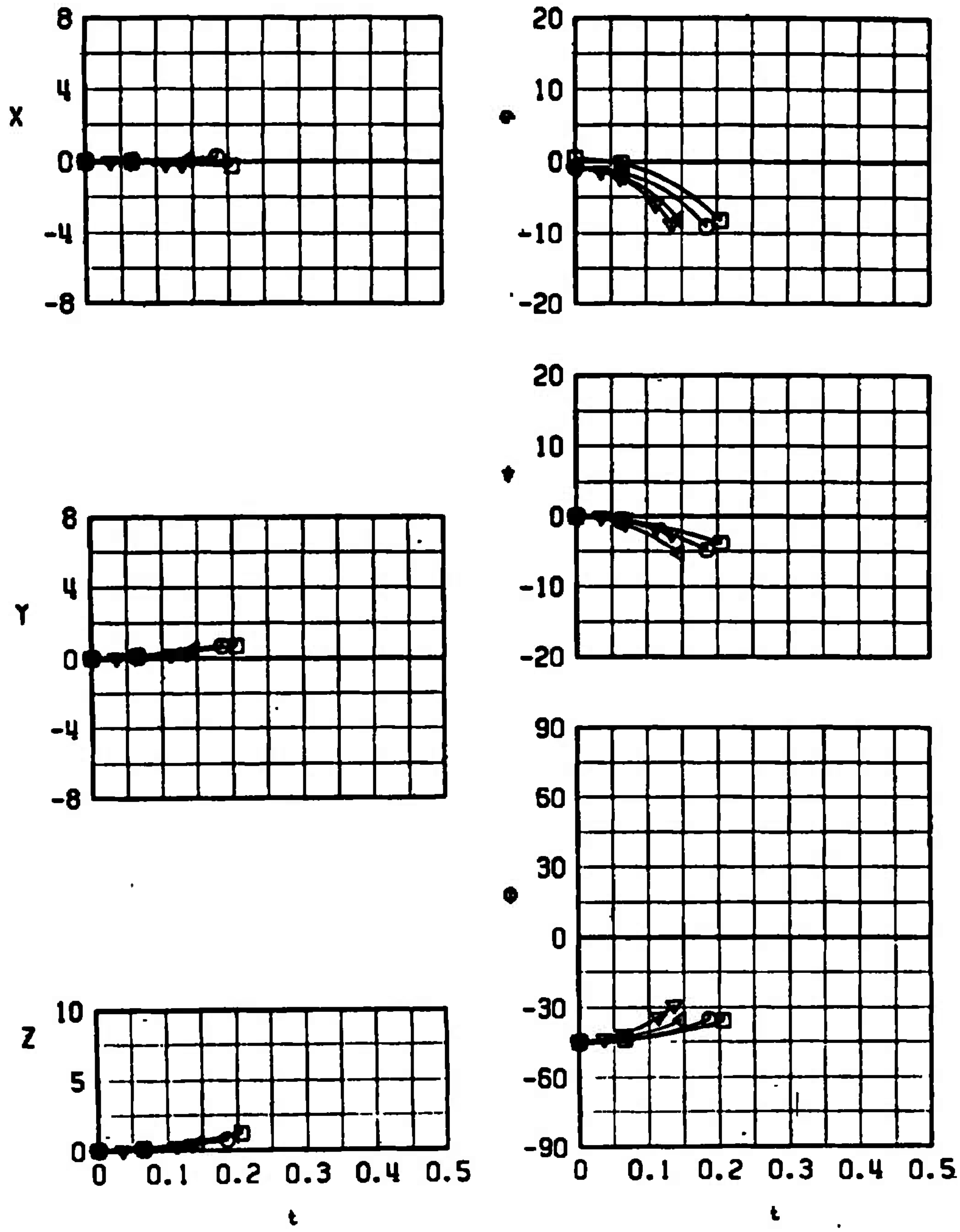

c. Configuration 5R
Fig. 22 Continued

SYMBOL	CONF	M_∞	α	H	δ	EJECTOR FORCE
□	6R	0.730	3.4	4000	0	5
○*	6R	0.780	2.2	7000	-70	5
◁*	6R	0.860	2.1	7000	-70	5
▽*	6R	0.950	2.0	7000	-70	5

*FINS DEPLOYED AT Z = 1.0 FT

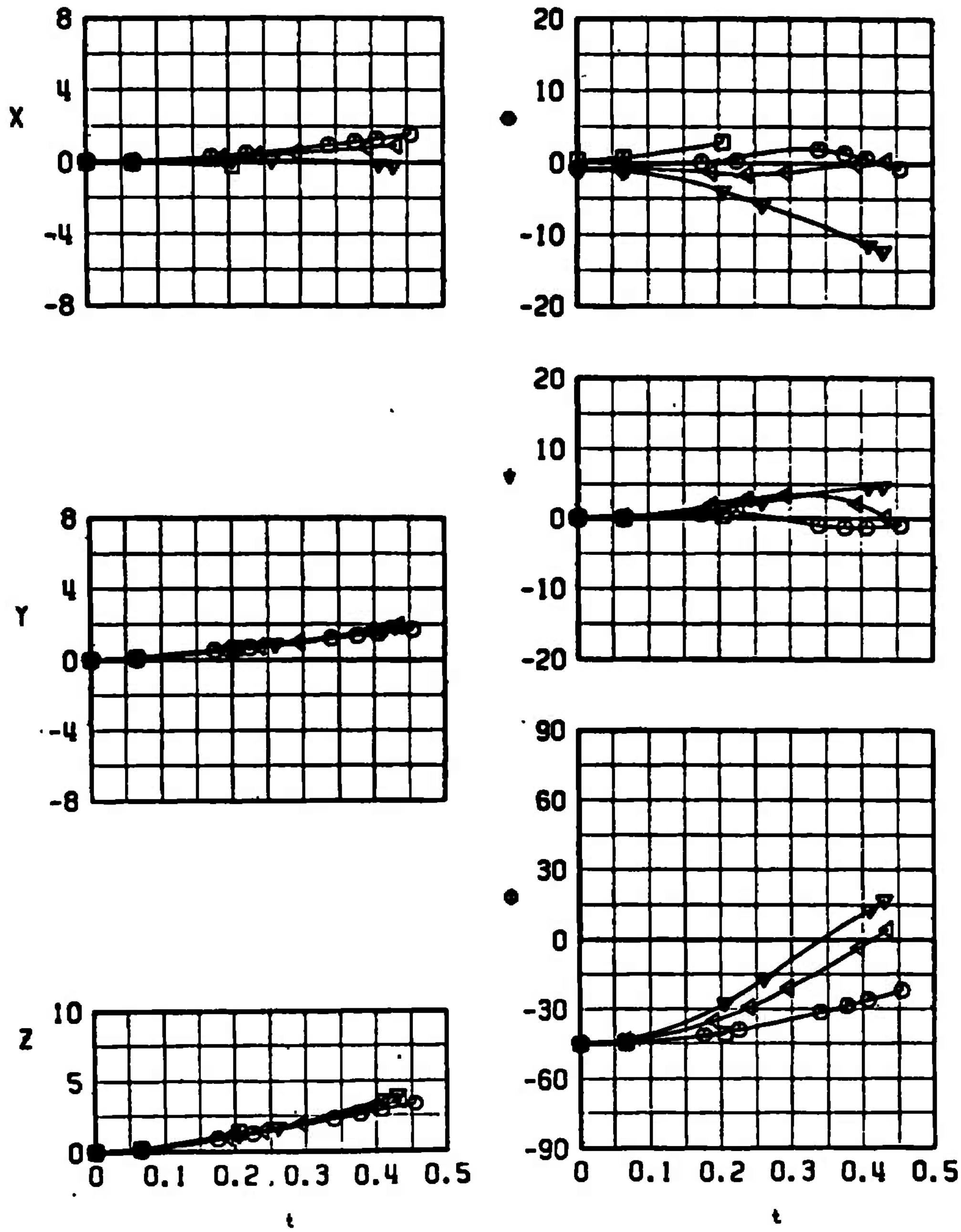

d. Configuration 6R
Fig. 22 Continued

SYMBOL	CONF	M_∞	α	H	$\bar{\theta}$	EJECTOR FORCE
□	7R	0.730	3.4	4000	0	5
▽*	7R	0.950	2.0	7000	-70	5

*FINS DEPLOYED AT Z = 1.0 FT

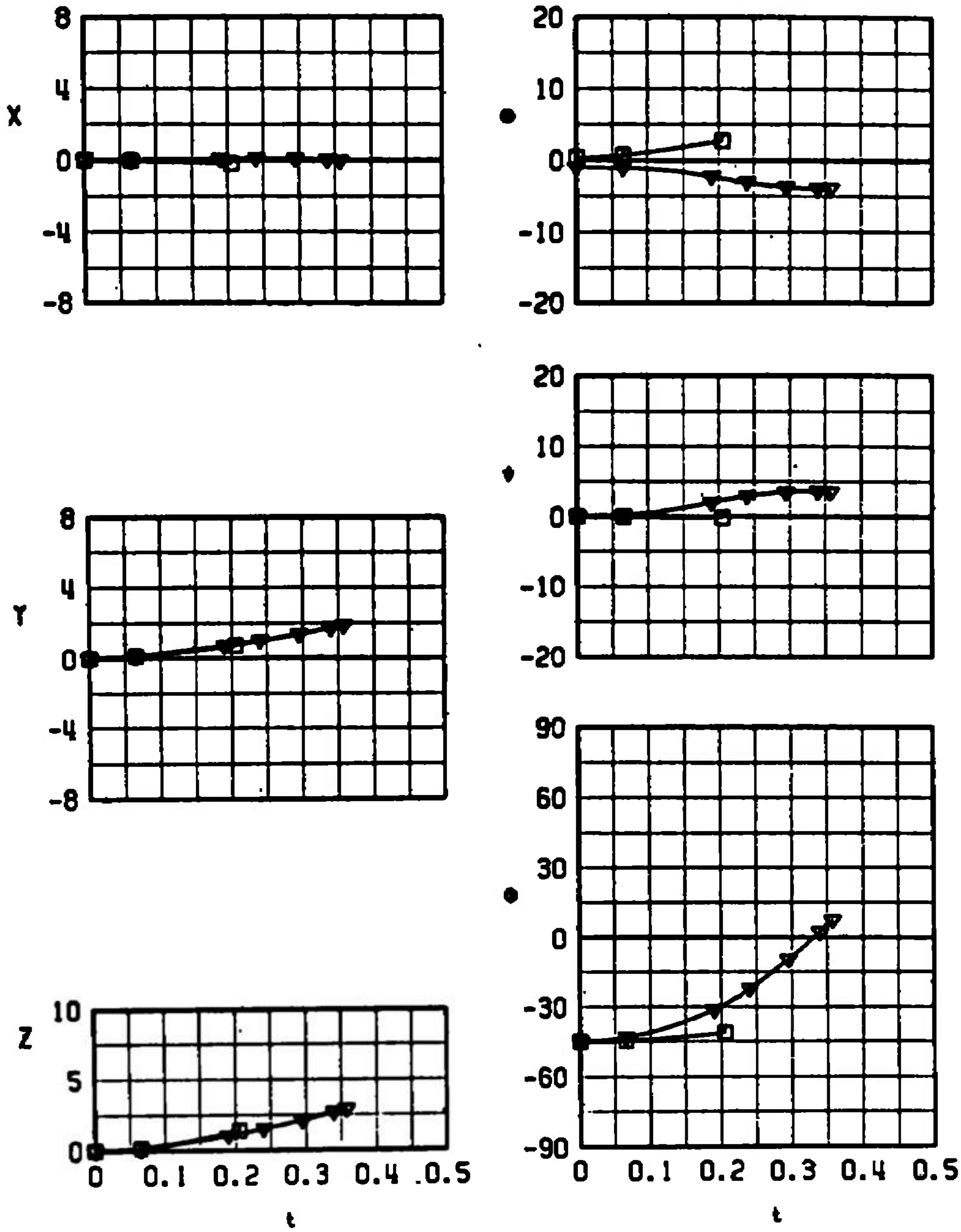

e. Configuration 7R
Fig. 22 Continued

SYMBOL	CONF	M_∞	α	H	$\bar{\phi}$	EJECTOR FORCE
□	8R	0.730	3.4	4000	0	5
◁	8R	0.860	2.1	7000	-70	5
▽	8R	0.950	2.0	7000	-70	5

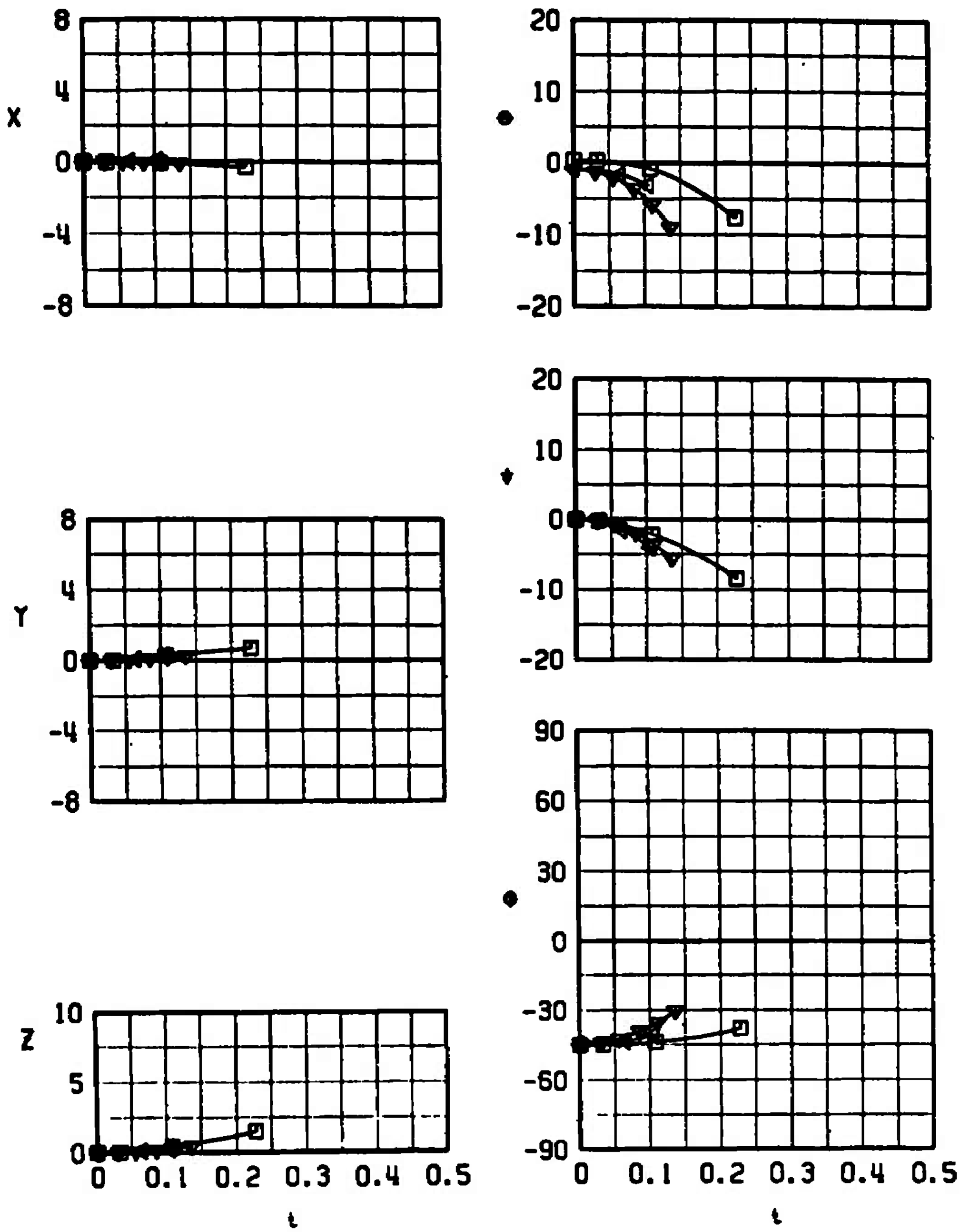

f. Configuration 8R
Fig. 22 Continued

SYMBOL	CONF	M_∞	α	H	$\bar{\theta}$	EJECTOR FORCE
□	9R	0.730	3.4	4000	0	S
○	9R	0.780	2.2	7000	-70	S
◁*	9R	0.860	2.1	7000	-70	S
▽*	9R	0.950	2.0	7000	-70	S

*FINS DEPLOYED AT Z = 1.0 FT

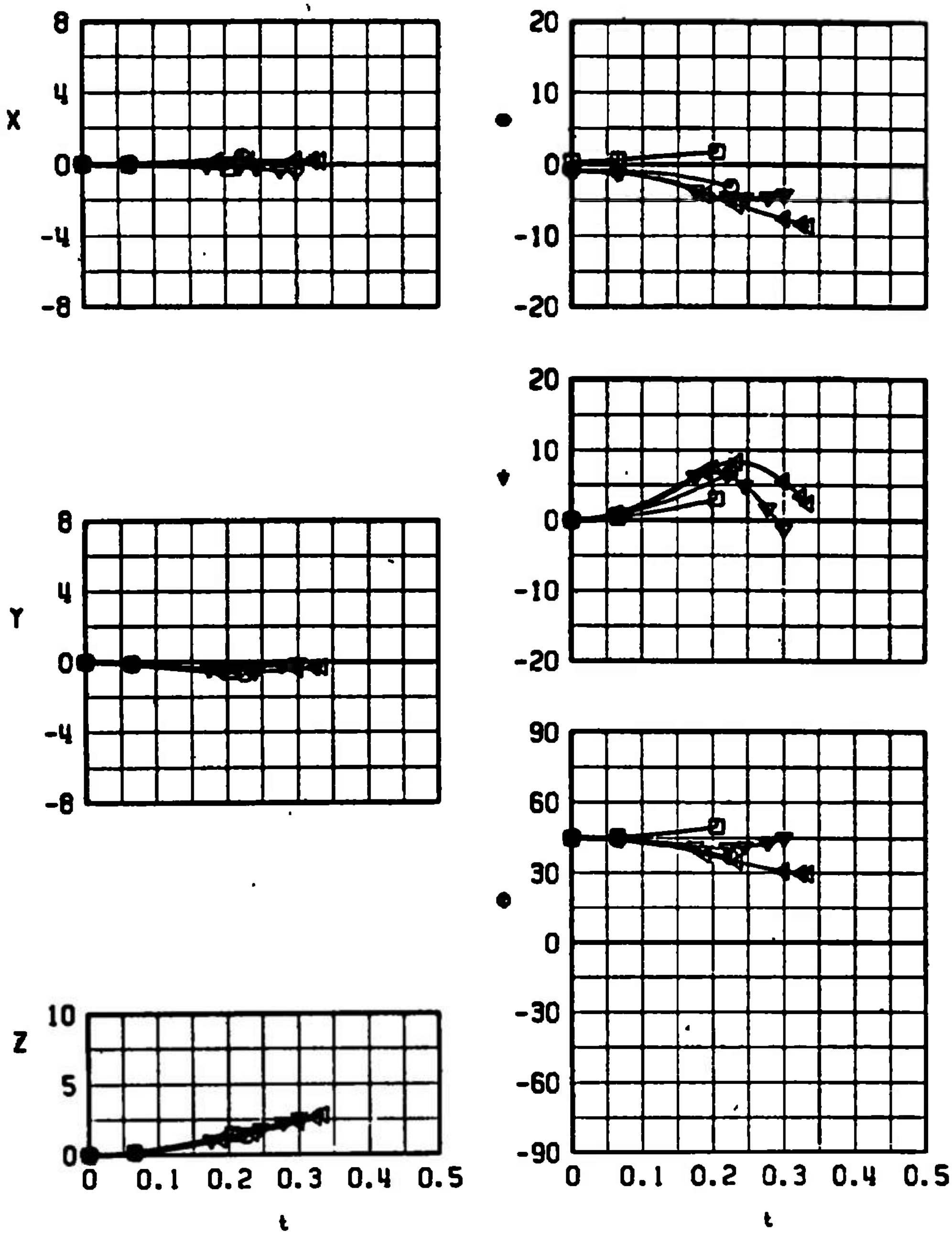

g. Configuration 9R
Fig. 22 Continued

SYMBOL	CONF	M_∞	α	H	$\bar{\theta}$	EJECTOR FORCE
⊙	10R	0.780	2.2	7000	-70	5
◁	10R	0.860	2.1	7000	-70	5
▽	10R	0.950	2.0	7000	-70	5

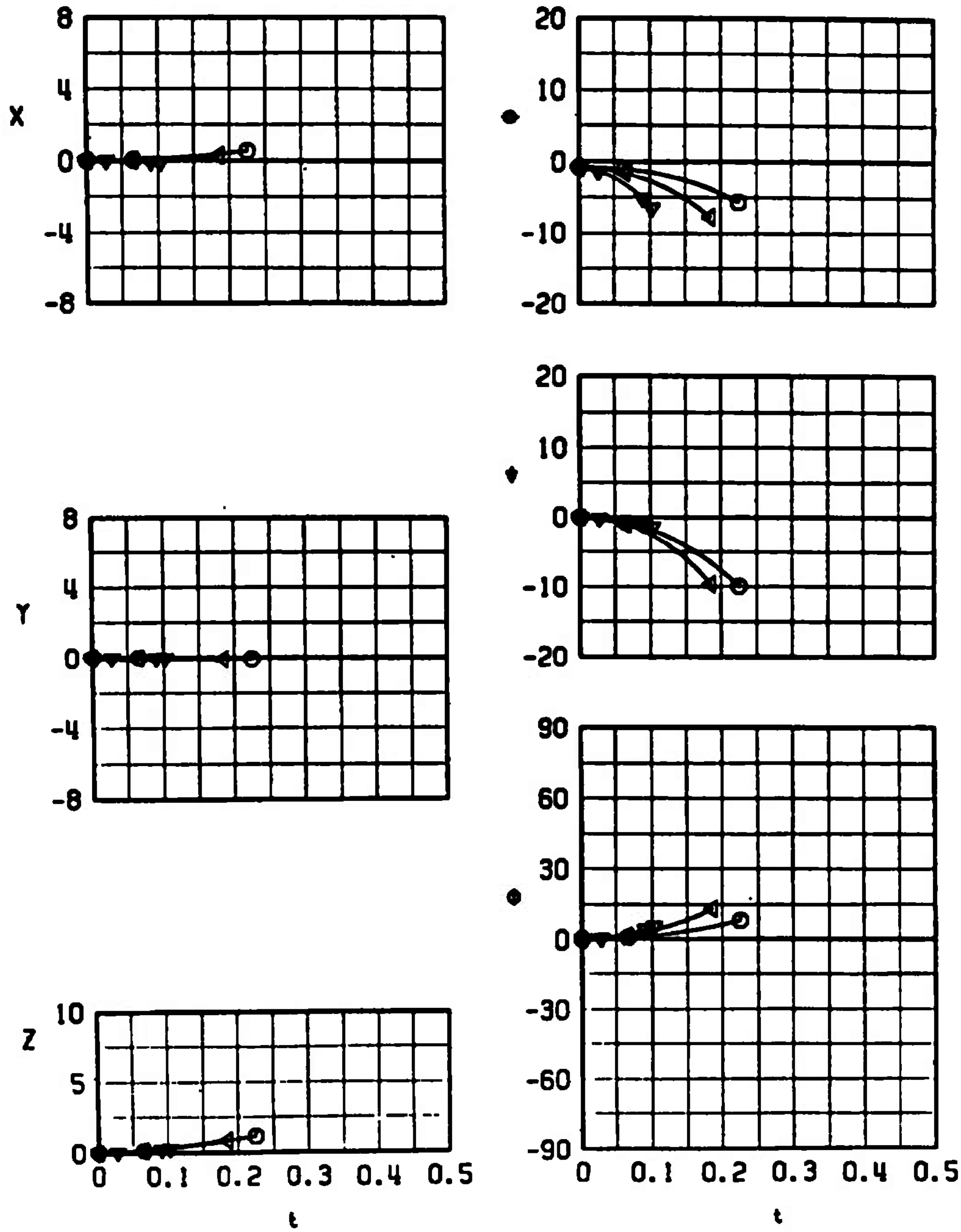

h. Configuration 10R
Fig. 22 Continued

SYMBOL	CONF	M_∞	α	H	$\bar{\theta}$	EJECTOR FORCE
⊙*	11R	0.780	2.2	7000	-70	5
◁*	11R	0.860	2.1	7000	-70	5
▽*	11R	0.950	2.0	7000	-70	5

*FINS DEPLOYED AT Z = 1.0 FT

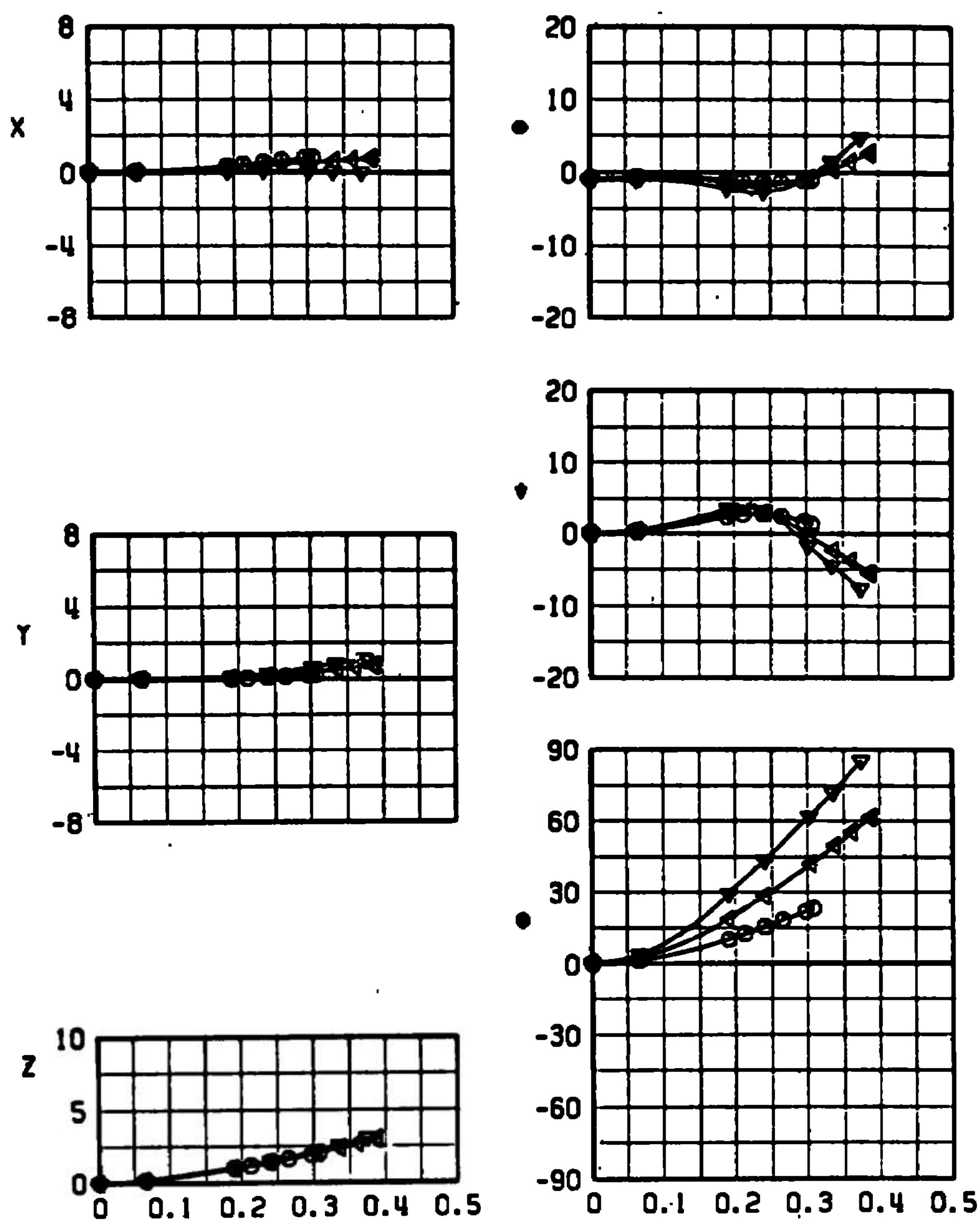

i. Configuration 11R
Fig. 22 Continued

SYMBOL	CONF	M_∞	α	H	θ	EJECTOR FORCE
⊙	12R	0.780	2.2	7000	-70	5
◁	12R	0.860	2.1	7000	-70	5
▽	12R	0.950	2.0	7000	-70	5

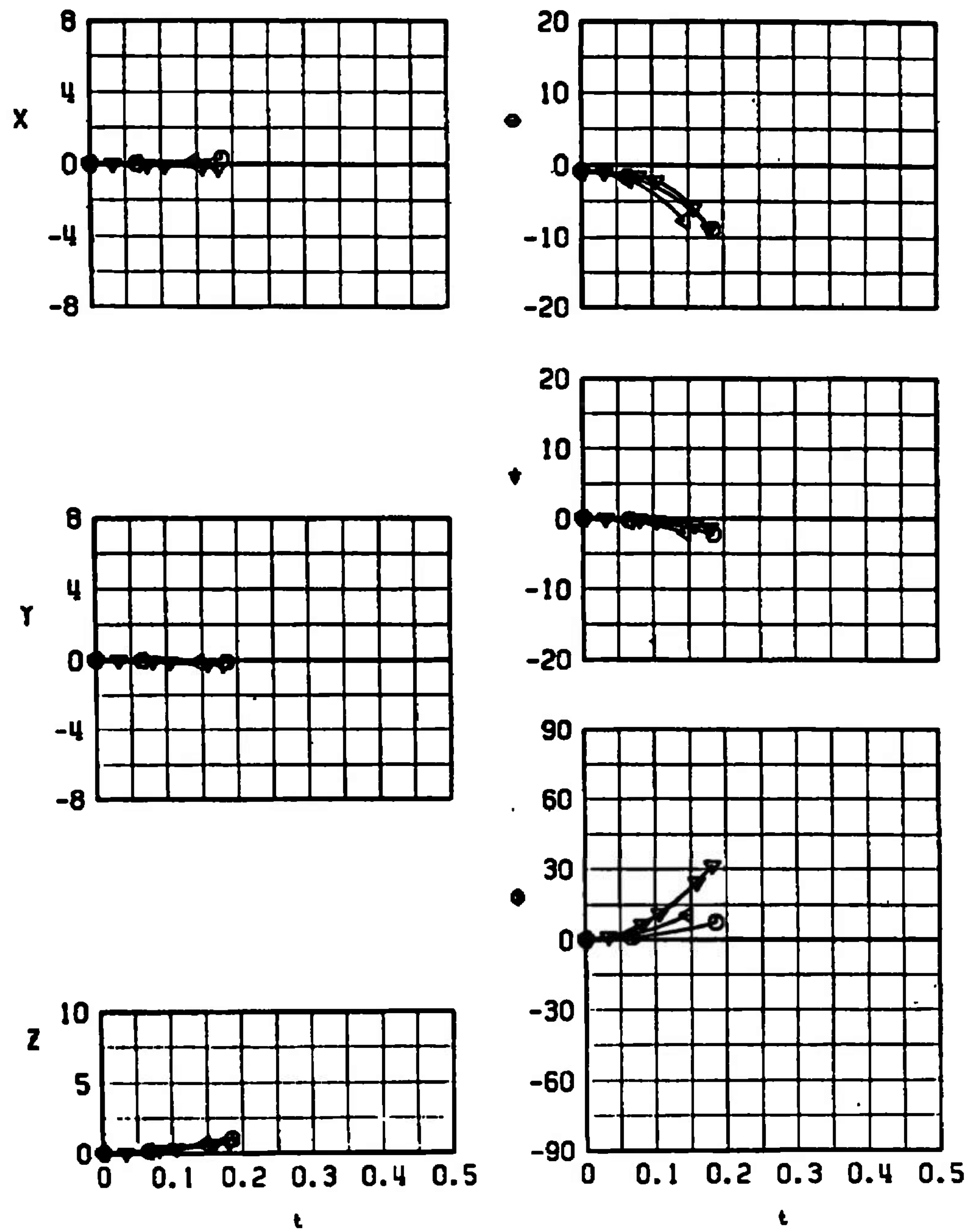

j. Configuration 12R
Fig. 22 Concluded

SYMBOL	CONF	M_∞	α	H	$\bar{\phi}$	EJECTOR FORCE
□	3L	0.730	3.4	4000	0	5
○	3L	0.780	2.2	7000	-70	5
◁	3L	0.860	2.1	7000	-70	5
▽	3L	0.950	2.0	7000	-70	5

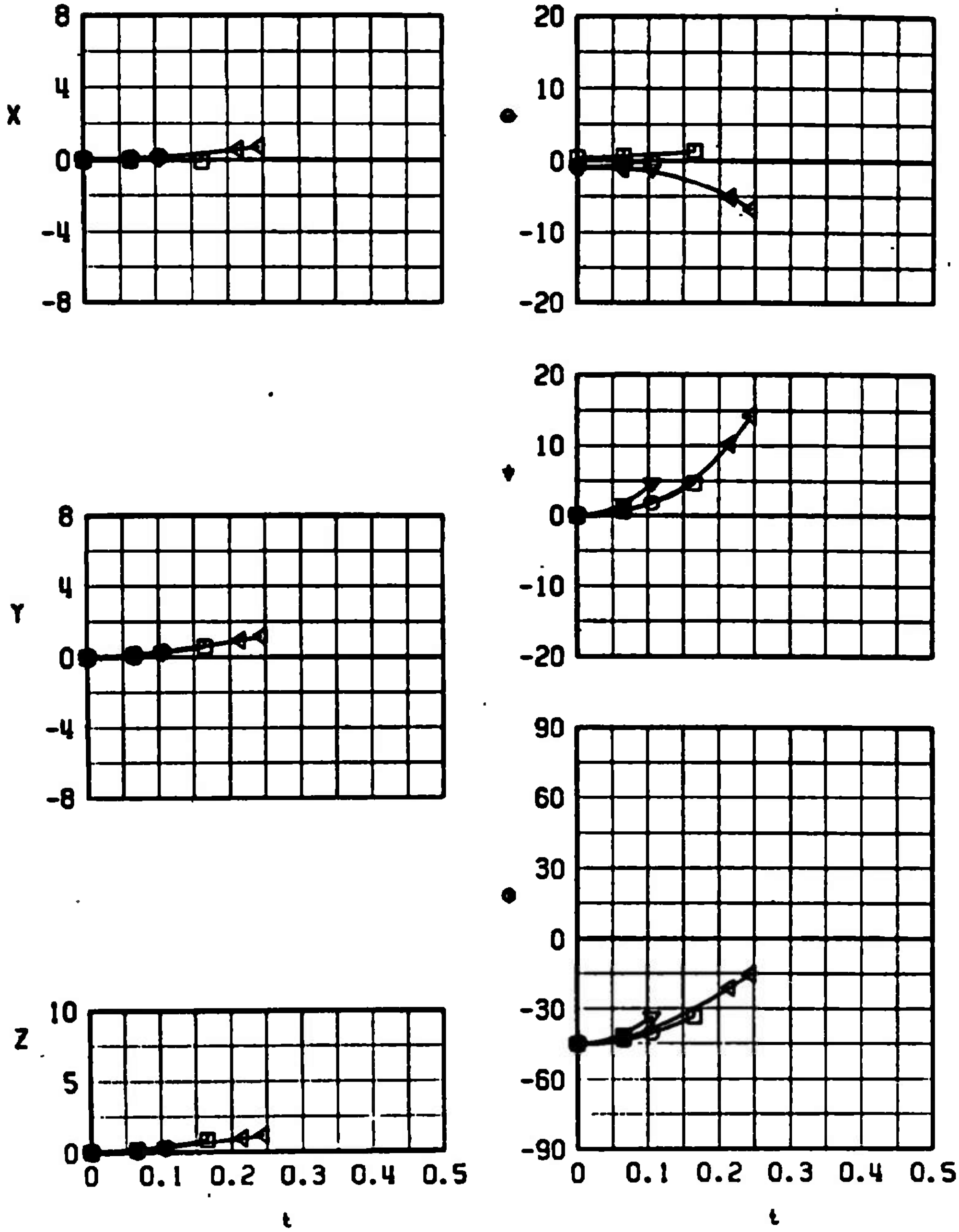

a. Configuration 3L

Fig. 23 Separation Characteristics of the MK-20 Rockeye Bomb from the MER on the Outboard Pylon Station; Inboard Pylon Empty and MER with Six MK-20 Bombs on Center Pylon

SYMBOL	CONF	M_∞	α	H	$\bar{\theta}$	EJECTOR FORCE
□	4L	0.730	3.4	4000	0	5
○*	4L	0.780	2.2	7000	-70	5
▽*	4L	0.950	2.0	7000	-70	5

*FINS DEPLOYED AT Z = 1.0 FT

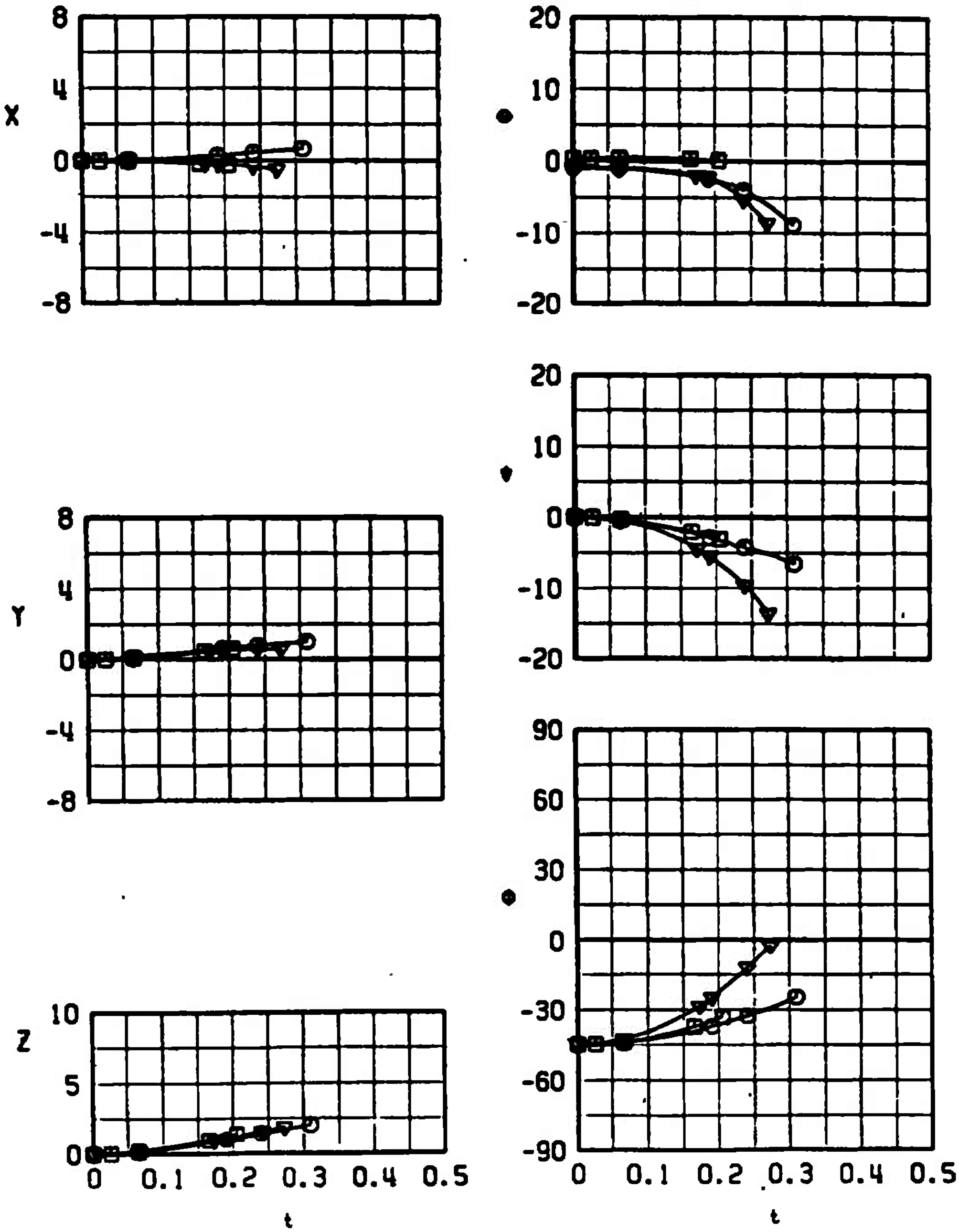

b. Configuration 4L
Fig. 23 Continued

SYMBOL	CONF	M_∞	α	H	$\bar{\theta}$	EJECTOR FORCE
○*	5L	0.780	2.2	7000	-70	5
◁*	5L	0.860	2.1	7000	-70	5
▽	5L	0.950	2.0	7000	-70	5

*FINS DEPLOYED AT Z = 1.0 FT

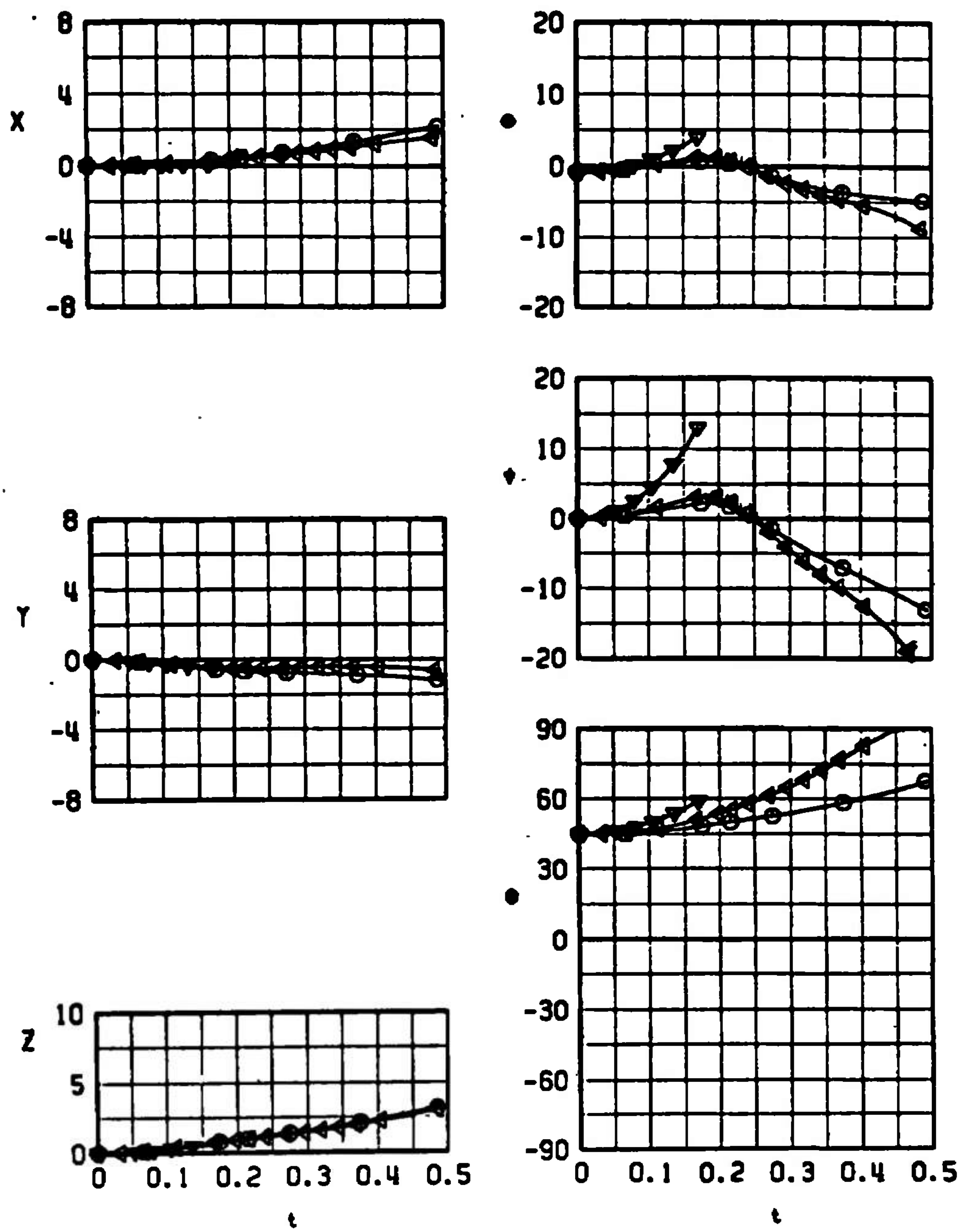

c. Configuration 5L
Fig. 23 Continued

SYMBOL	CONF	M_∞	α	H	$\bar{\theta}$	EJECTOR FORCE
□	6L	0.730	3.4	4000	0	5
○	6L	0.780	2.2	7000	-70	5
◁*	6L	0.860	2.1	7000	-70	5
▽*	6L	0.950	2.0	7000	-70	5

*FINS DEPLOYED AT Z = 1.0 FT

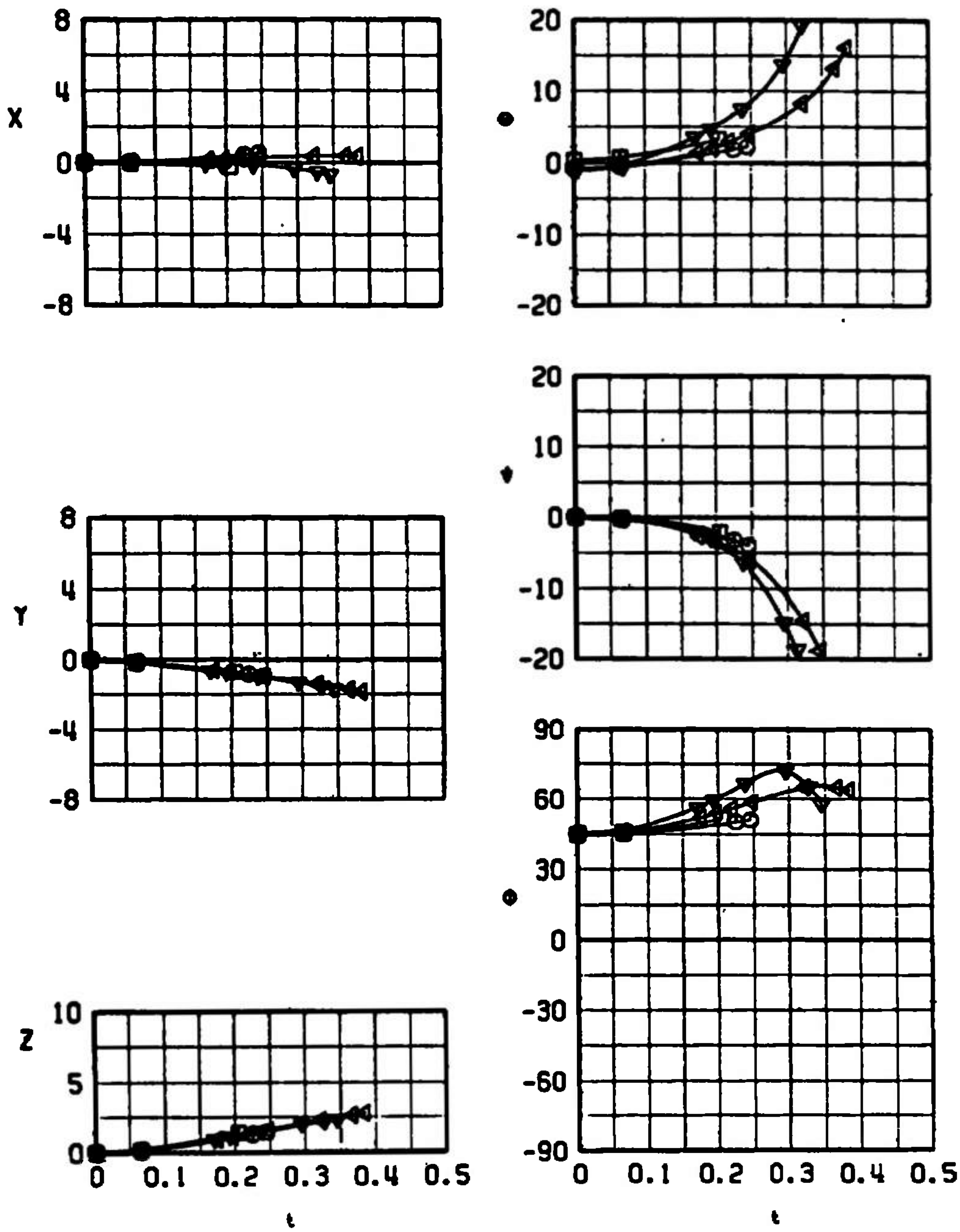

d. Configuration 6L
Fig. 23 Continued

SYMBOL	CONF	M_∞	α	H	$\bar{\theta}$	EJECTOR FORCE
□	7L	0.730	3.4	4000	0	5
○*	7L	0.780	2.2	7000	-70	5
◁	7L	0.860	2.1	7000	-70	5
▽*	7L	0.950	2.0	7000	-70	5

*FINS DEPLOYED AT Z = 1.0 FT

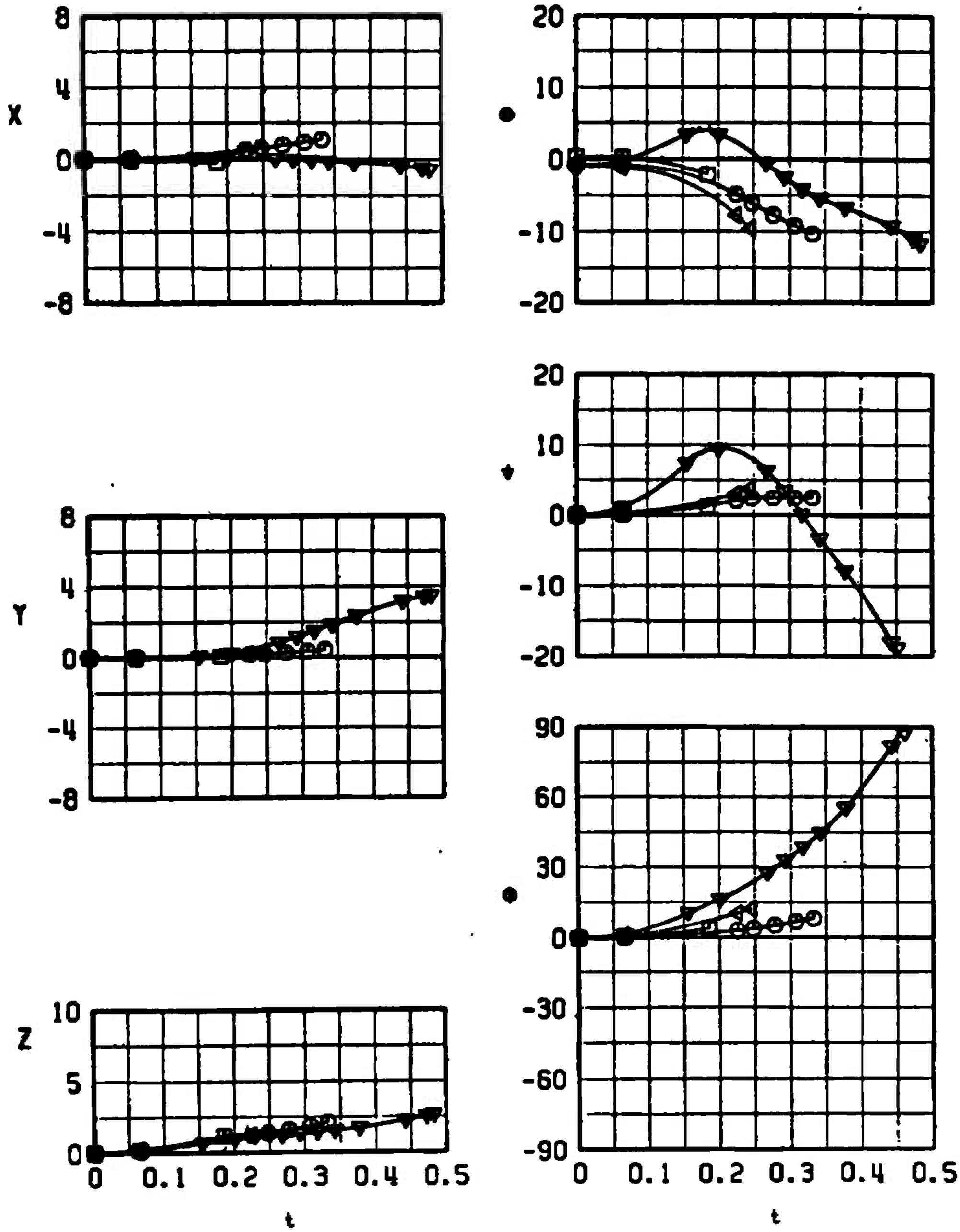

e. Configuration 7L
Fig. 23 Continued

SYMBOL	CONF	M_∞	α	H	$\bar{\theta}$	EJECTOR FORCE
□	8L	0.730	3.4	4000	0	5
○	8L	0.780	2.2	7000	-70	5
◁	8L	0.860	2.1	7000	-70	5
▽	8L	0.950	2.0	7000	-70	5

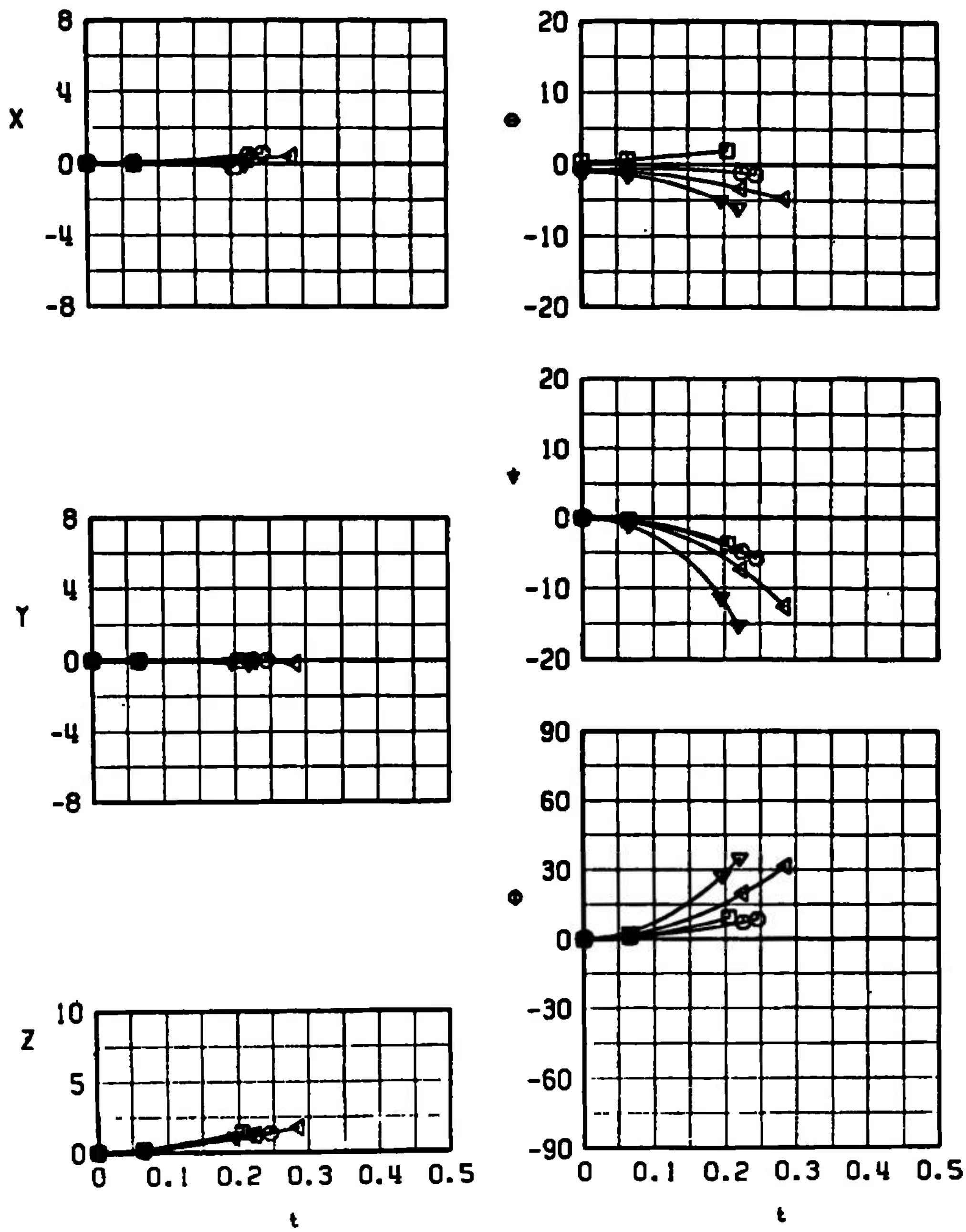

f. Configuration 8L
Fig. 23 Continued

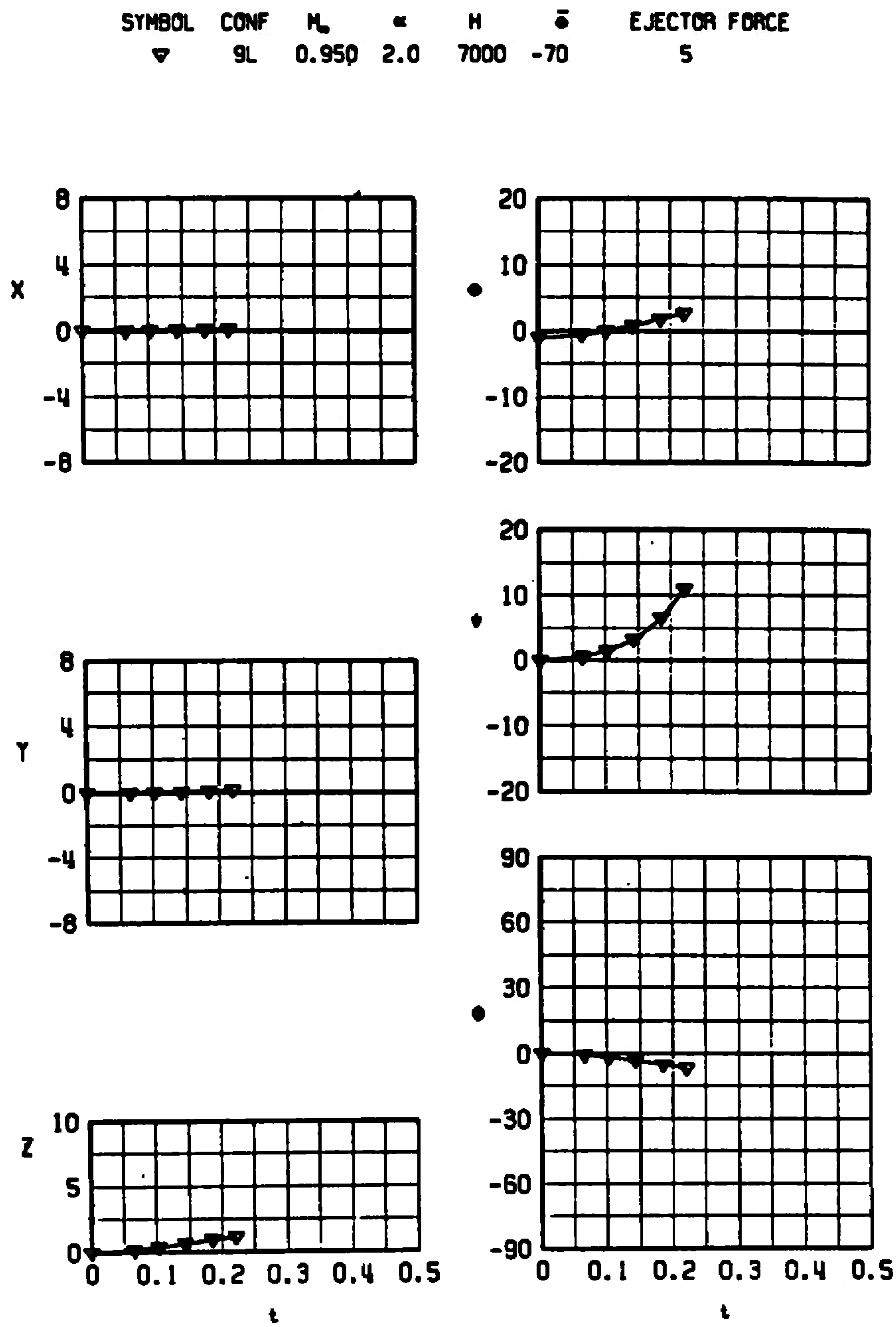

g. Configuration 9L
Fig. 23 Continued

SYMBOL	CONF	M_∞	α	H	$\bar{\theta}$	EJECTOR FORCE
◁*	10L	0.860	2.1	7000	-70	5
▽*	10L	0.950	2.0	7000	-70	5

*FINS DEPLOYED AT Z = 1.0 FT

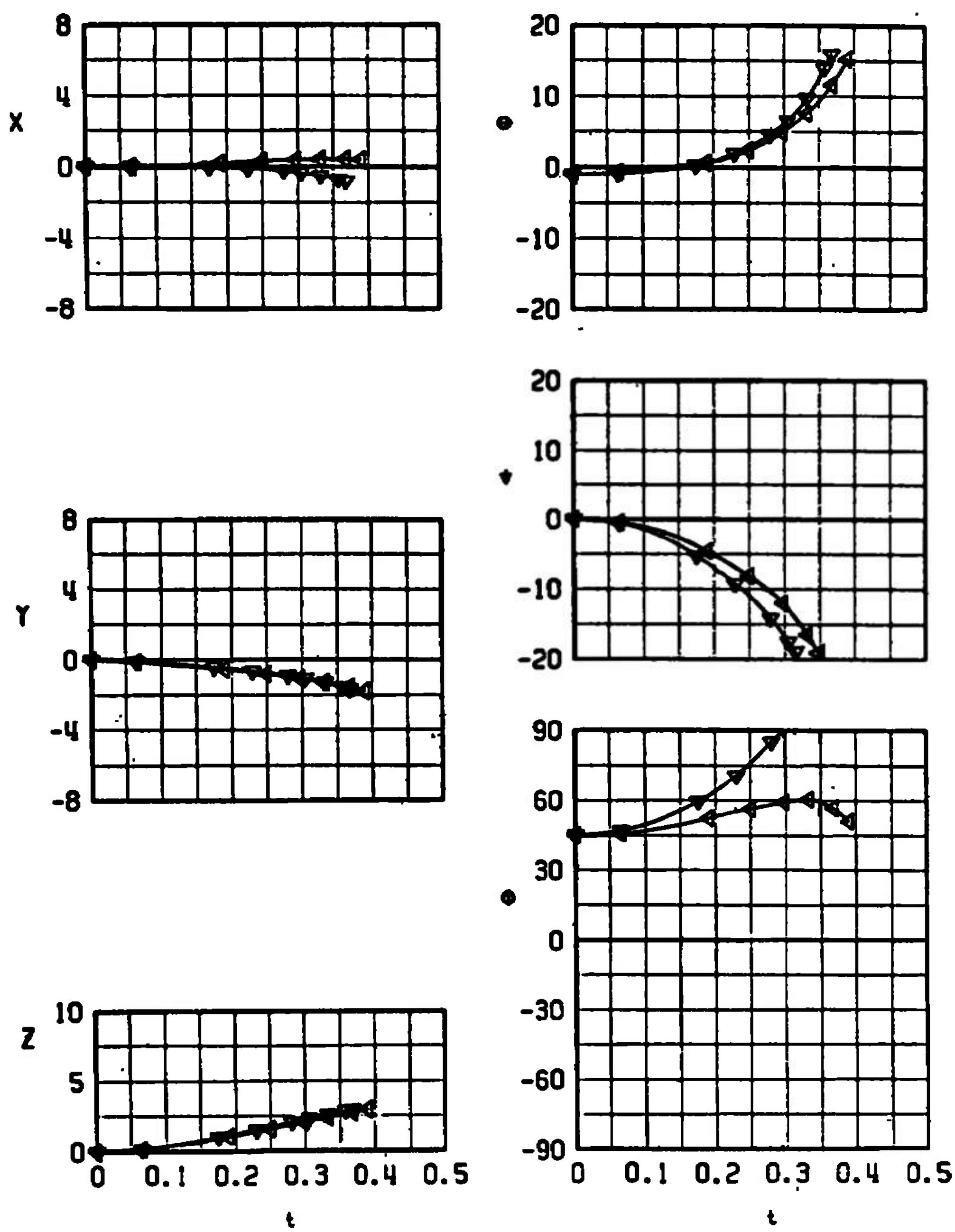

h. Configuration 10L
Fig. 23 Continued

SYMBOL	CONF	M_∞	α	H	$\bar{\theta}$	EJECTOR FORCE
⊙*	11L	0.780	2.2	7000	-70	5
▽*	11L	0.950	2.0	7000	-70	5

*FINS DEPLOYED AT Z = 1.0 FT

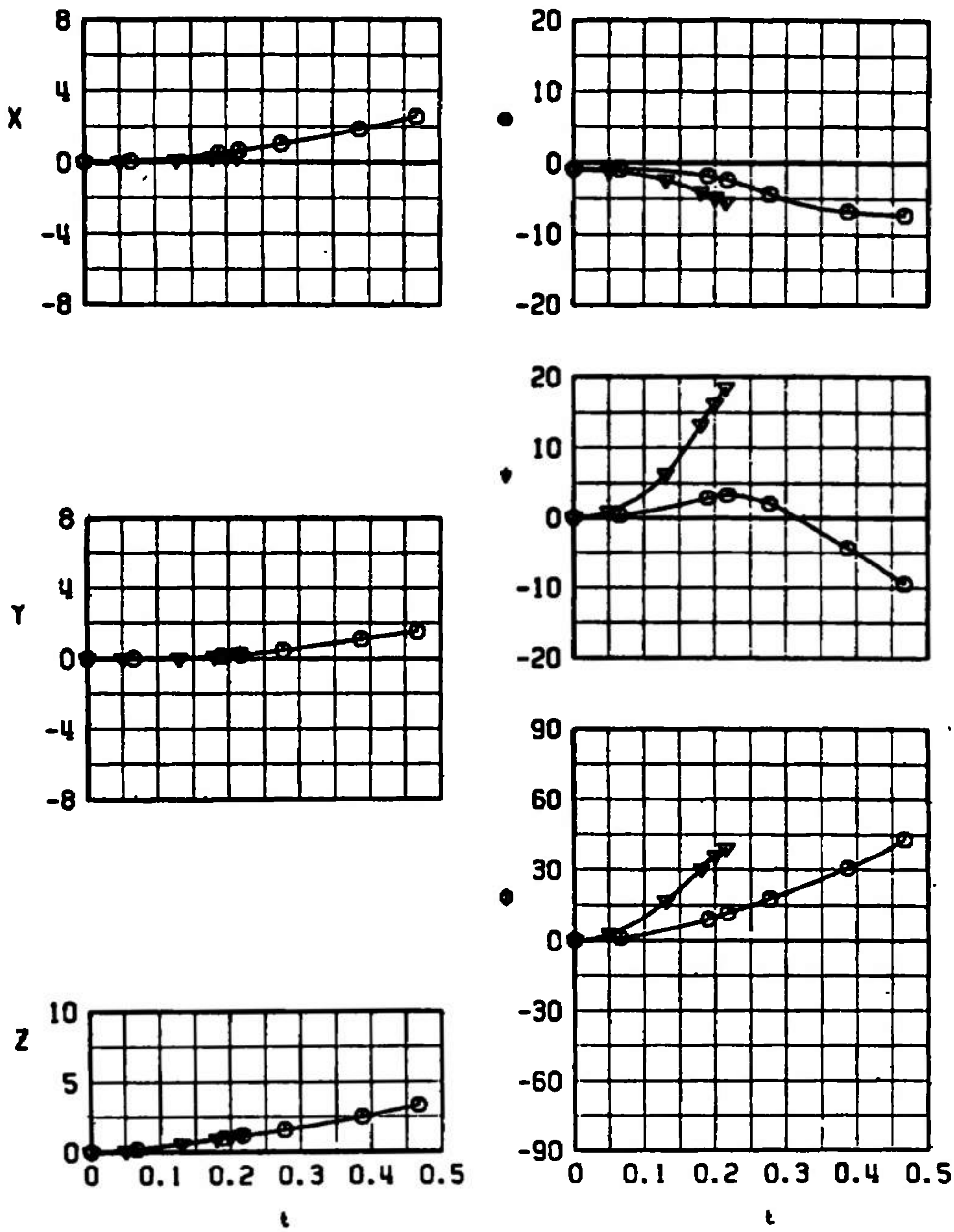

i. Configuration 11L
Fig. 23 Continued

SYMBOL	CONF	M_∞	α	H	$\bar{\theta}$	EJECTOR FORCE
○	12L	0.780	2.2	7000	-70	5
◁	12L	0.860	2.1	7000	-70	5
▽	12L	0.950	2.0	7000	-70	5

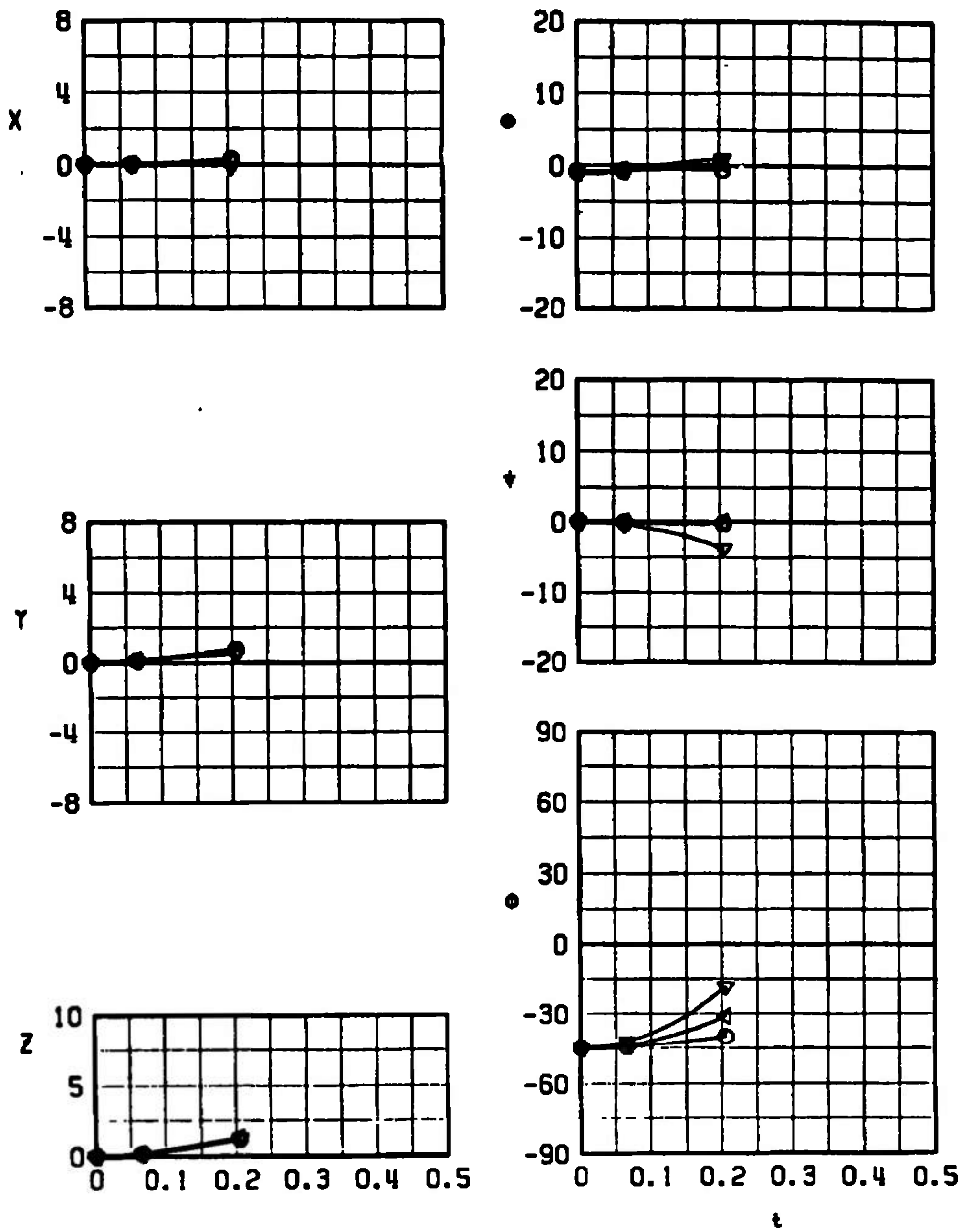

j. Configuration 12L
Fig. 23 Concluded

SYMBOL	CONF	M_∞	α	H	$\bar{\theta}$	EJECTOR FORCE
○	13R	0.780	2.2	7000	-70	5
◁	13R	0.860	2.1	7000	-70	5

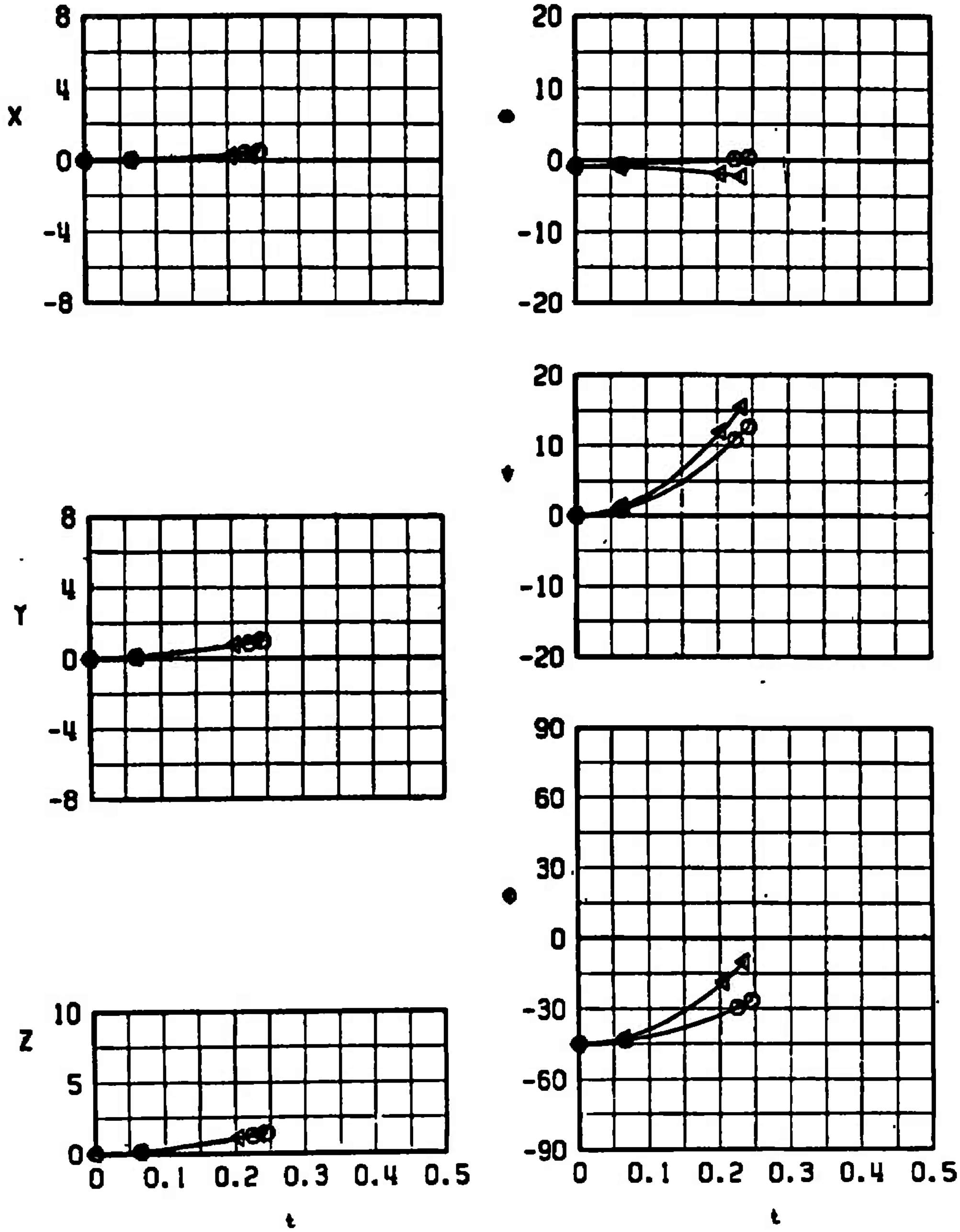

a. Configuration 13R

Fig. 24 Separation Characteristics of the MK-20 Rockeye Bomb from the MER on the Center Pylon Station; TER on the Outboard Pylon and 300-gal Fuel Tank on the Inboard Pylon

SYMBOL	CONF	M_∞	α	H	$\bar{\theta}$	EJECTOR FORCE
□	14R	0.730	3.4	4000	0	5
○	14R	0.780	2.2	7000	-70	5
◁	14R	0.860	2.1	7000	-70	5
▽	14R	0.950	2.0	7000	-70	5

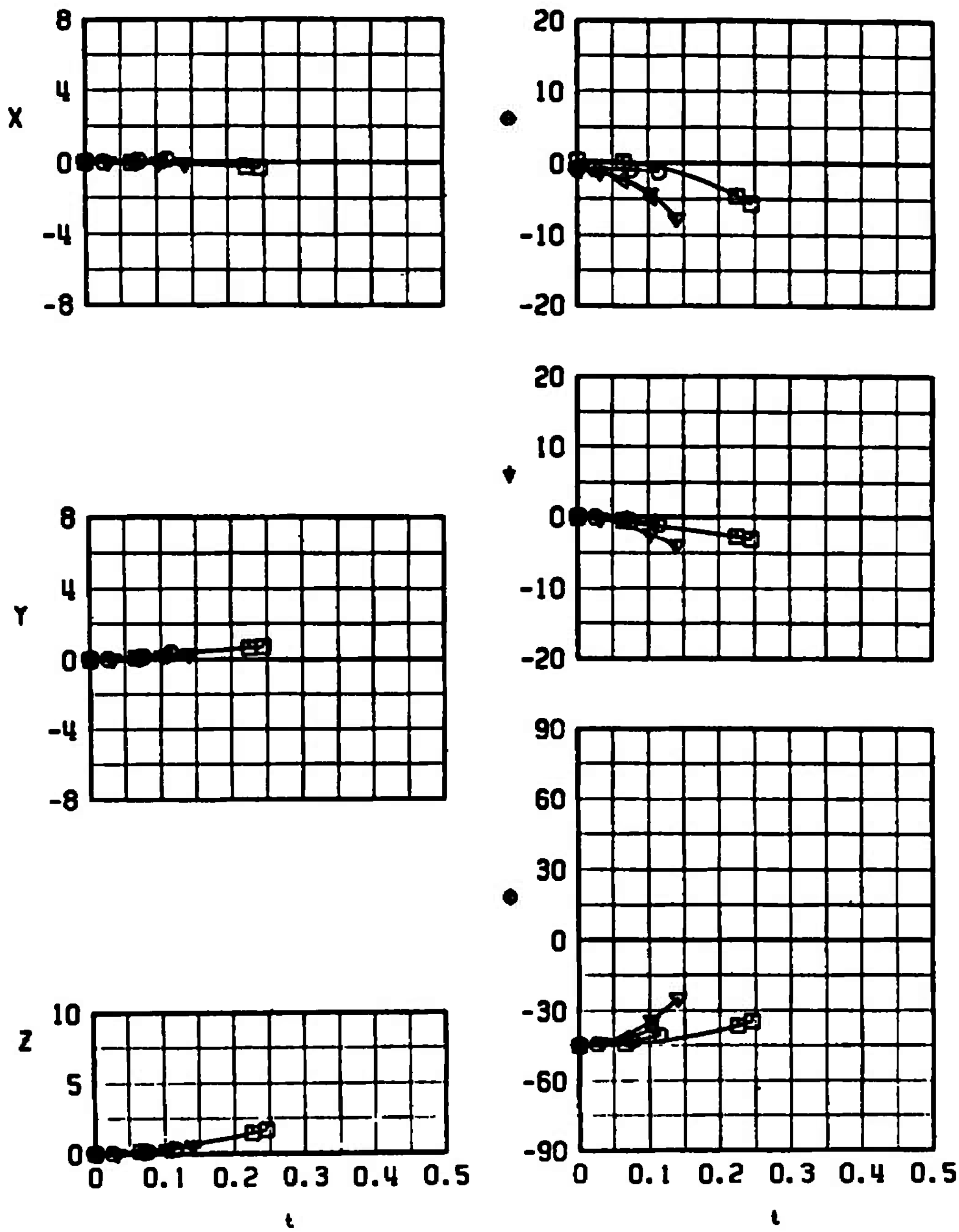

b. Configuration 14R
Fig. 24 Continued

SYMBOL	CONF	M_∞	α	H	δ	EJECTOR FORCE
□	15R	0.730	3.4	4000	0	5
◁*	15R	0.860	2.1	7000	-70	5
▽*	15R	0.950	2.0	7000	-70	5

*FINS DEPLOYED AT Z = 1.0 FT

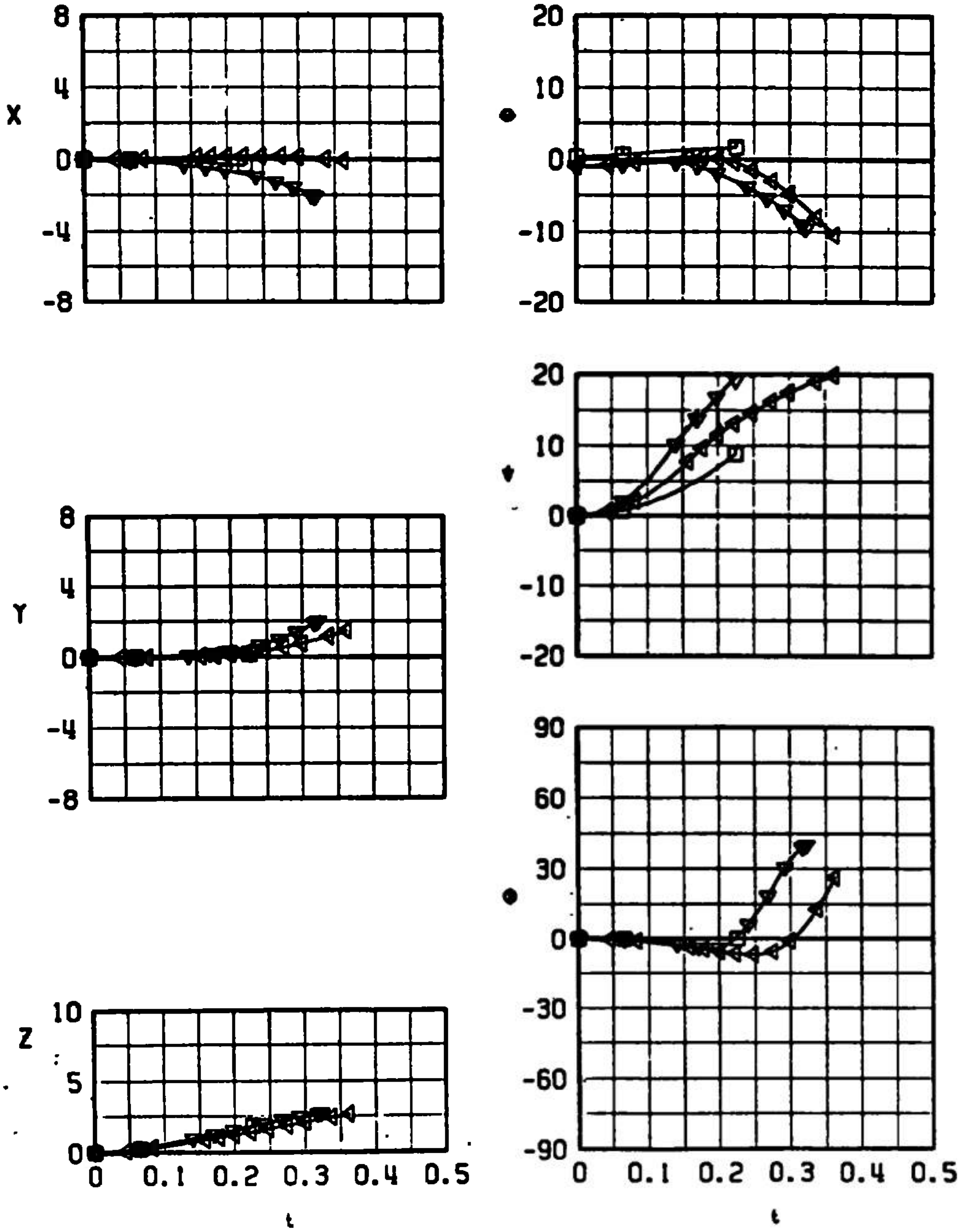

c. Configuration 15R
Fig. 24 Continued

SYMBOL	CONF	M_∞	α	H	$\bar{\theta}$	EJECTOR FORCE
□	16R	0.730	3.4	4000	0	5
○	16R	0.780	2.2	7000	-70	5
◁	16R	0.860	2.1	7000	-70	5
▽	16R	0.950	2.0	7000	-70	5

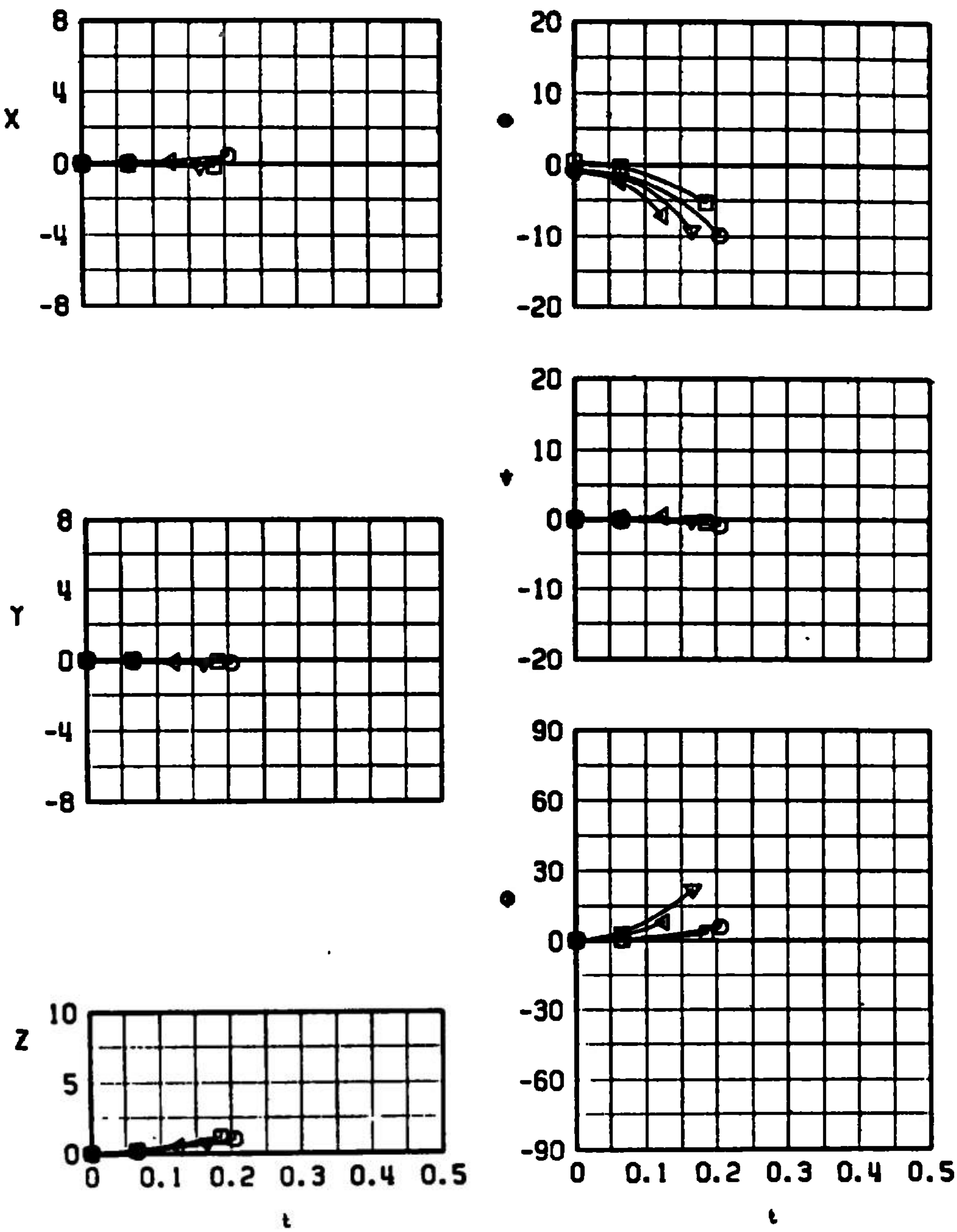

d. Configuration 16R
Fig. 24 Concluded

SYMBOL	CONF	M_∞	α	H	$\bar{\theta}$	EJECTOR FORCE
□	13L	0.730	3.4	4000	0	5
○	13L	0.780	2.2	7000	-70	5
◁	13L	0.860	2.1	7000	-70	5
▽	13L	0.950	2.0	7000	-70	5

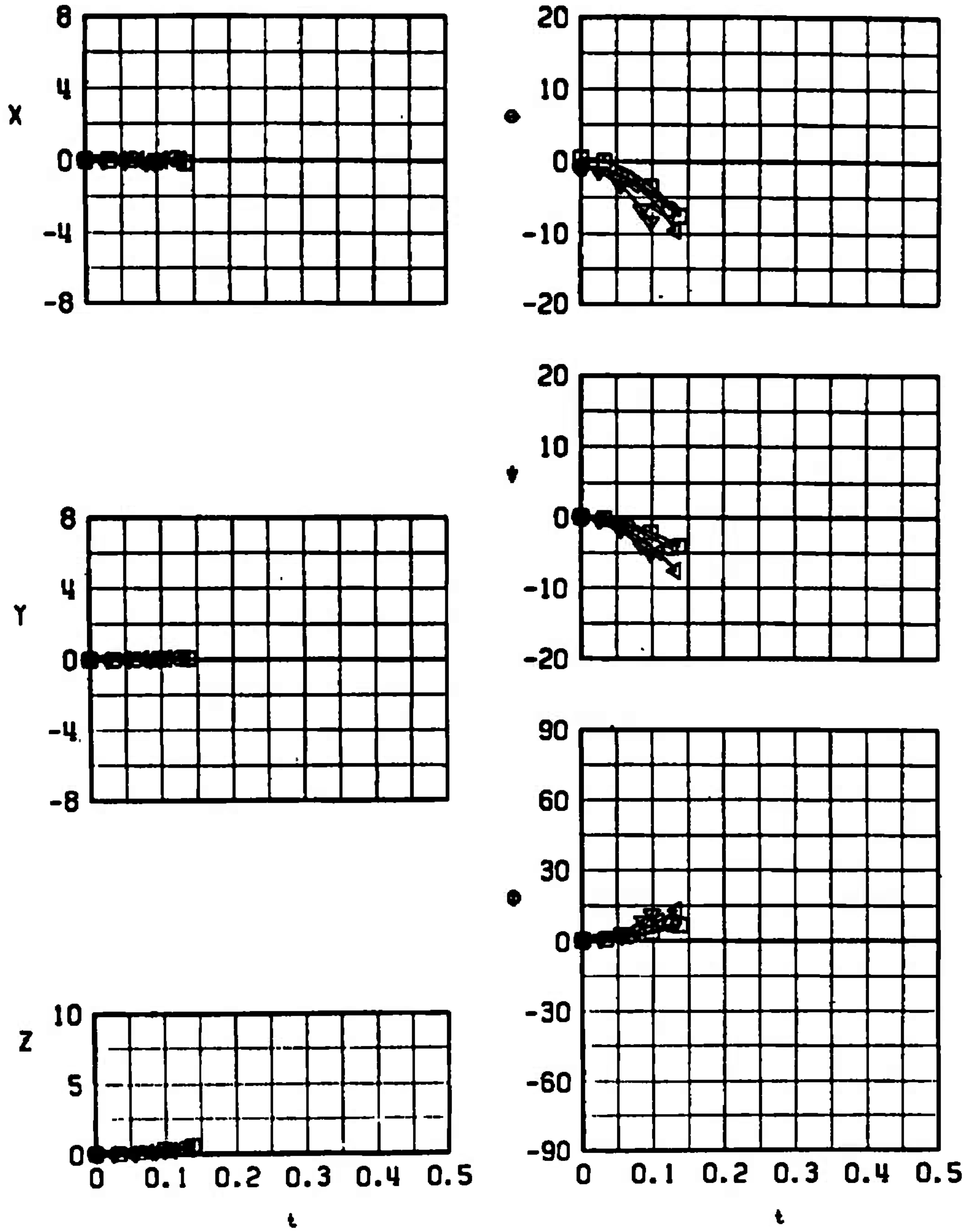

a. Configuration 13L

Fig. 25 Separation Characteristics of the MK-20 Rockeye Bomb from the TER on the Outboard Pylon Station; MER with Four MK-20 Bombs on the Center Pylon and 300-gal Fuel Tank on the Inboard Pylon

SYMBOL	CONF	M_∞	α	H	$\bar{\phi}$	EJECTOR FORCE
□	15L	0.730	3.4	4000	0	5
○	15L	0.780	2.2	7000	-70	5
◁	15L	0.860	2.1	7000	-70	5
▽	15L	0.950	2.0	7000	-70	5

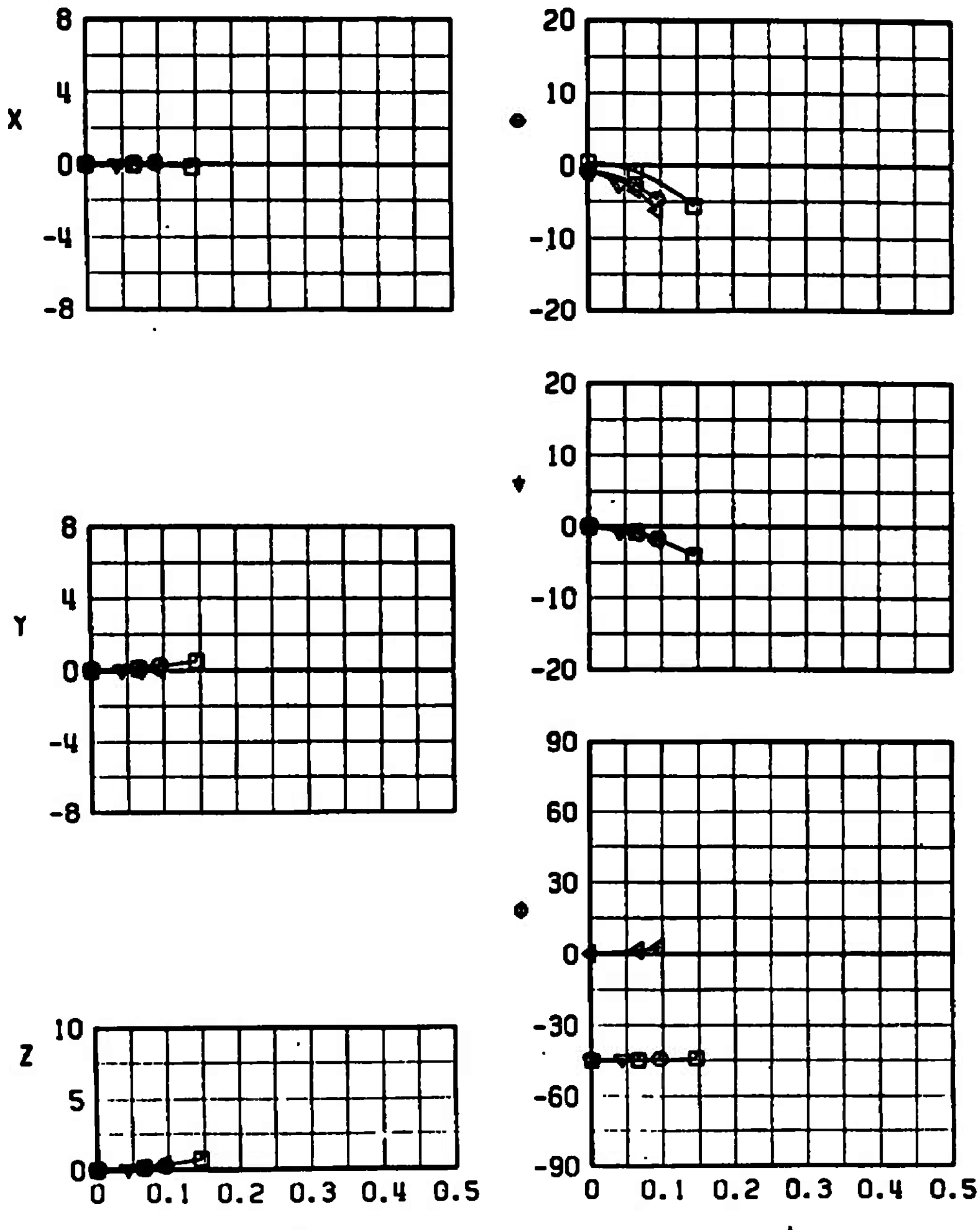

b. Configuration 15L
Fig. 25 Continued

SYMBOL	CONF	M_∞	α	H	$\dot{\theta}$	EJECTOR FORCE
□	16L	0.730	3.4	4000	0	5
○	16L	0.780	2.2	7000	-70	5
◁	16L	0.860	2.1	7000	-70	5
▽	16L	0.950	2.0	7000	-70	5

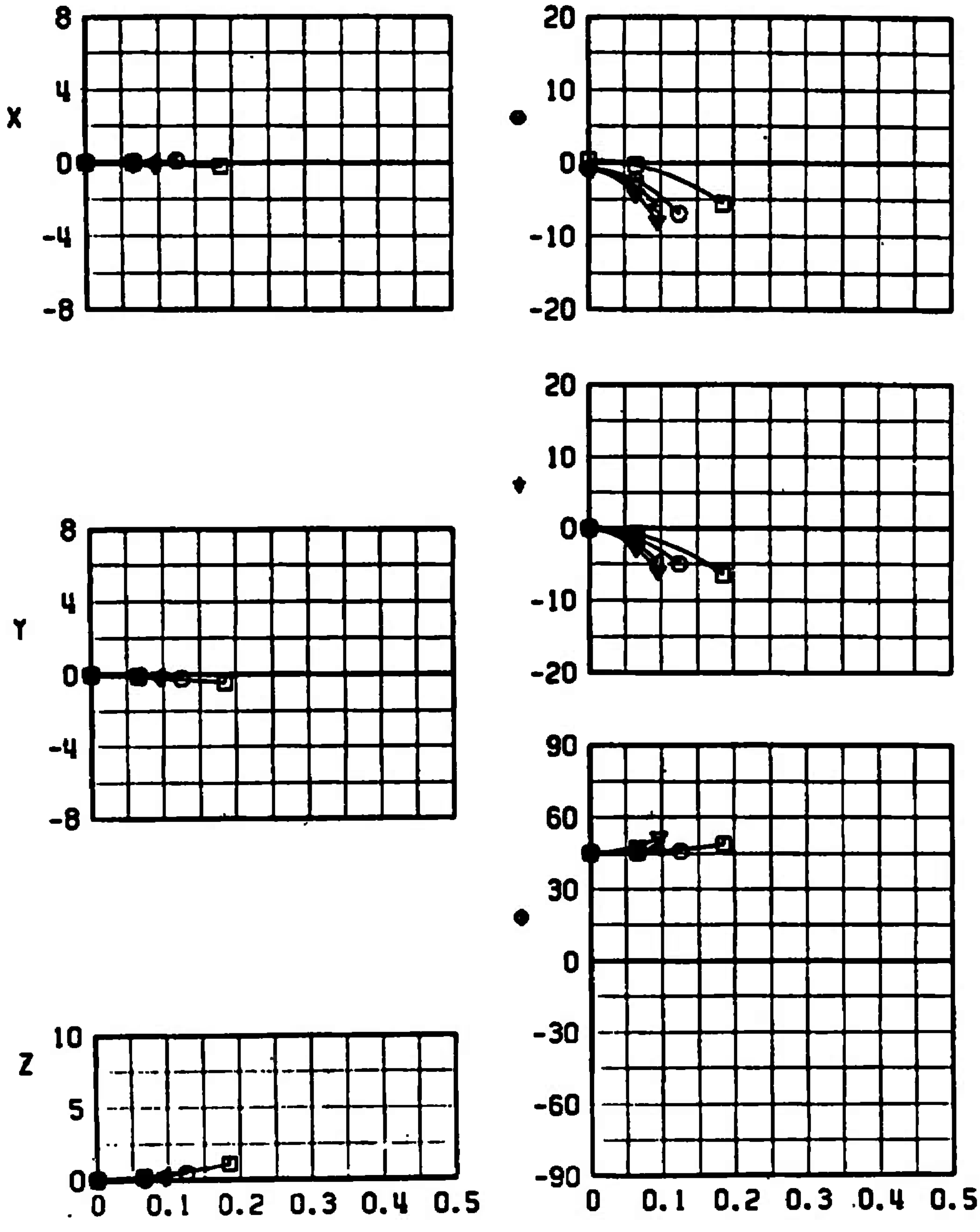

c. Configuration 16L
Fig. 25 Concluded

SYMBOL	CONF	M_∞	α	H	$\bar{\delta}$	EJECTOR FORCE
□	17R	0.407	9.4	4000	0	6
○	17R	0.488	6.8	4000	0	6
△	17R	0.650	4.1	4000	0	6
◁	17R	0.814	3.2	4000	0	6

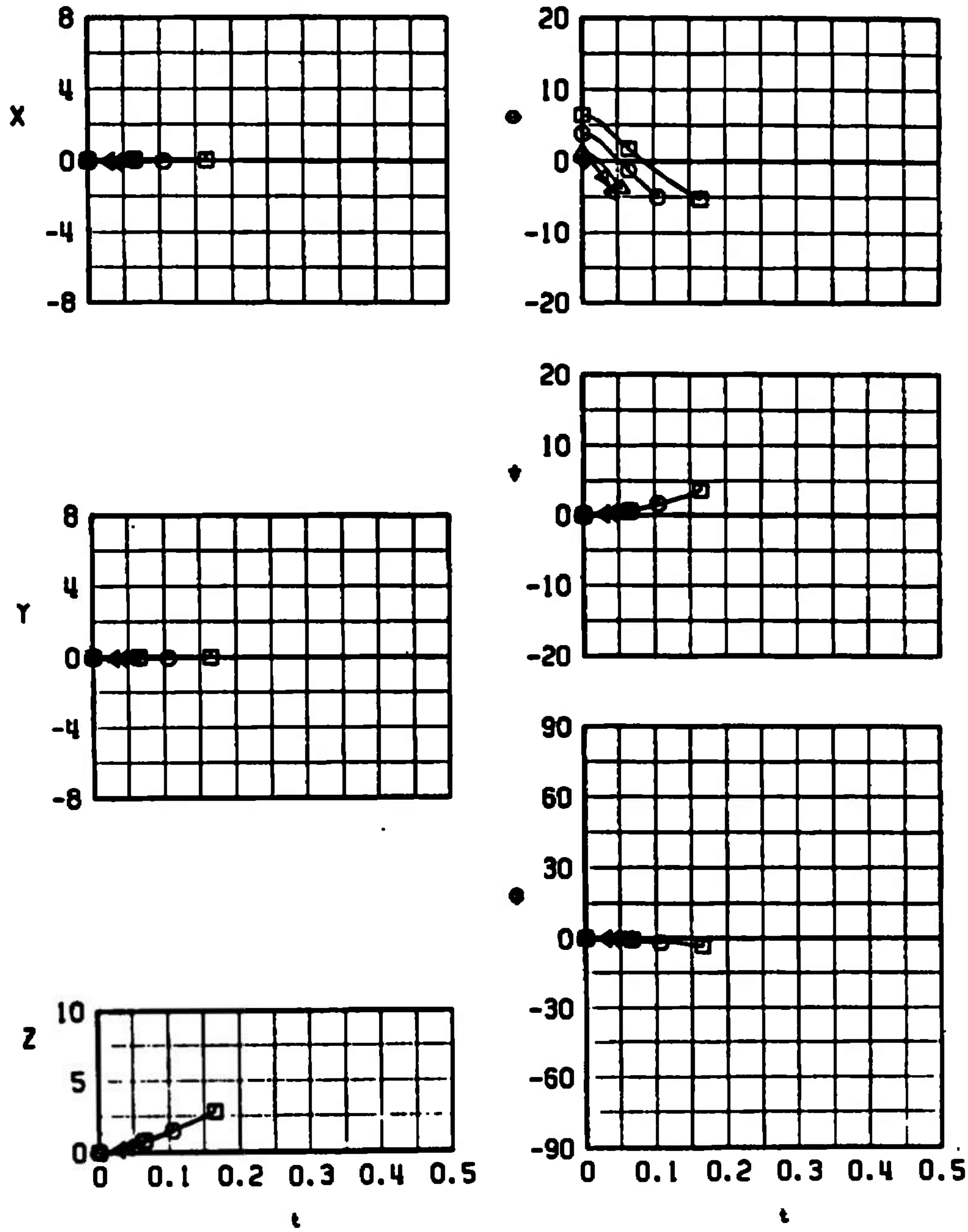

a. Fuel Tank (Empty)

Fig. 26 Separation Characteristics of the 300-gal Fuel Tank from the Inboard Pylon, Configuration 17R

SYMBOL	CONF	M_∞	α	H	$\bar{\phi}$	EJECTOR FORCE
□	17R	0.407	9.4	4000	0	7
○	17R	0.488	6.8	4000	0	7
△	17R	0.650	4.1	4000	0	7
◁	17R	0.814	3.2	4000	0	7

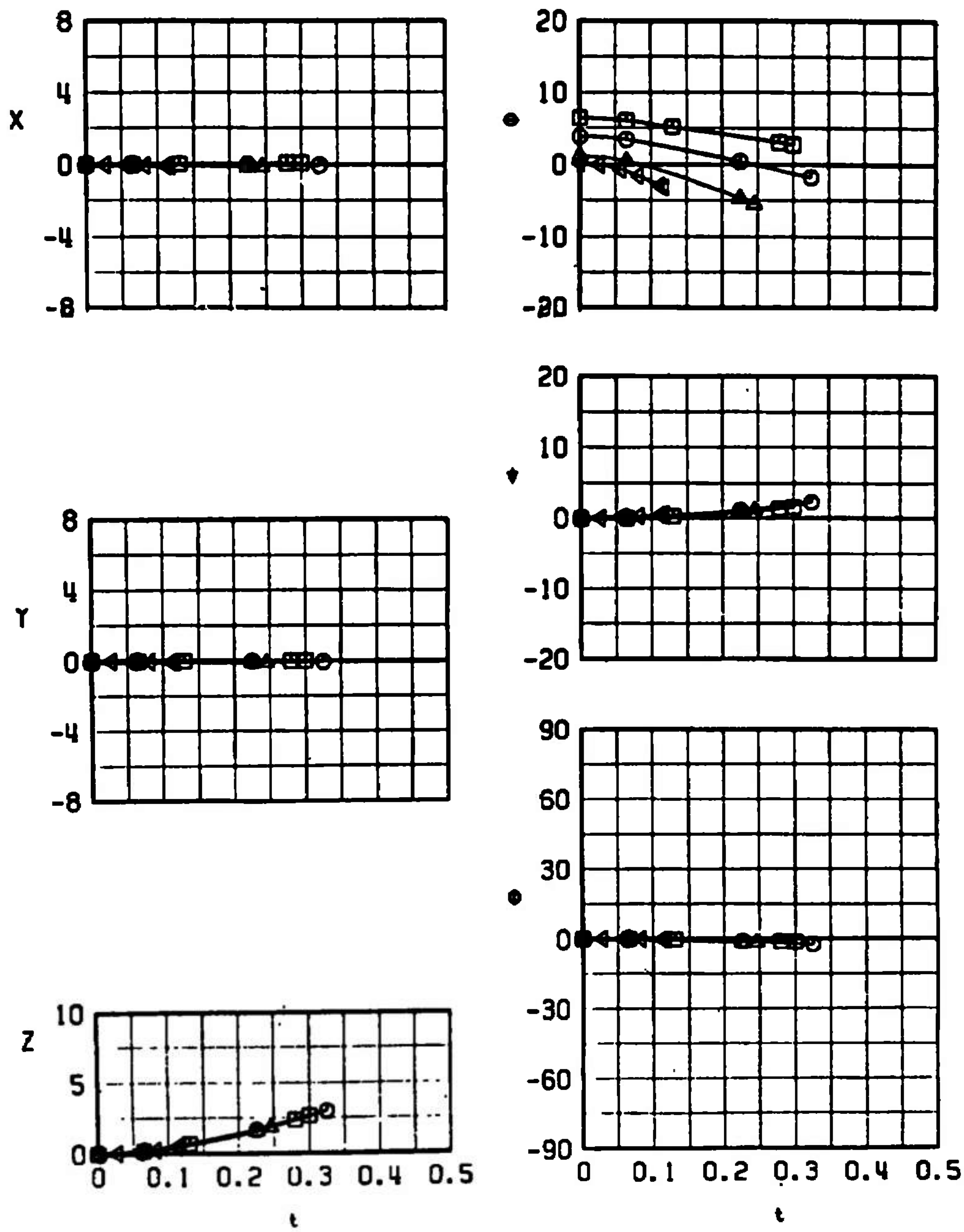

b. Fuel Tank (Full)
Fig. 26 Continued

SYMBOL	CONF	M_∞	α	H	ψ	EJECTOR FORCE
□	17R	0.407	9.4	4000	0	12
○	17R	0.650	4.1	4000	0	12
△	17R	0.814	-3.2	4000	0	12

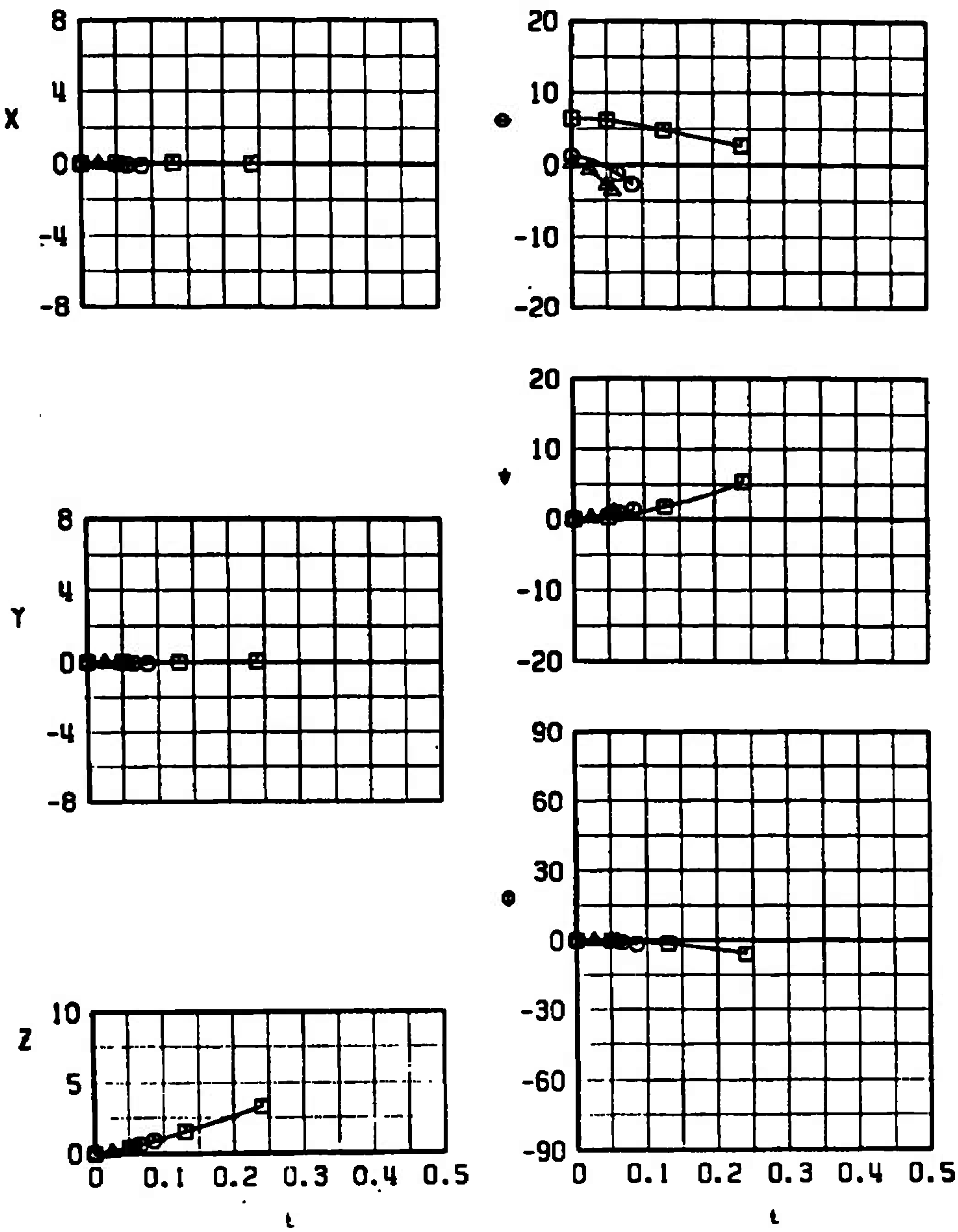

c. Fuel Tank (Cargo No. 1)
Fig. 26 Continued

SYMBOL	CONF	M_∞	α	H	$\bar{\phi}$	EJECTOR FORCE
☐	17R	0.407	9.4	4000	0	13
○	17R	0.650	4.1	4000	0	13
△	17R	0.814	3.2	4000	0	13

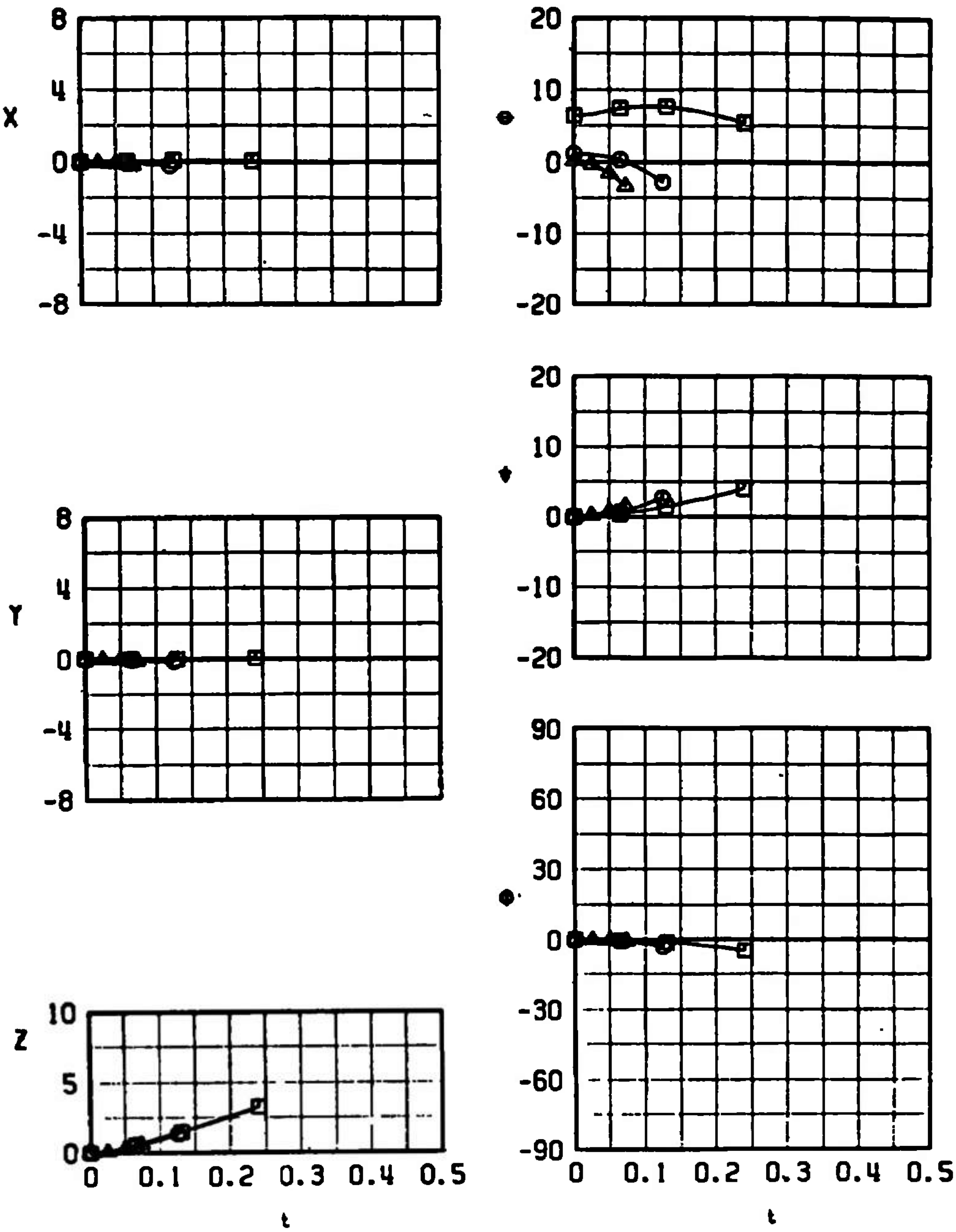

d. Fuel Tank (Cargo No. 2)
Fig. 26 Continued

SYMBOL	CONF	M_∞	α	H	δ	EJECTOR FORCE
□	17R	0.407	9.4	4000	0	14
○	17R	0.650	4.1	4000	0	14
△	17R	0.814	3.2	4000	0	14

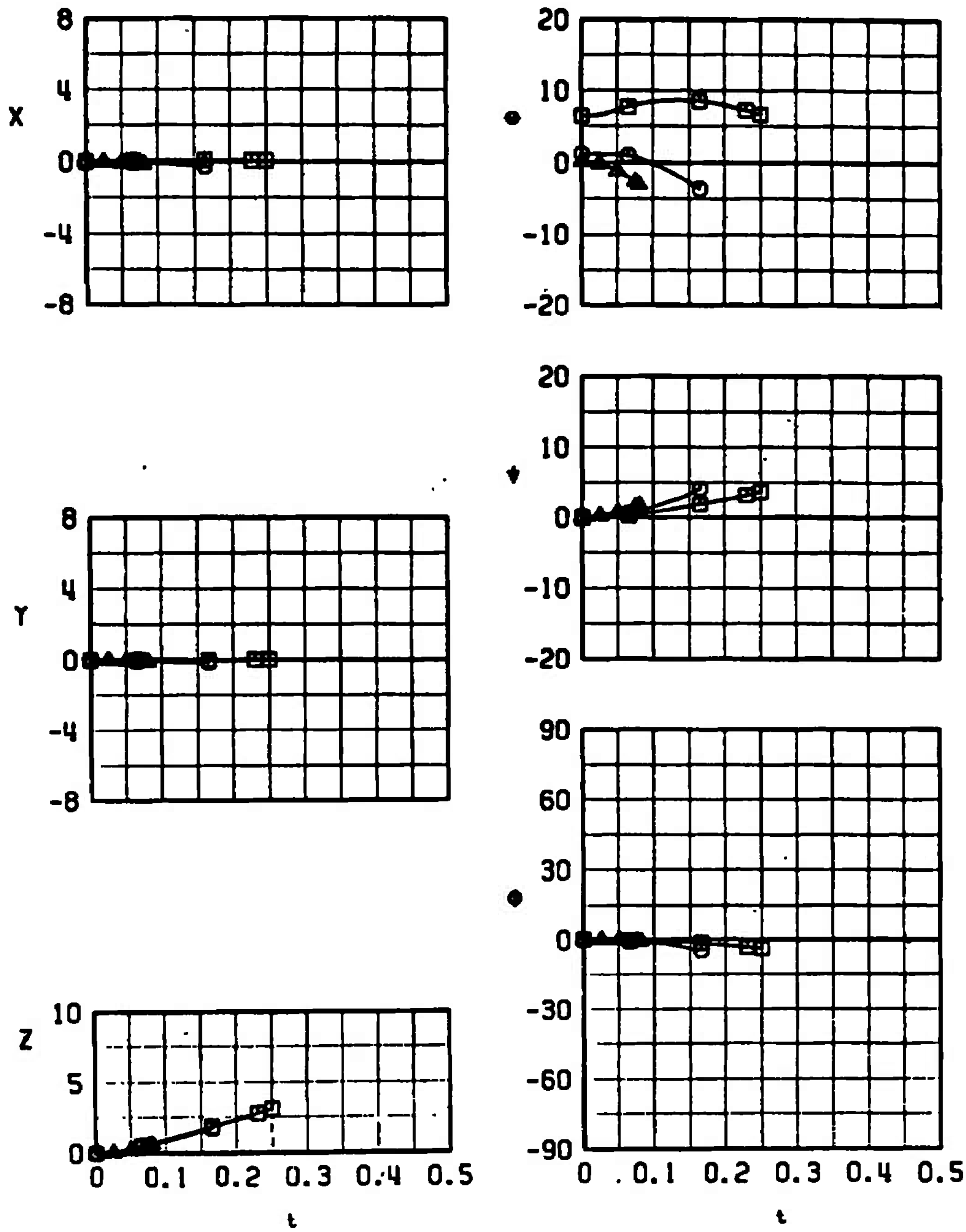

e. Fuel Tank (Cargo No. 3)
Fig. 26 Continued

SYMBOL	CONF	M_∞	α	H	$\bar{\theta}$	EJECTOR FORCE
□	17R	0.407	9.4	4000	0	15
○	17R	0.650	4.1	4000	0	15
△	17R	0.814	3.2	4000	0	15

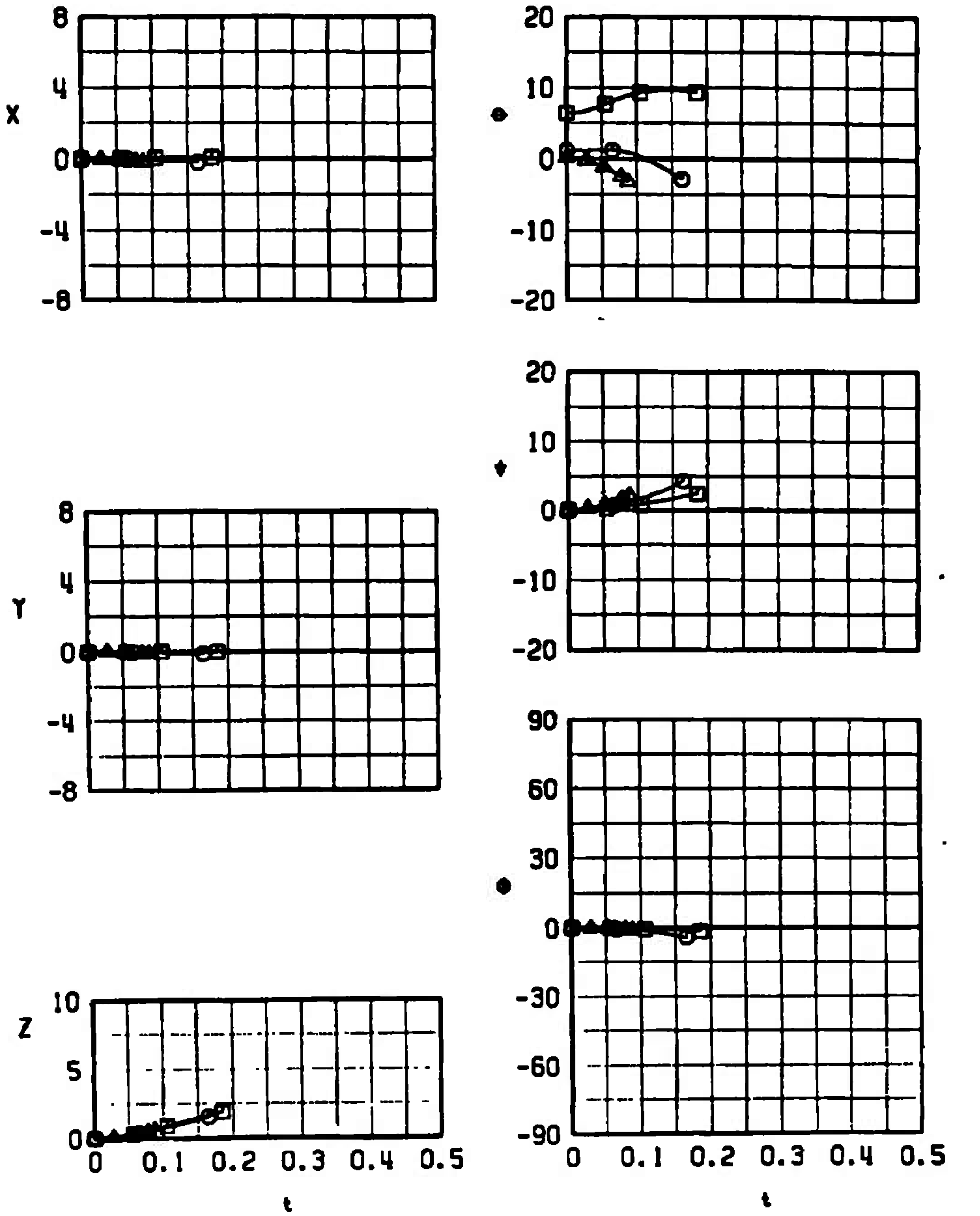

f. Fuel Tank (Cargo No. 4)
Fig. 26 Concluded

SYMBOL	CONF	M_∞	α	H	$\bar{\delta}$	EJECTOR FORCE
□	17L	0.407	9.4	4000	0	6
○	17L	0.488	6.8	4000	0	6
△	17L	0.650	4.1	4000	0	6
◁	17L	0.814	3.2	4000	0	6

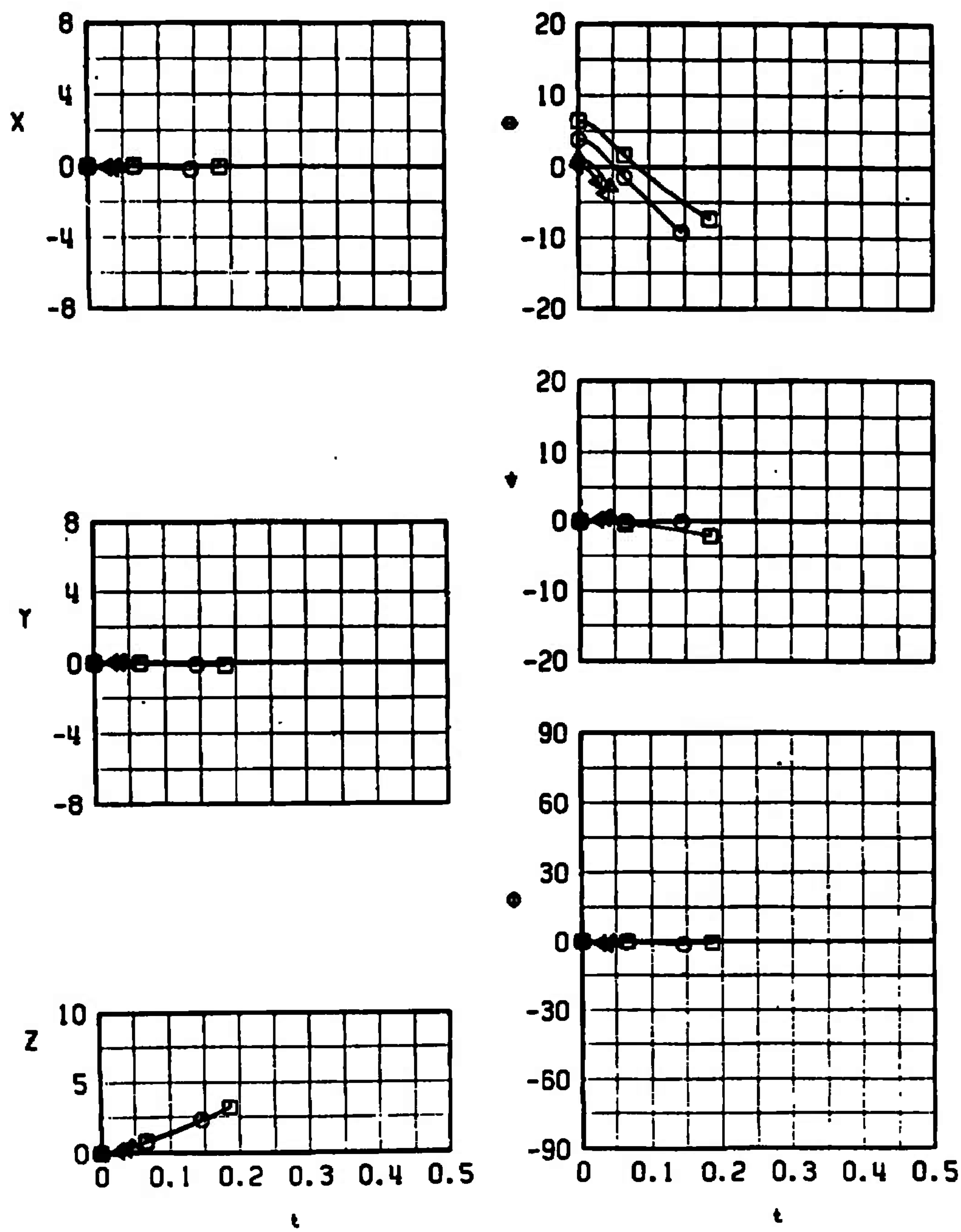

a. Fuel Tank (Empty)

Fig. 27 Separation Characteristics of the 300-gal Fuel Tank from the Inboard Pylon, Configuration 17L

SYMBOL	CONF	M_∞	α	H	γ	EJECTOR FORCE
□	17L	0.407	9.4	4000	0	7
○	17L	0.488	6.8	4000	0	7
△	17L	0.650	4.1	4000	0	7
◁	17L	0.814	3.2	4000	0	7

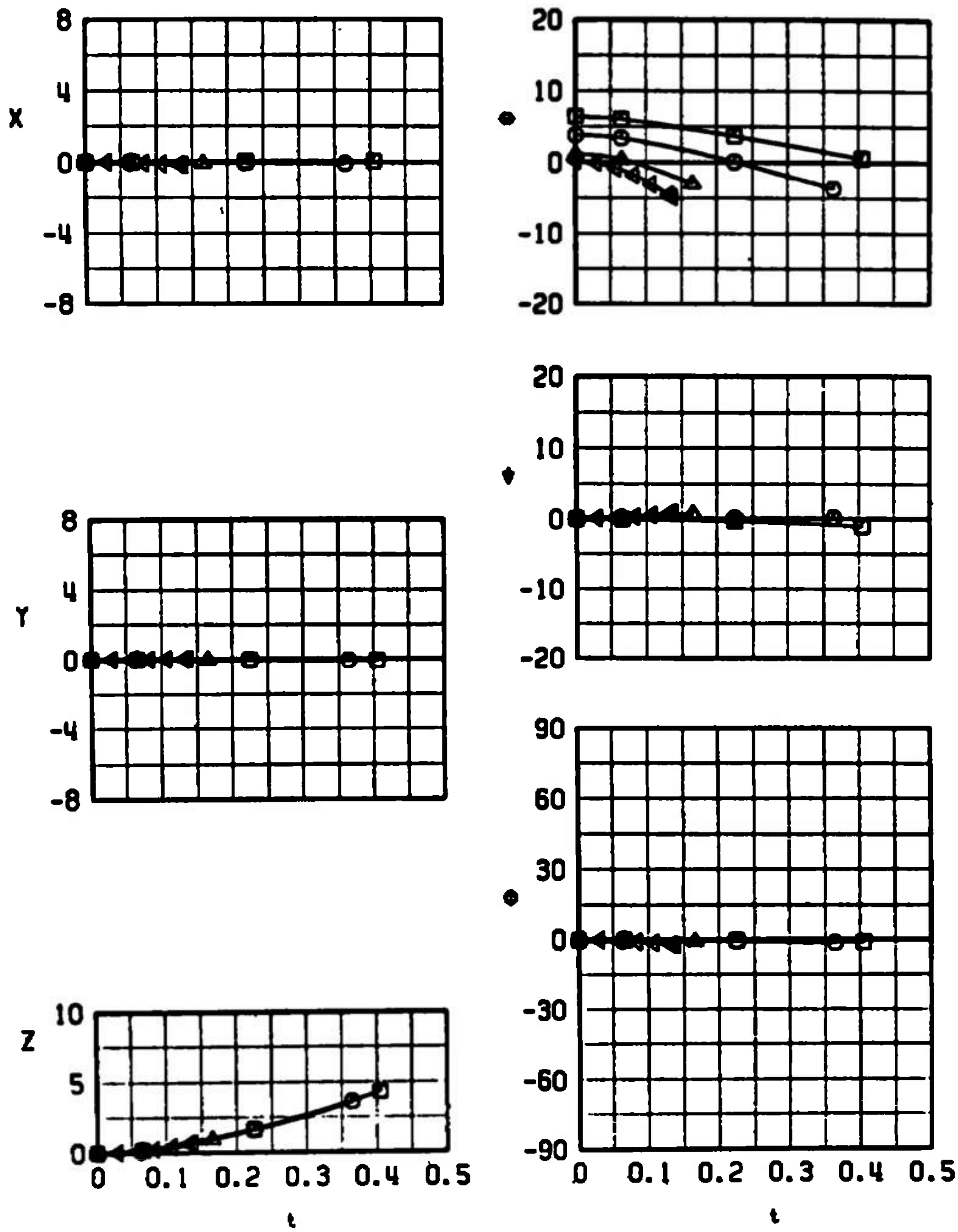

b. Fuel Tank (Full)
Fig. 27 Concluded

SYMBOL	CONF	M_∞	α	H	$\bar{\theta}$	EJECTOR FORCE
□	18R	0.814	2.8	4000	0	8
○	18R	0.814	2.8	4000	0	9

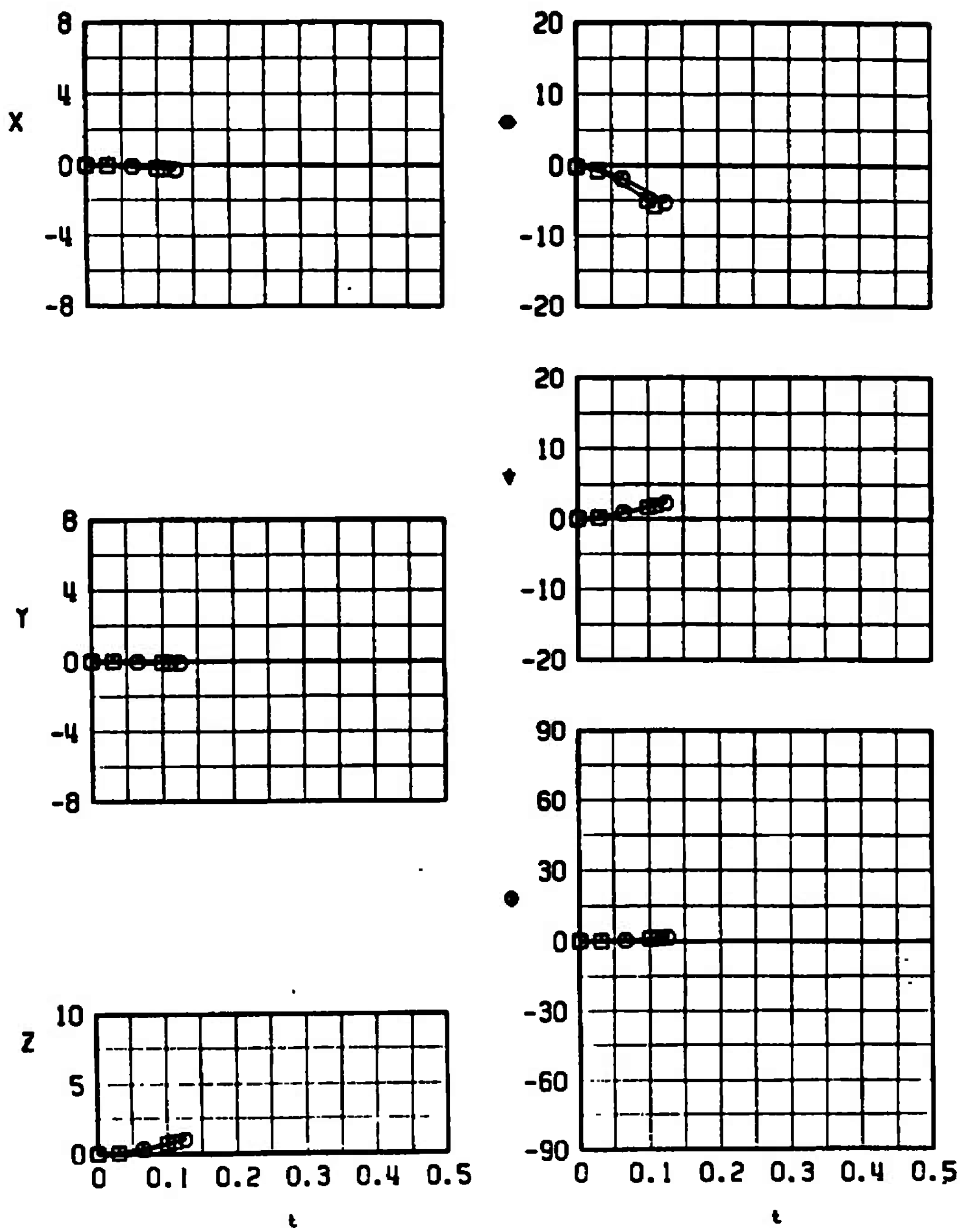

a. $M_\infty = 0.814$

Fig. 28 Separation Characteristics of the CBU-52B/B Dispenser from the Center Pylon Station, Configuration 18R

SYMBOL	CONF	M_∞	α	H	$\bar{\theta}$	EJECTOR FORCE
□	18R	0.860	2.0	7000	-70	8
○	18R	0.860	2.0	7000	-70	9

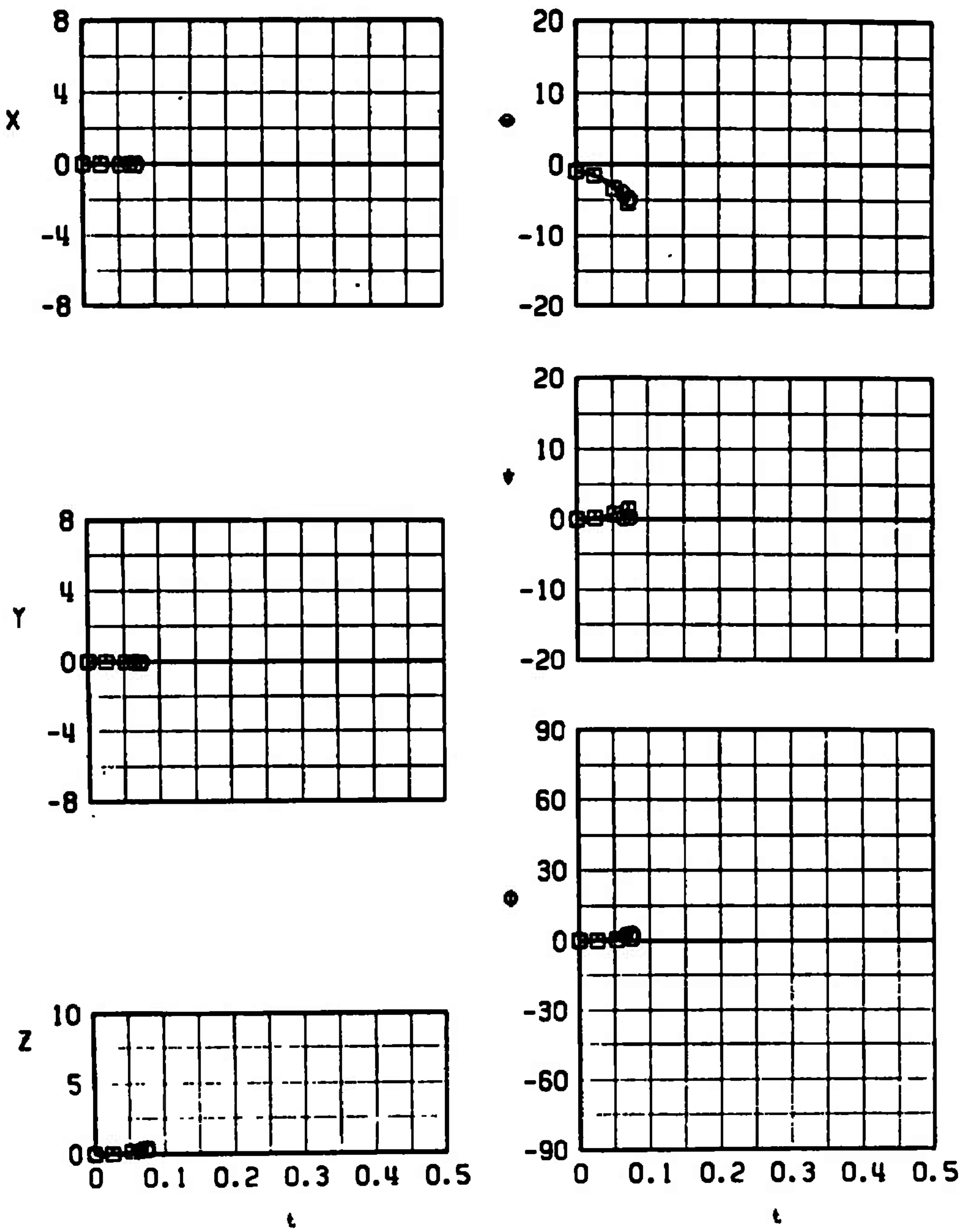

b. $M_\infty = 0.860$
Fig. 28 Continued

SYMBOL	CONF	M_∞	α	H	δ	EJECTOR FORCE
□	18R	0.950	1.9	7000	-70	8
○	18R	0.950	1.9	7000	-70	9

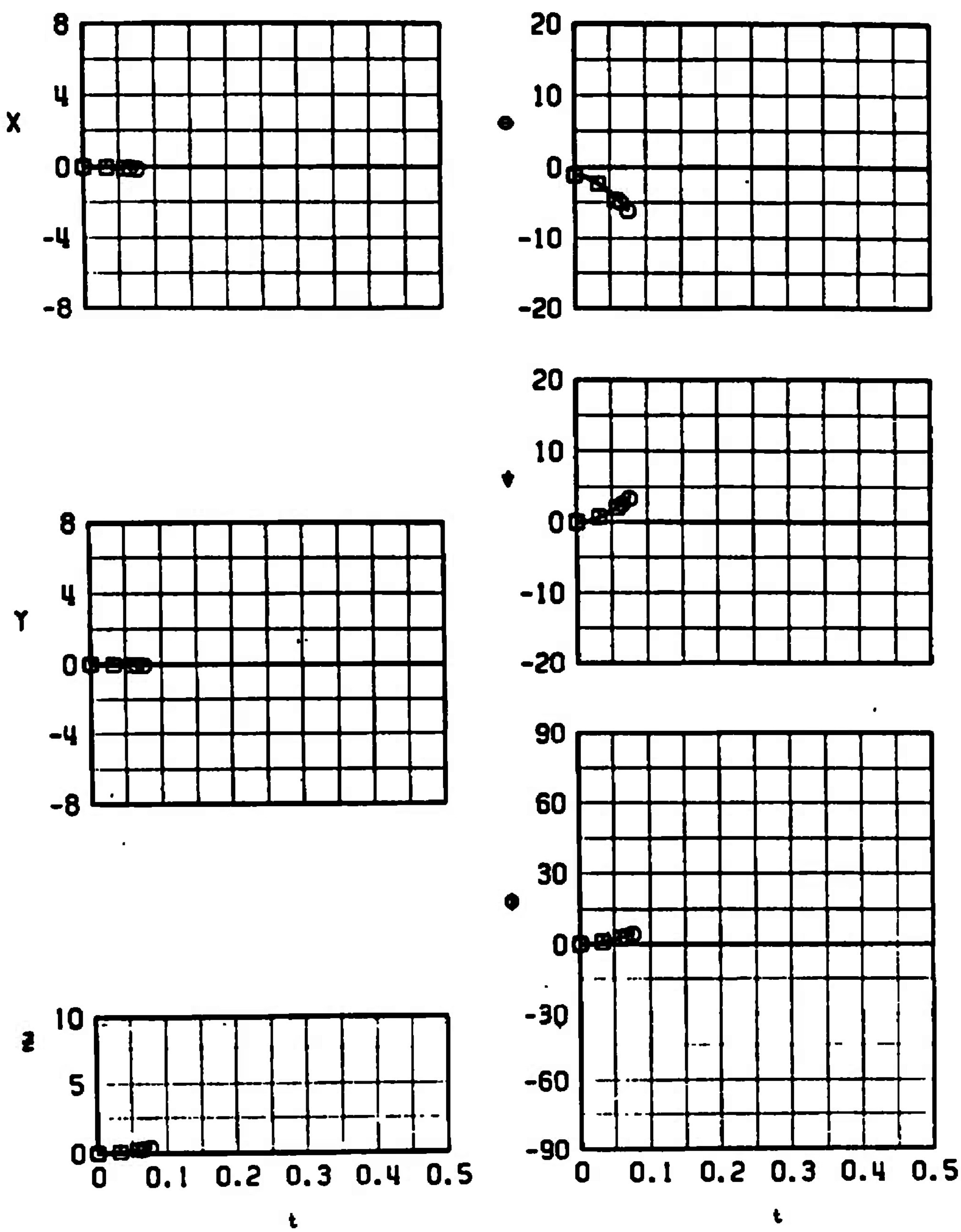

c. $M_\infty = 0.950$
Fig. 28 Concluded

SYMBOL	CONF	M_∞	α	H	$\bar{\theta}$	EJECTOR FORCE
□	18L	0.814	2.8	4000	0	8
○	18L	0.814	2.8	4000	0	9

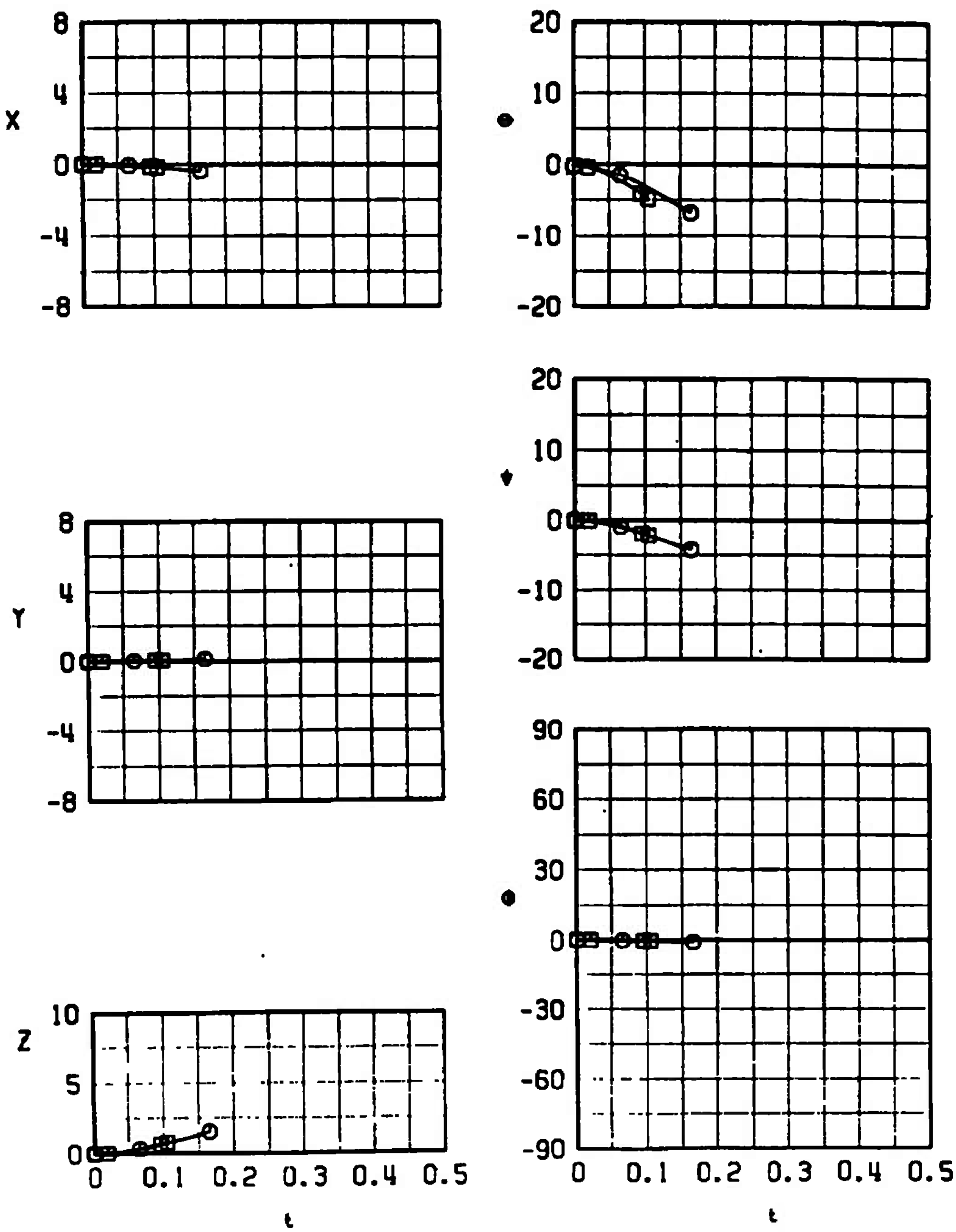

a. $M_\infty = 0.814$

Fig. 29 Separation Characteristics of the CBU-52B/B Dispenser from the Outboard Pylon Station, Configuration 18L

SYMBOL	CONF	M_∞	α	H	$\bar{\theta}$	EJECTOR FORCE
□	18L	0.860	2.0	7000	-70	8
○	18L	0.860	2.0	7000	-70	9

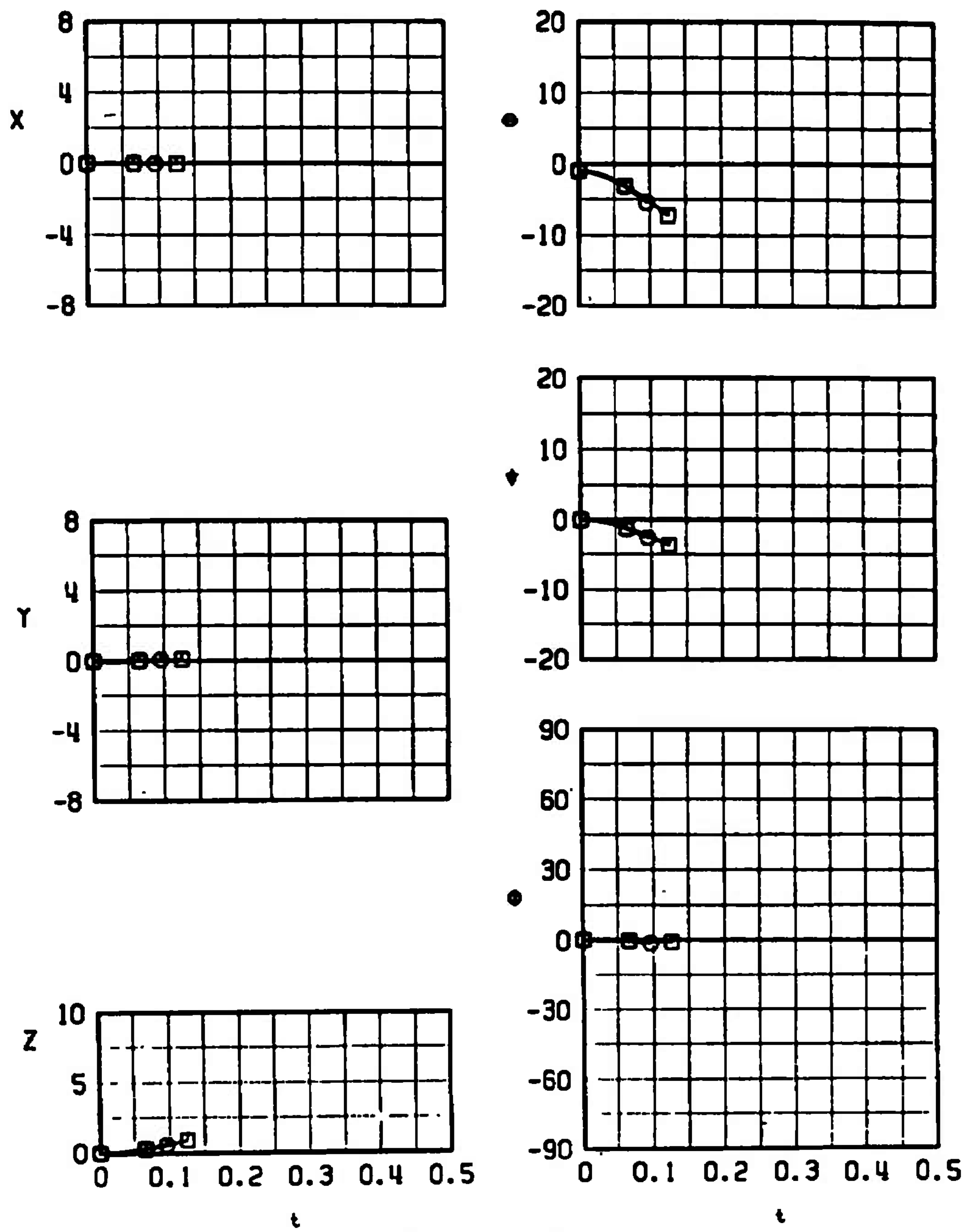

b. M_∞ = 0.860

Fig. 29 Continued

SYMBOL	CONF	M_∞	α	H	$\bar{\theta}$	EJECTOR FORCE
□	18L	0.950	1.9	7000	-70	8
○	18L	0.950	1.9	7000	-70	9

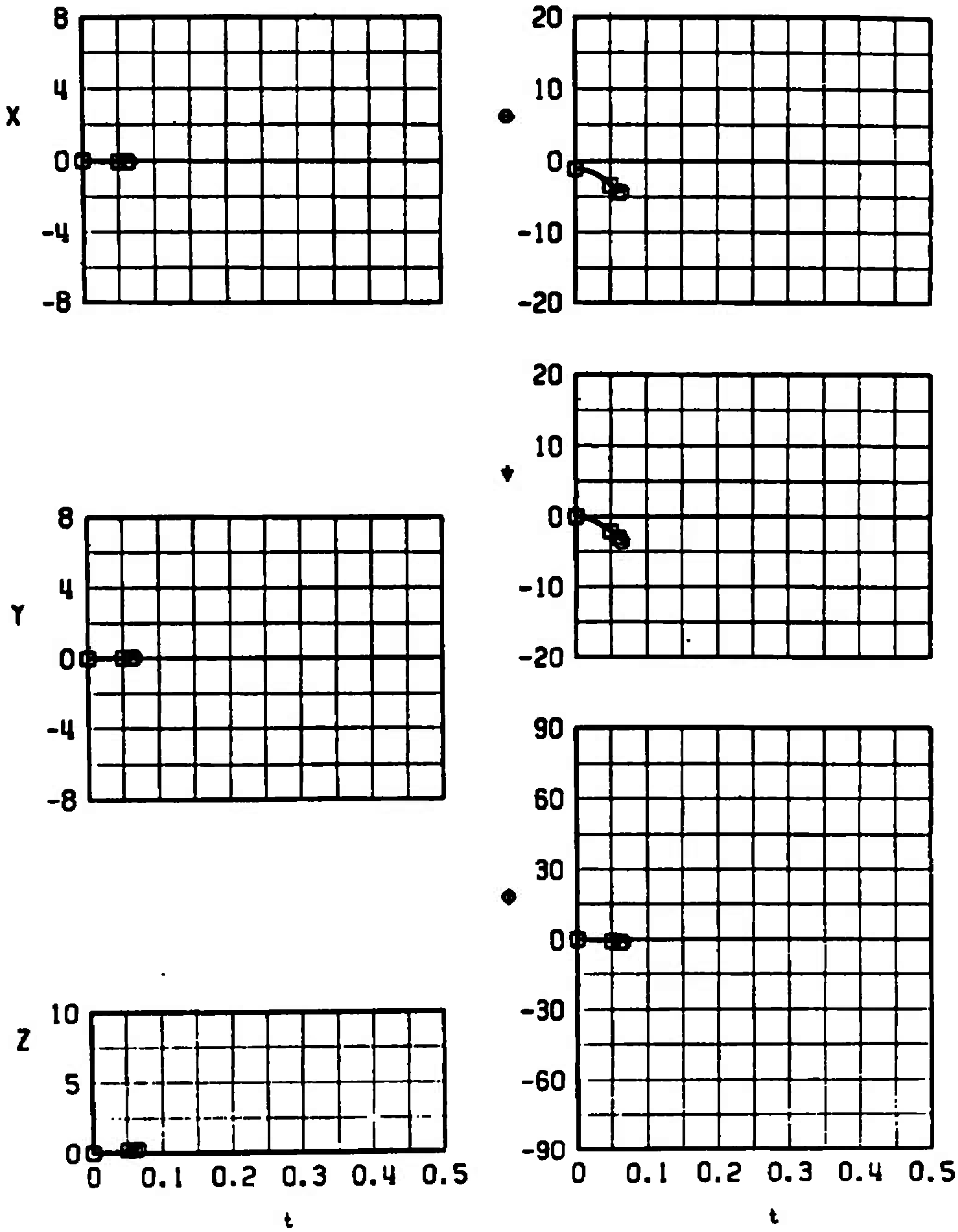

c. M_∞ = 0.950
Fig. 29 Concluded

SYMBOL	CONF	M_∞	α	H	$\bar{\phi}$	EJECTOR FORCE
□	20R	0.814	2.8	4000	0	8
○	20R	0.814	2.8	4000	0	9

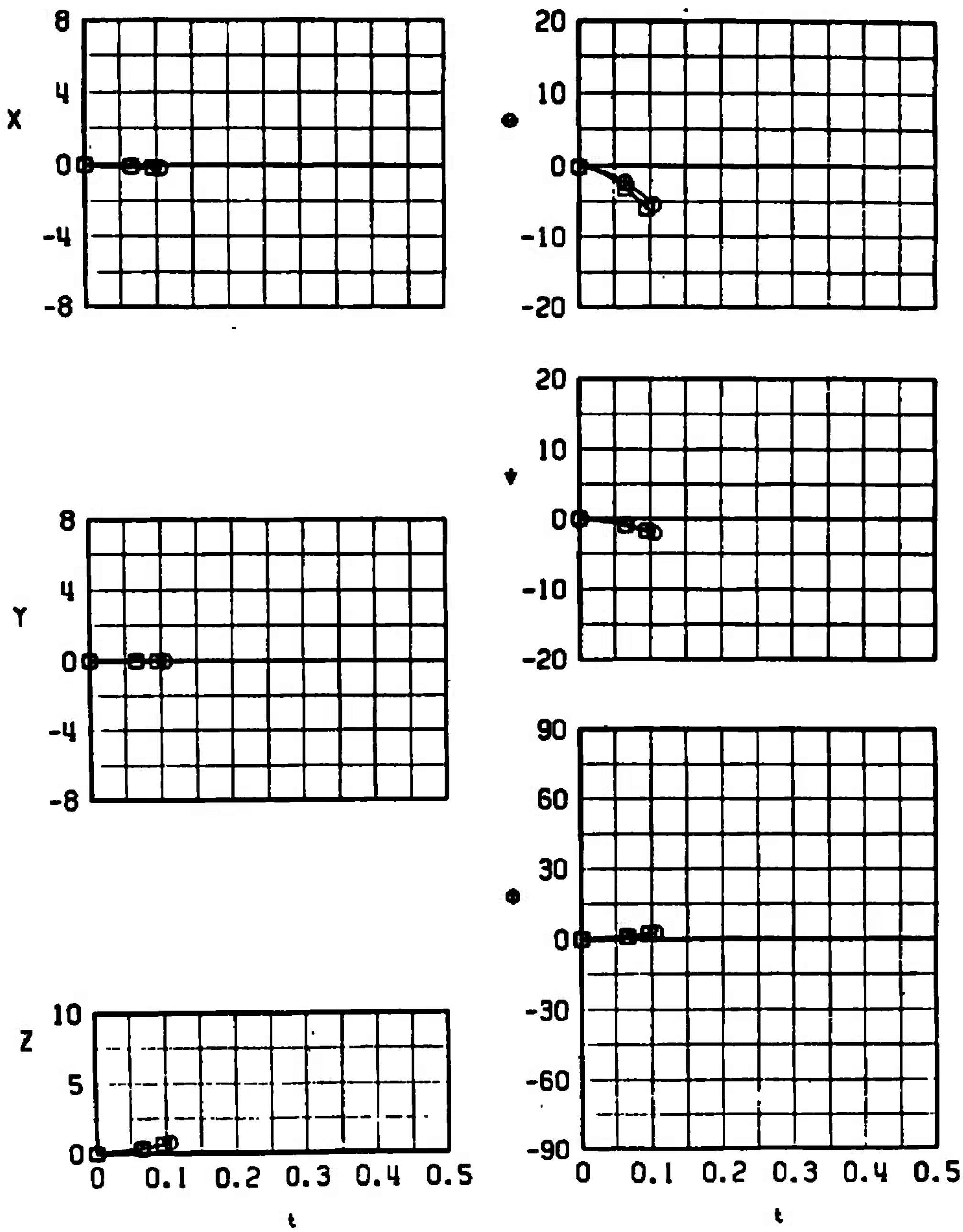

a. $M_\infty = 0.814$

Fig. 30 Separation Characteristics of the CBU-52B/B Dispenser from the Inboard Pylon Station, Configuration 20R

SYMBOL	CONF	M_∞	α	H	$\bar{\theta}$	EJECTOR FORCE
□	20R	0.860	2.0	7000	-70	8
○	20R	0.860	2.0	7000	-70	9

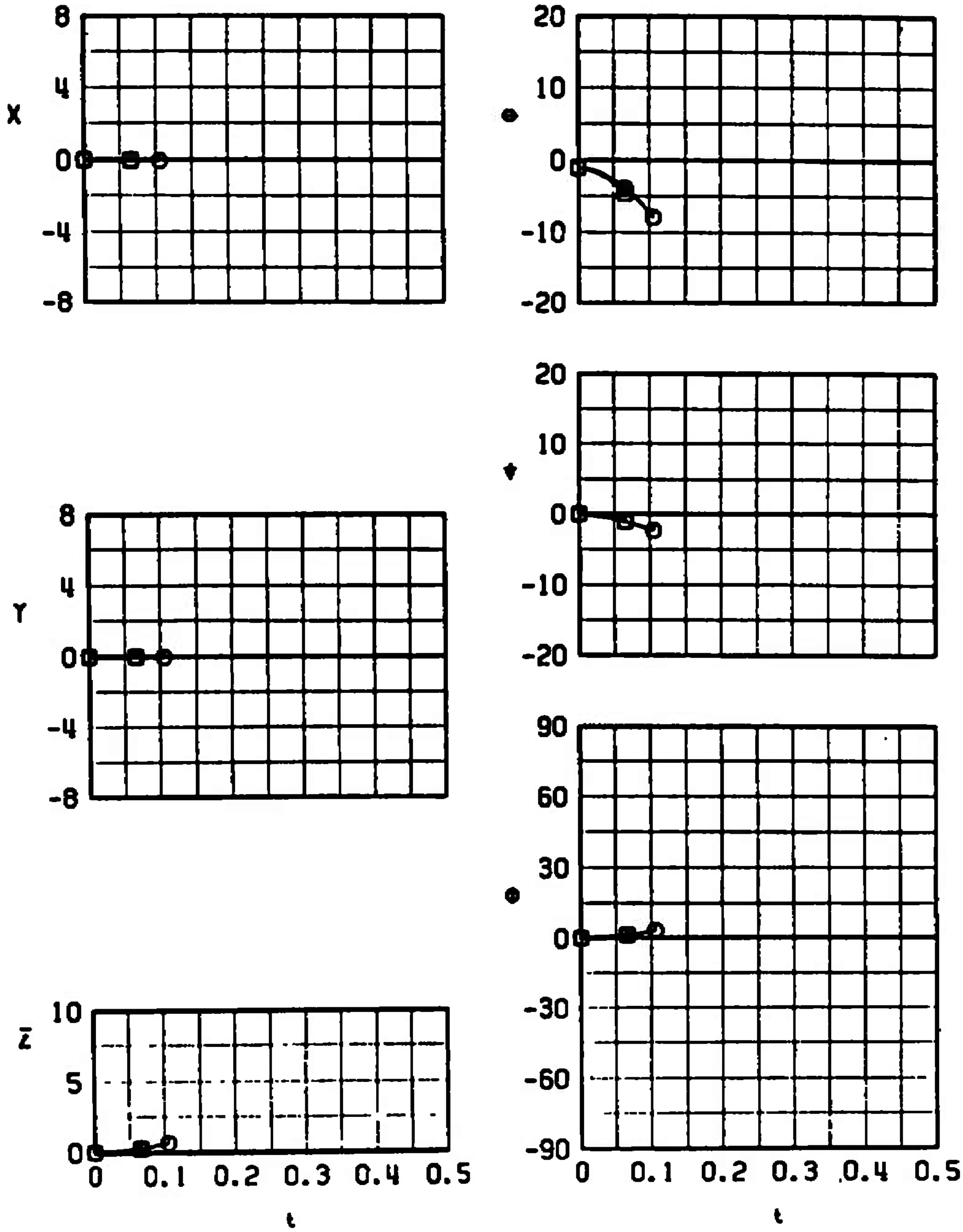

b. $M_\infty = 0.860$
Fig. 30 Continued

SYMBOL	CONF	M_∞	α	H	$\bar{\theta}$	EJECTOR FORCE
□	20R	0.950	1.9	7000	-70	8
○	20R	0.950	1.9	7000	-70	9

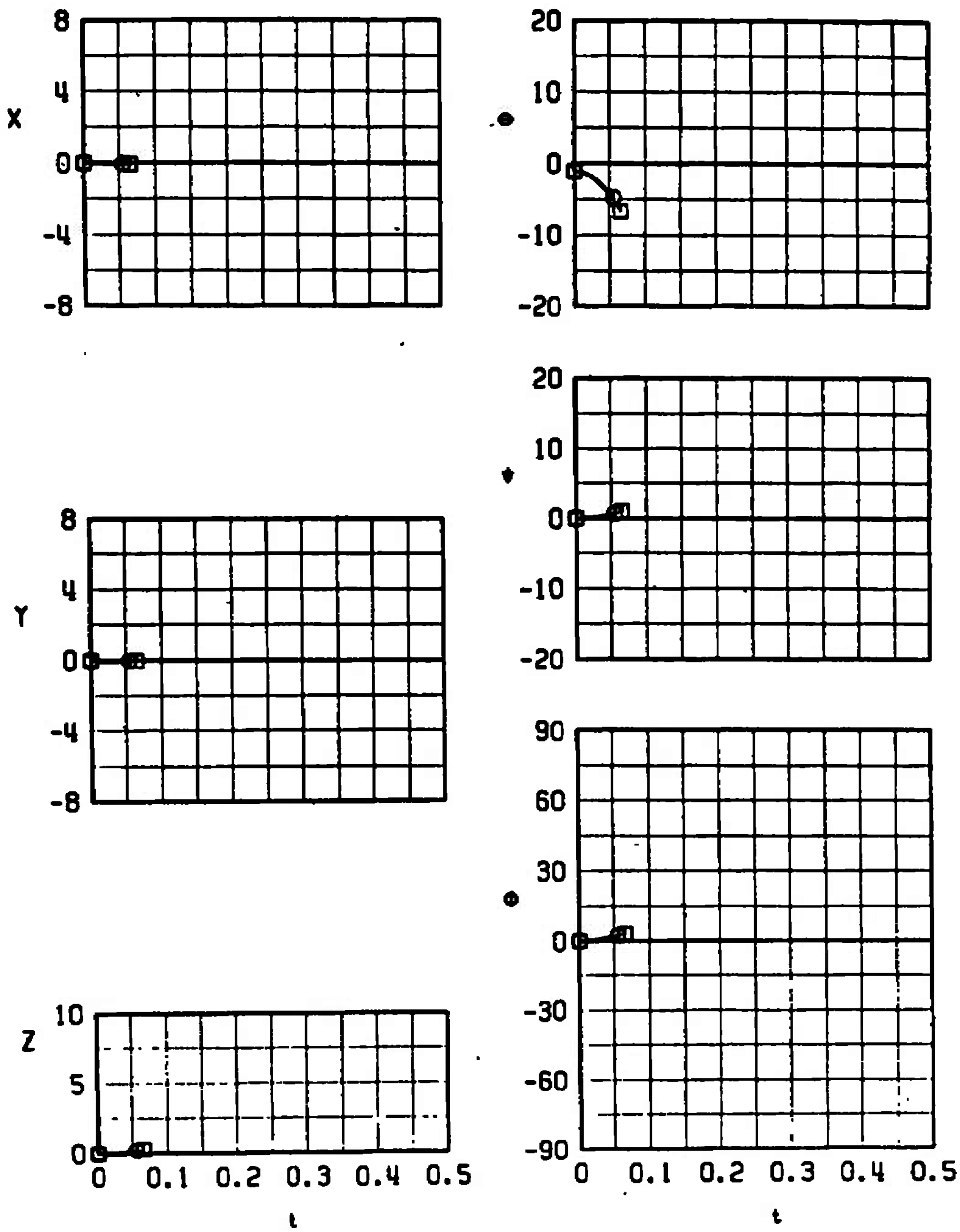

c. M_∞ = 0.950
Fig. 30 Concluded

SYMBOL	CONF	M_∞	α	H	$\bar{\phi}$	EJECTOR FORCE
□	19R	0.730	3.0	4000	0	10
○	19R	0.730	3.0	4000	0	11

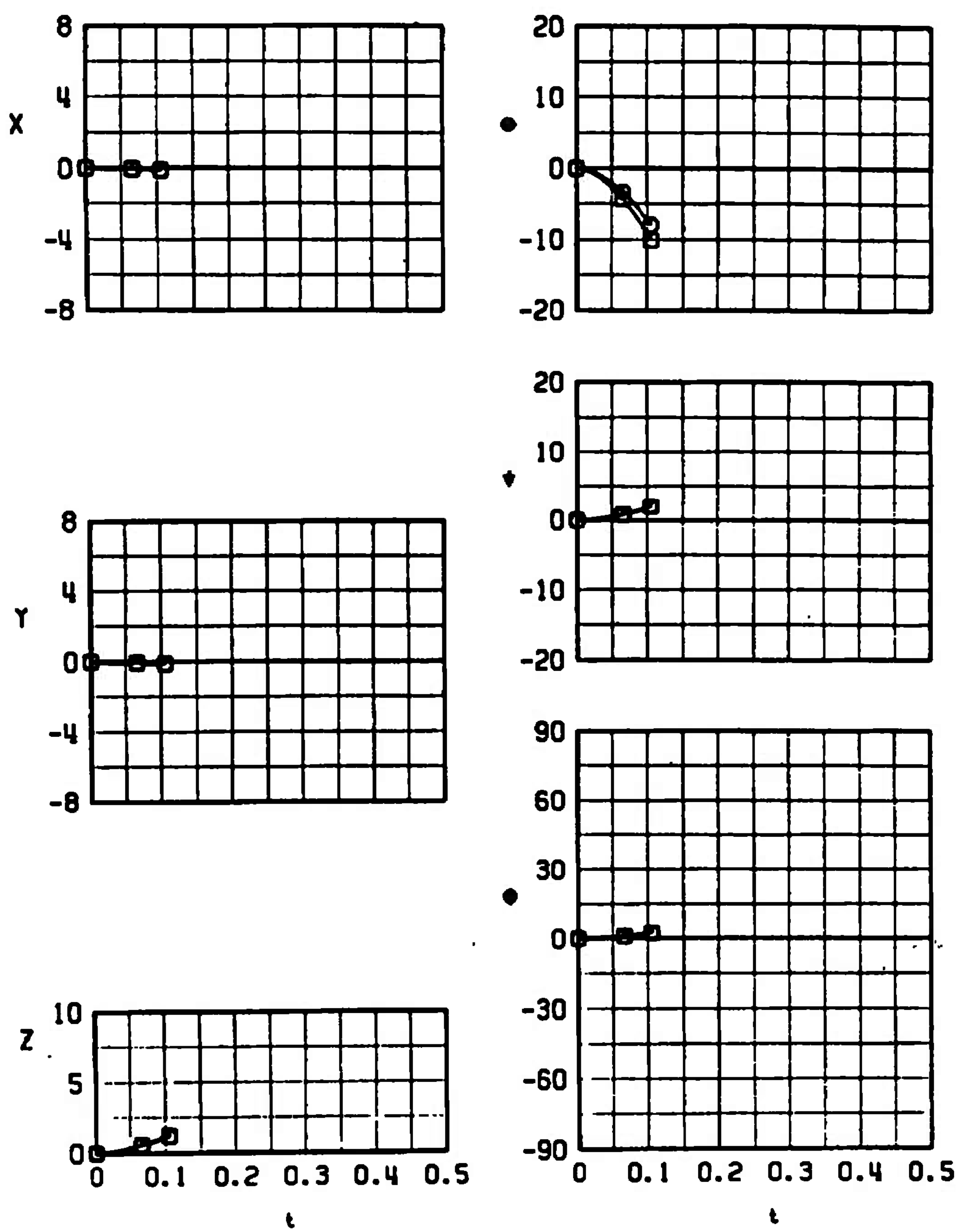

a. $M_\infty = 0.730$

Fig. 31 Separation Characteristics of the BLU-52A/B Bomb from the Center Pylon Station, Configuration 19R

SYMBOL	CONF	M_∞	α	H	$\bar{\theta}$	EJECTOR FORCE
□	19R	0.760	2.7	6000	-50	10
○	19R	0.760	2.7	6000	-50	11

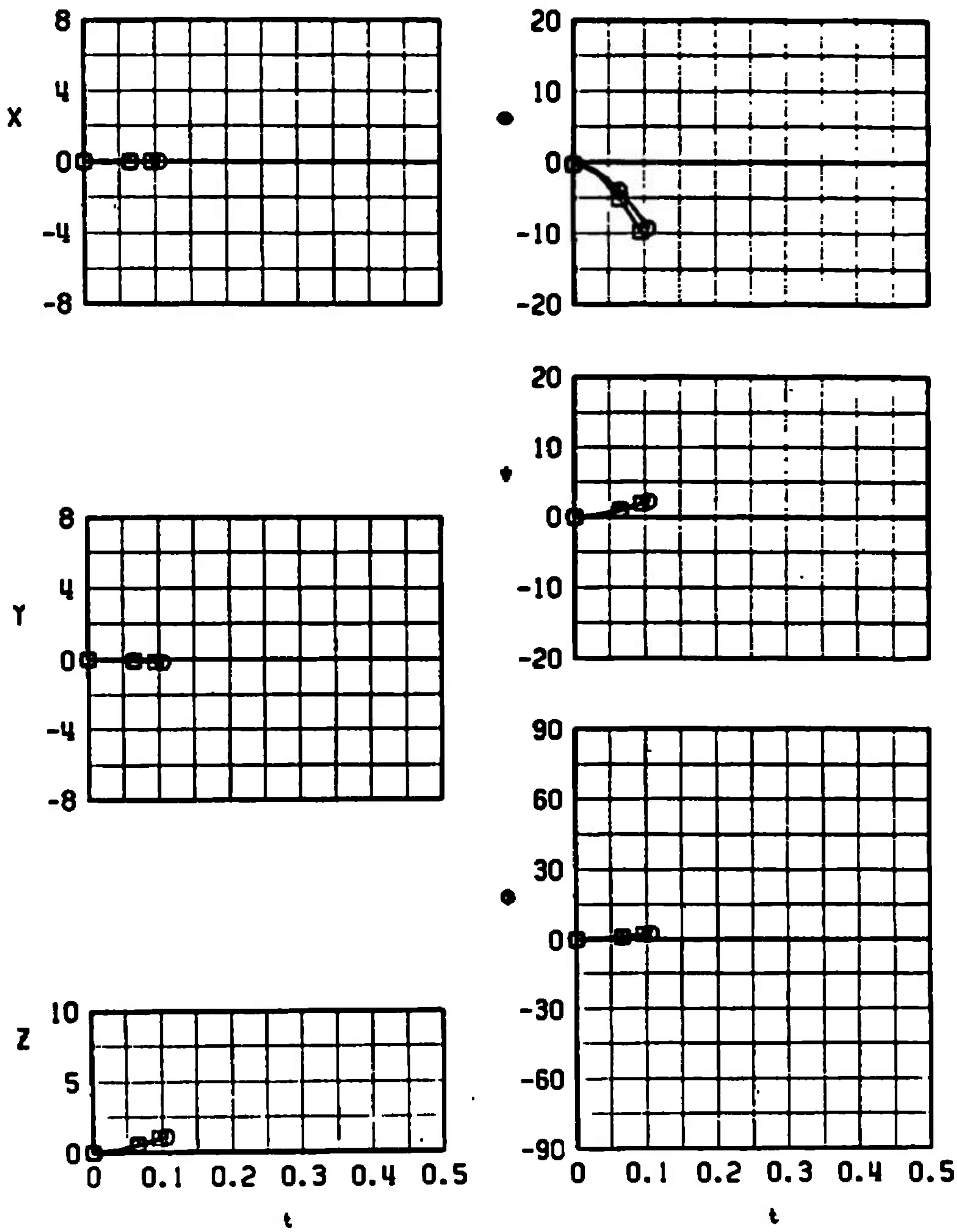

b. $M_\infty = 0.760$
Fig. 31 Continued

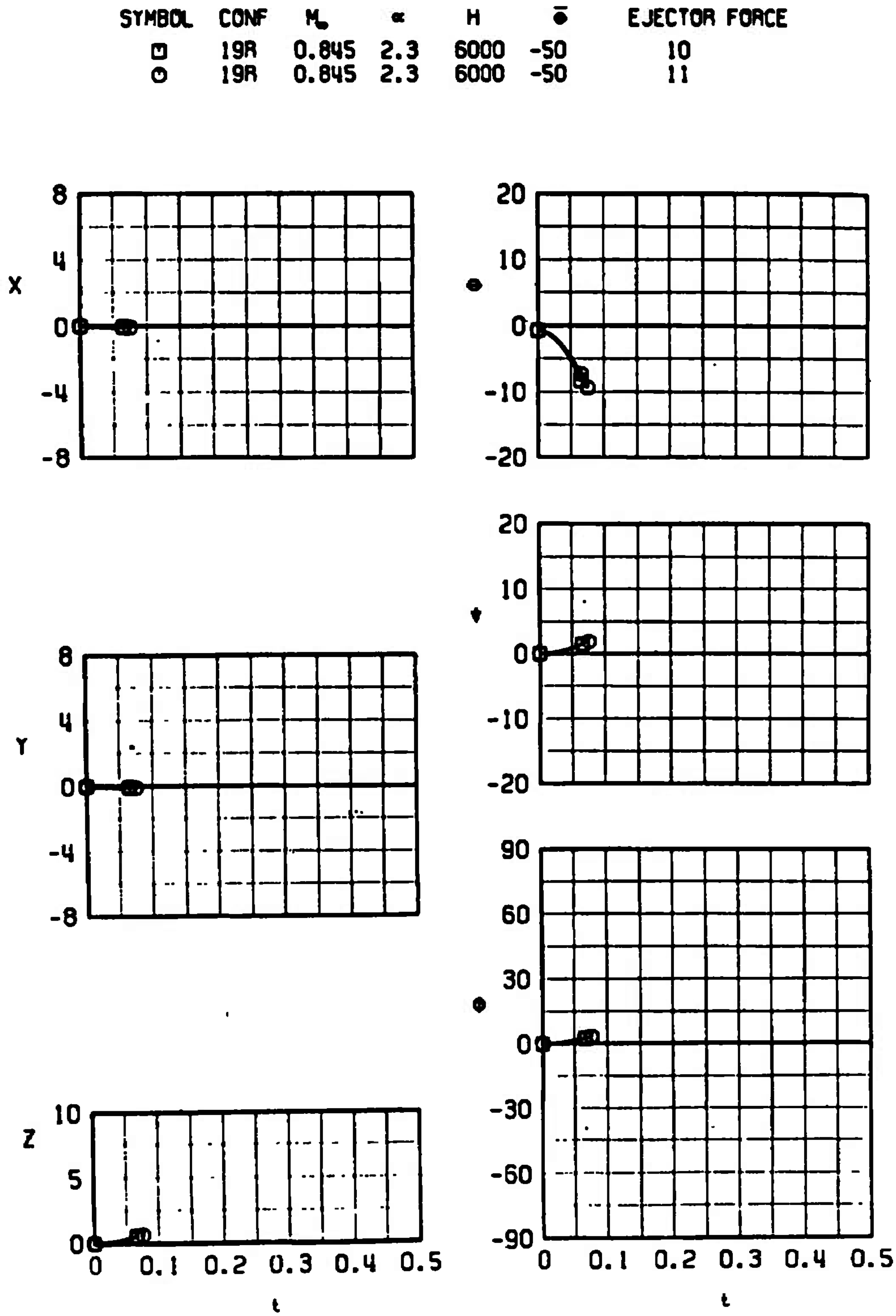

c. $M_\infty = 0.845$

Fig. 31 Concluded

SYMBOL	CONF	M_∞	α	H	$\bar{\theta}$	EJECTOR FORCE
□	19L	0.730	3.0	4000	0	10
○	19L	0.730	3.0	4000	0	11

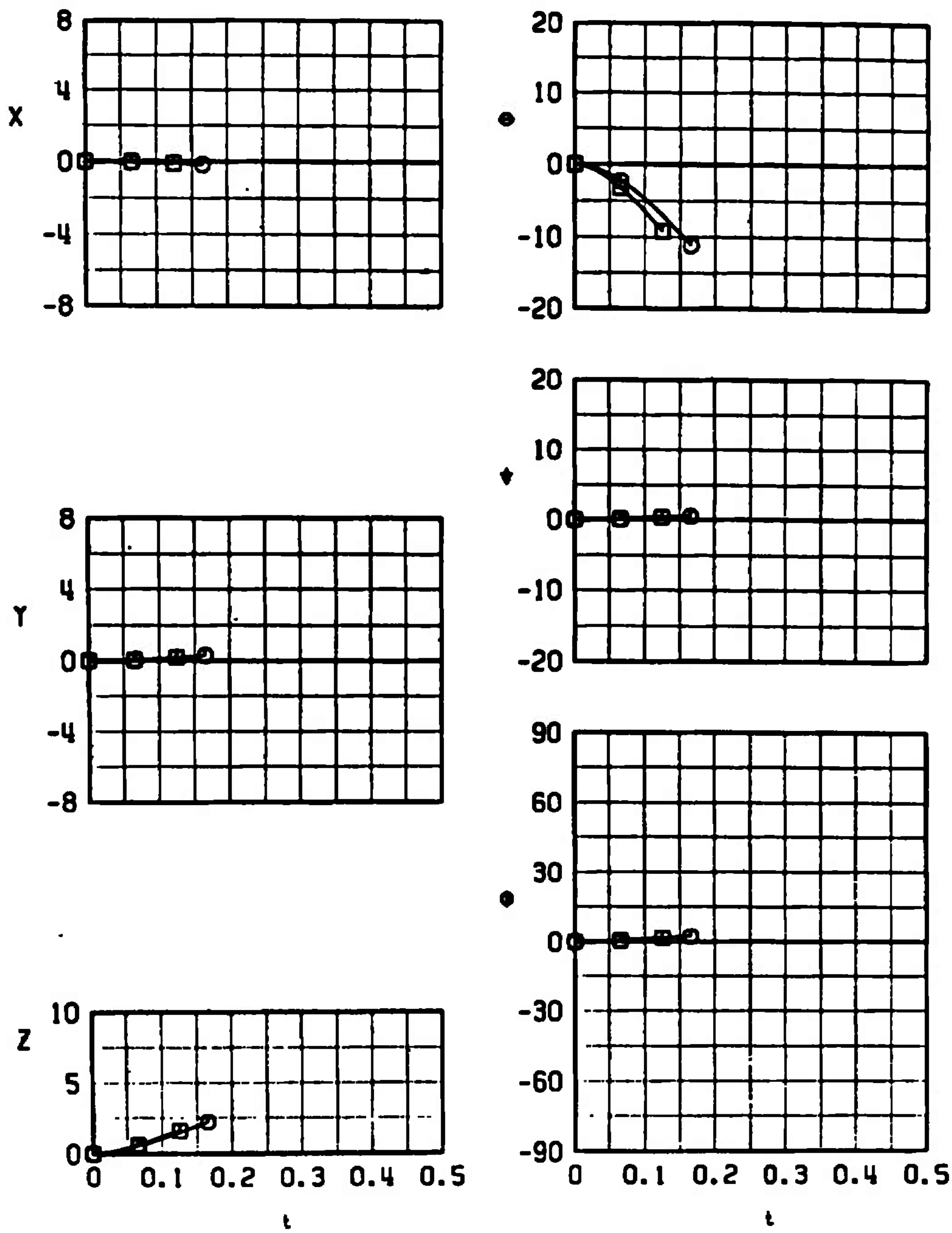

a. $M_\infty = 0.730$

Fig. 32 Separation Characteristics of the BLU-52A/B Bomb from the Outboard Pylon Station, Configuration 19L

SYMBOL	CONF	M_∞	α	H	$\bar{\theta}$	EJECTOR FORCE
□	19L	0.760	2.7	6000	-50	10
○	19L	0.760	2.7	6000	-50	11

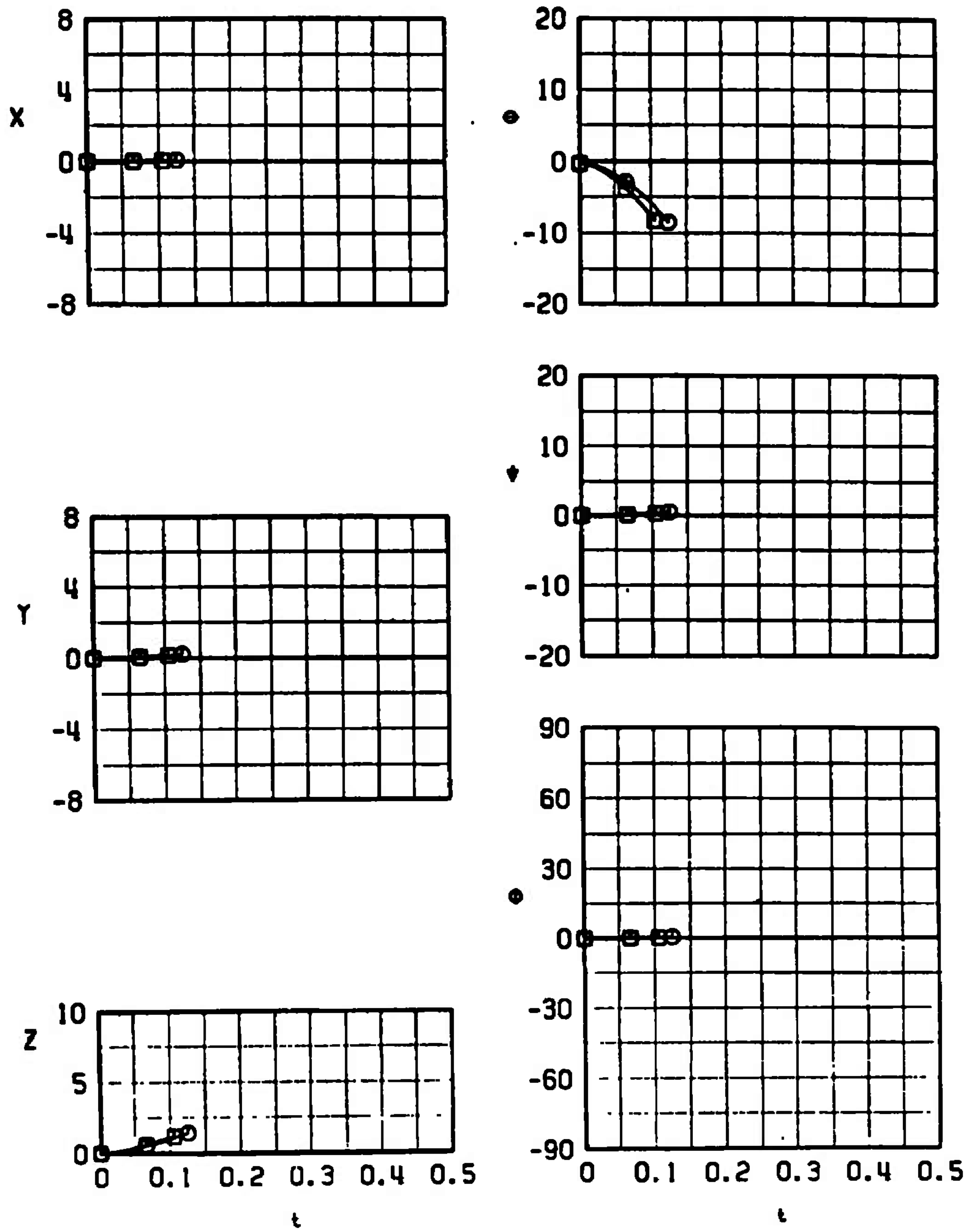

b. M_∞ = 0.760
Fig. 32 Continued

SYMBOL	CONF	M_∞	α	H	$\bar{\theta}$	EJECTOR FORCE
□	19L	0.845	2.3	6000	-50	10
○	19L	0.845	2.3	6000	-50	11

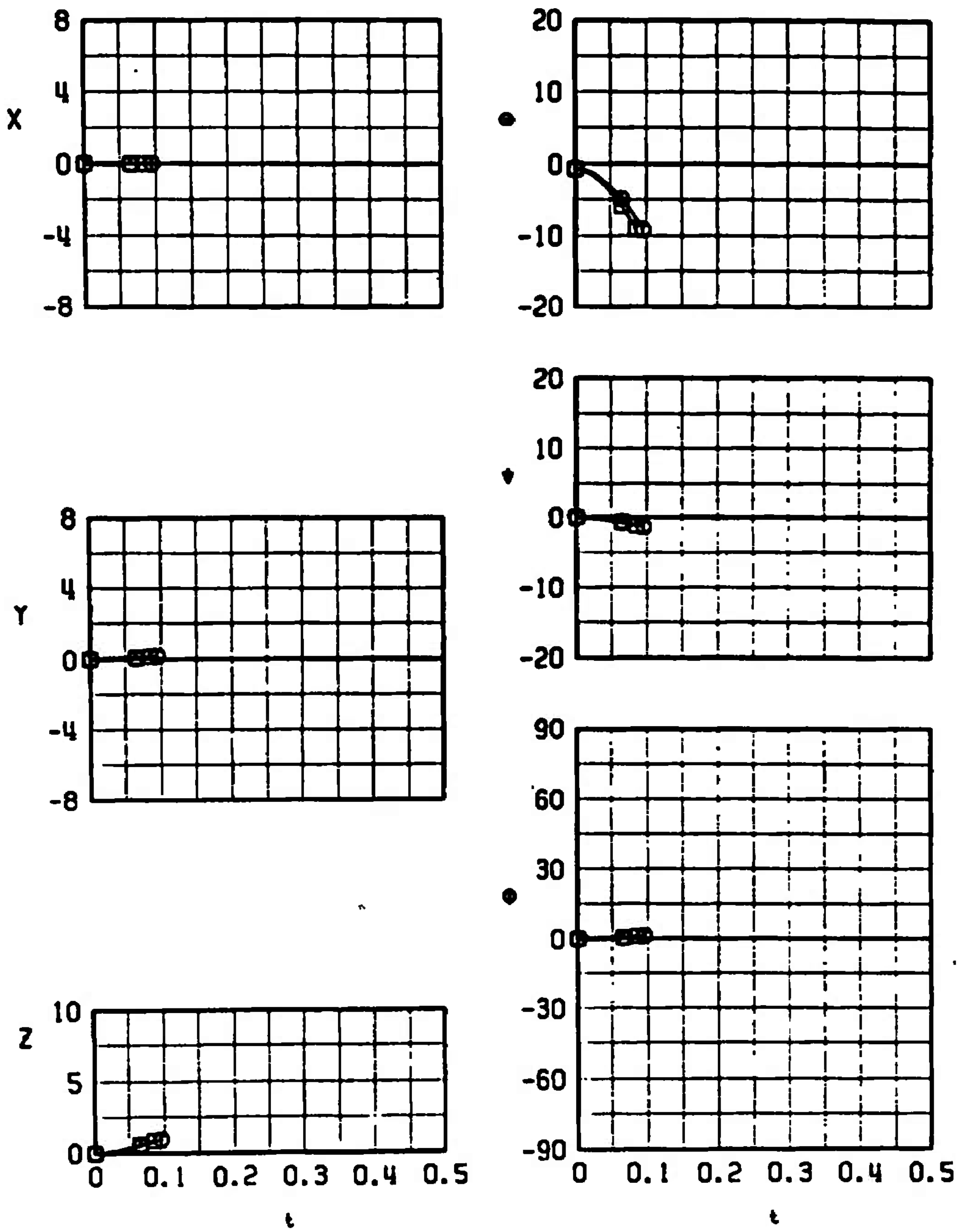

c. $M_\infty = 0.845$

Fig. 32 Concluded

SYMBOL	CONF	M_∞	α	H	ϕ	EJECTOR FORCE
□	21R	0.73	3.0	4000	0	10
○	21R	0.73	3.0	4000	0	11

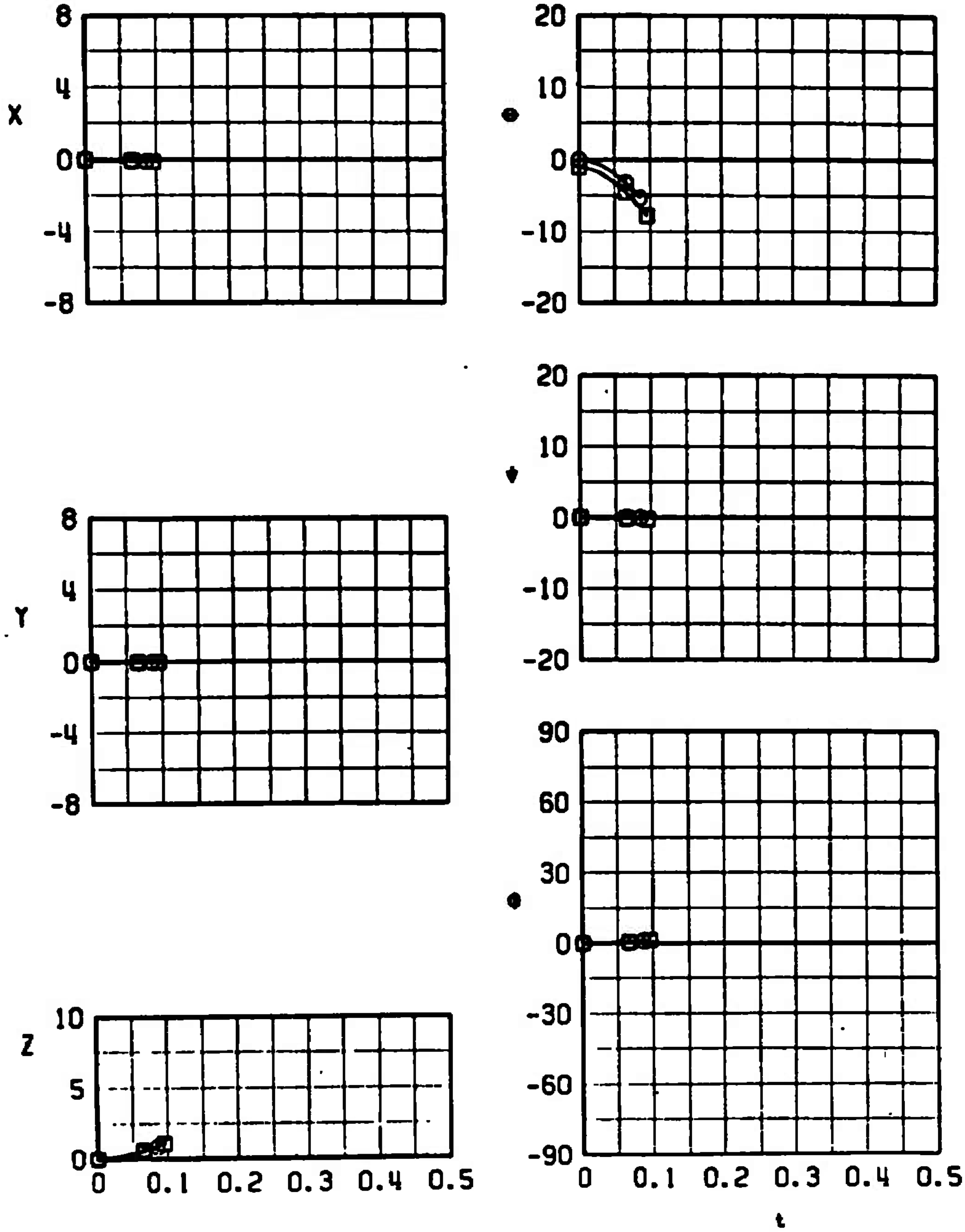

a. $M_\infty = 0.730$

Fig. 33 Separation Characteristics of the BLU-52A/B Bomb from the Inboard Pylon Station, Configuration 21R

SYMBOL	CONF	M_∞	α	H	$\bar{\Phi}$	EJECTOR FORCE
□	21R	0.760	2.7	6000	-50	10
○	21R	0.760	2.7	6000	-50	11

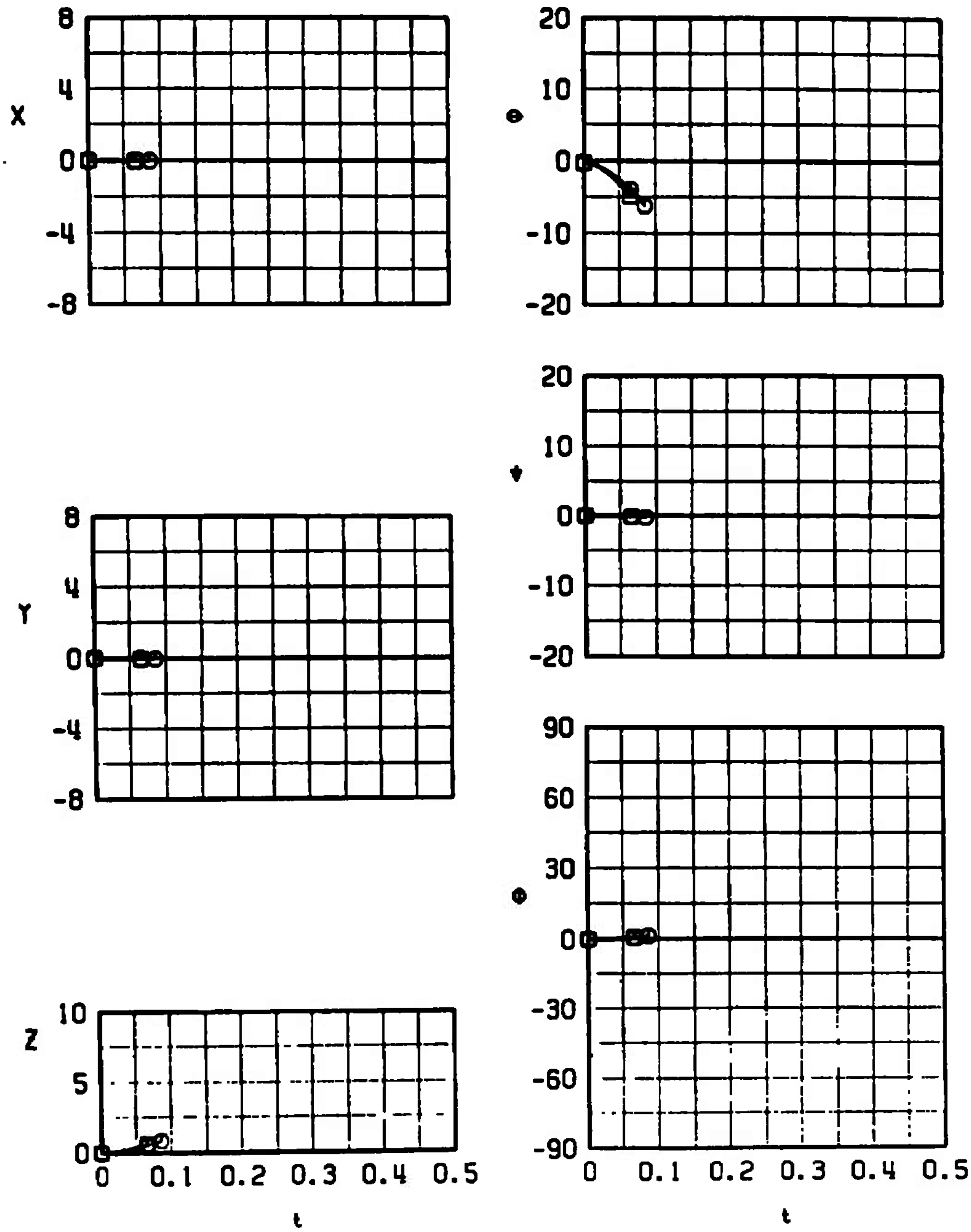

b. $M_\infty = 0.760$
Fig. 33 Continued

SYMBOL	CONF	M_∞	α	H	$\bar{\theta}$	EJECTOR FORCE
□	21R	0.845	2.3	6000	-50	10
○	21R	0.845	2.3	6000	-50	11

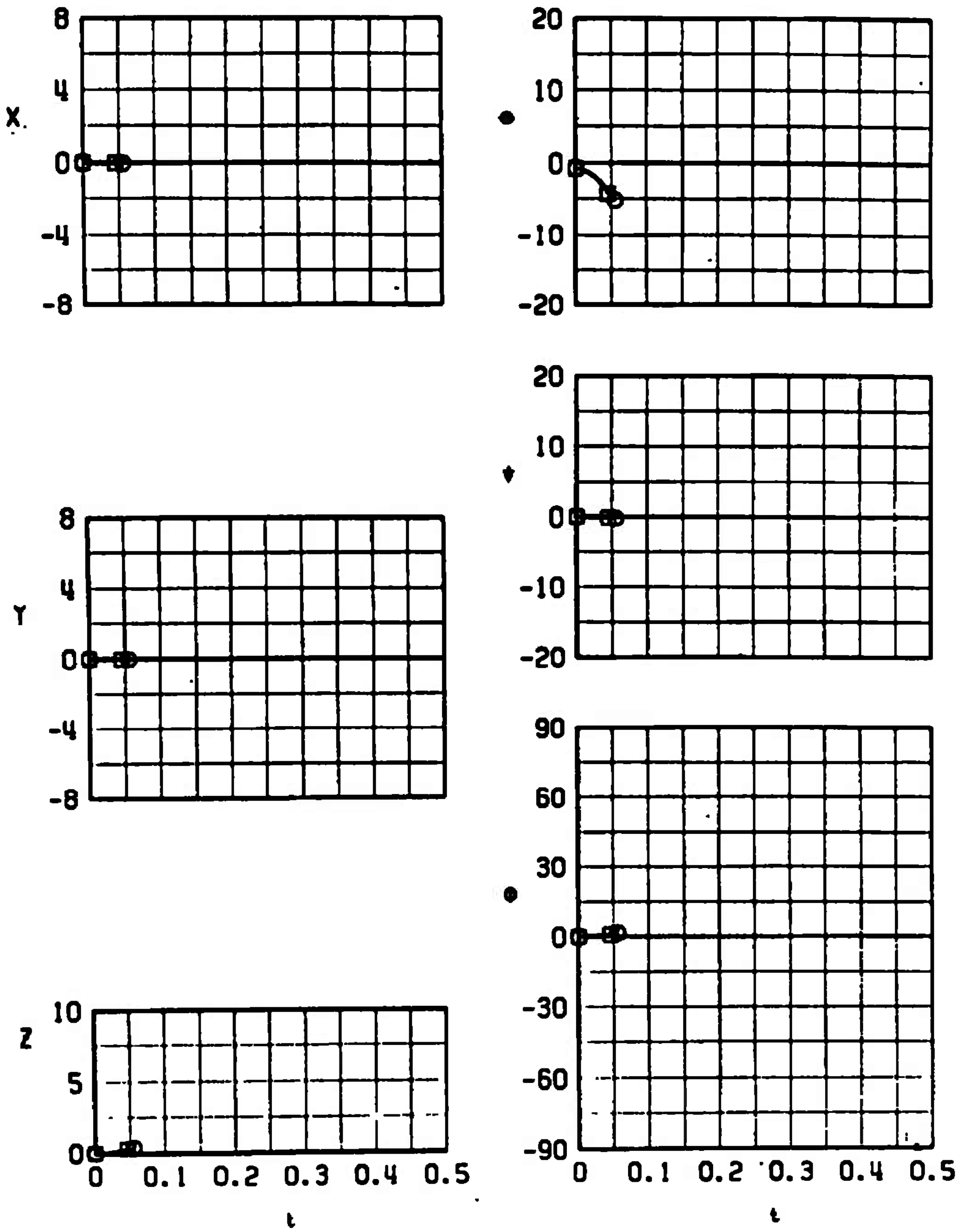

c. M_∞ = 0.845
Fig. 33 Concluded

TABLE I
STORE EJECTION FORCES

Ejector Force No.	F_{Z_1}, lb	F_{Z_2}, lb	F_Z, lb
1	1230	2070	
2	1450	1460	
3	1360	2140	
4	1880	1630	
5	---	---	1170
6	2040	1190	
7	2020	1740	
8	2020	1400	
9	1780	1580	
10	2130	1290	
11	1570	1530	
12	2120	1270	
13	2140	1330	
14	2130	1370	
15	2100	1380	

For store launches from the pylon, the ejector stroke length ZE = 0.34167 ft.

For store launches from the MER or TER, ZE = 0.24167 ft.

TABLE II
FULL-SCALE STORE PARAMETERS USED IN TRAJECTORY CALCULATIONS

	SUU-25C/A (Empty)	SUU-25C/A (Full)	MK-20	CBU-52B/B	BLU-52A/B	300-gal Fuel Tank (Empty)	300-gal Fuel Tank (Full)	300-gal Fuel Tank (Cargo No. 1)	300-gal Fuel Tank (Cargo No. 2)	300-gal Fuel Tank (Cargo No. 3)	300-gal Fuel Tank (Cargo No. 4)
C_{m_q}, per radian	-51.0	-51.0	-52.0	-54.0	-48.0	-133.1	-133.1	-133.1	-133.1	-133.1	-133.1
C_{n_r}, per radian	-51.0	-51.0	-52.0	-54.0	-48.0	-93.6	-93.6	-93.8	-93.6	-93.8	-93.6
C_{ℓ_p}, per radian	0.0	0.0	-0.8	-1.9	-0.6	-1.0	-1.0	-1.0	-1.0	-1.0	-1.0
$\overline{m}$, slugs	8.2	15.4	15.1	24.5	11.2	7.1	68.0	10.2	13.3	16.4	19.6
X_{cg}, ft	4.125	4.692	3.733	2.925	5.417	9.608	8.475	7.725	7.033	6.767	6.583
b, ft	1.167	1.187	1.103	1.333	1.550	2.208	2.208	2.208	2.208	2.208	2.208
S, ft^2	1.069	1.069	0.955	1.396	1.886	3.828	3.828	3.828	3.828	3.828	3.828
X_L, ft			-0.130								
X_{L_1}	1.375	1.942		0.683	0.875	2.483	1.350	0.600	-0.092	-0.358	-0.542
X_{L_2}	-0.292	0.275		-0.983	-0.792	0.817	-0.317	-1.087	-1.758	-2.025	-2.208
I_{xx}, slug-ft^2	2.5	4.5	2.6	2.8	3.5	5.8	45.0	8.0	10.0	13.0	15.0
I_{yy}, slug-ft^2	50.4	88.7	53.2	57.0	69.8	115.5	943.6	147.0	182.0	218.0	219.0
I_{zz}, slug-ft^2	50.4	88.7	53.2	57.0	69.8	115.5	943.6	147.0	182.0	218.0	219.0

TABLE III
MAXIMUM FULL-SCALE POSITION UNCERTAINTIES CAUSED BY BALANCE PRECISION LIMITATIONS

	M_∞	ΔX, ft	ΔY, ft	ΔZ, ft	$\Delta\theta$, deg	$\Delta\psi$, deg	$\Delta\phi$, deg
SUU-25C/A (Empty)	0.325	±0.012	±0.020	±0.012	±0.160	±0.240	±1.257
	0.814	±0.021	±0.034	±0.021	±0.272	±0.408	±2.134
SUU-25C/A (Full)	0.325	±0.006	±0.010	±0.006	±0.091	±0.136	±0.698
	0.814	±0.011	±0.018	±0.011	±0.154	±0.232	±1.186
MK-20	0.730	±0.009	±0.015	±0.009	±0.208	±0.312	±1.655
	0.950	±0.015	±0.025	±0.015	±0.352	±0.528	±2.804
BLU-52A/B	0.730	±0.012	±0.020	±0.012	±0.158	±0.237	±1.226
	0.845	±0.017	±0.027	±0.017	±0.212	±0.318	±1.644
CBU-52B/B	0.730	±0.006	±0.009	±0.006	±0.194	±0.291	±1.535
	0.845	±0.007	±0.012	±0.007	±0.259	±0.389	±2.057
300-gal-Fuel Tank (Empty)	0.407	±0.015	±0.006	±0.015	±0.082	±0.049	±0.427
	0.814	+0.060	±0.025	±0.060	±0.329	±0.197	±1.700
300-gal Fuel Tank (Full)	0.407	±0.001	±0.001	±0.001	±0.010	±0.010	±0.055
	0.814	±0.006	±0.002	±0.006	±0.040	±0.024	±0.220

TABLE IV
A-7D LOAD CONFIGURATIONS

Configuration	Launch Store Model	Inboard Pylon	Center Pylon	Outboard Pylon
1L	SUU-25C/A	Empty	MER	SUU-25C/A (Launch)
2R	SUU-25C/A	M-117	MER: M-117 (Dummy) Sta. 1, 2, 5, 6	SUU-25C/A (Launch)
2L	SUU-25C/A	MK-82 S. E.	MER: MK-82 S. E. (Dummy) Sta. 1, 2, 3, 4, 5, 6	SUU-25C/A (Launch)
3R	MK-20	Empty	MER: MK-20 (Dummy) Sta. 4 MK-20 (Launch) Sta. 3	MER
3L	MK-20	Empty	MER: MK-20 (Dummy) Sta. 1, 2, 3, 4, 5, 6	MER: MK-20 (Dummy) Sta. 3, 4, 6 MK-20 (Launch) Sta. 5
4R	MK-20	Empty	MER: MK-20 (Launch) Sta. 4	MER
4L	MK-20	Empty	MER: MK-20 (Dummy) Sta. 1, 2, 3, 4, 5, 6	MER: MK-20 (Dummy) Sta. 3, 4 MK-20 (Launch) Sta. 6
5R	MK-20	Empty	MER: MK-20 (Dummy) Sta. 3, 4, 6 MK-20 (Launch) Sta, 5	MER
5L	MK-20	Empty	MER: MK-20 (Dummy) Sta. 1, 2, 3, 4, 5, 6	MER: MK-20 (Dummy) Sta. 4 MK-20 (Launch) Sta. 3
6R	MK-20	Empty	MER: MK-20 (Dummy) Sta. 3, 4 MK-20 (Launch) Sta 6	MER
6L	MK-20	Empty	MER: MK-20 (Dummy) Sta. 1, 2, 3, 4, 5, 6	MER: MK-20 (Launch) Sta. 4
7R	MK-20	Empty	MER: MK-20 (Launch) Sta. 6	MER
7L	MK-20	Empty	MER: MK-20 (Dummy) Sta. 1, 2, 3, 4, 5, 6	MER: MK-20 (Dummy) Sta. 2, 3, 4, 5, 6 MK-20 (Launch) Sta. 1

TABLE IV (Continued)

Configuration	Launch Store Model	Inboard Pylon	Center Pylon	Outboard Pylon
8R	MK-20	Empty	MER: MK-20 (Dummy) Sta. 6 MK-20 (Launch) Sta. 5	MER
8L	MK-20	Empty	MER: MK-20 (Dummy) Sta. 1, 2, 3, 4, 5, 6	MER: MK-20 (Dummy) Sta. 3, 4, 5, 6 MK-20 (Launch) Sta. 2
9R	MK-20	Empty	MER: MK-20 (Dummy) Sta. 5, 6 MK-20 (Launch) Sta. 4	MER
9L	MK-20	Empty	MER: MK-20 (Dummy) Sta. 1, 2, 3, 4, 5, 6	MER. MK-20 (Dummy) Sta. 4, 5, 6 MK-20 (Launch) Sta. 3
10R	MK-20	Empty	MER: MK-20 (Dummy) Sta. 4, 5, 6 MK-20 (Launch) Sta. 3	MER
10L	MK-20	Empty	MER: MK-20 (Dummy) Sta. 1, 2, 3, 4, 5, 6	MER: MK-20 (Dummy) Sta. 5, 6 MK-20 (Launch) Sta. 4
11R	MK-20	Empty	MER: MK-20 (Dummy) Sta. 3, 4, 5, 6 MK-20 (Launch) Sta. 2	MER
11L	MK-20	Empty	MER: MK-20 (Dummy) Sta. 1, 2, 3, 4, 5, 6	MER: MK-20 (Dummy) Sta. 6 MK-20 (Launch) Sta. 5
12R	MK-20	Empty	MER: MK-20 (Dummy) Sta. 2, 3, 4, 5, 6 MK-20 (Launch) Sta. 1	MER
12L	MK-20	Empty	MER: MK-20 (Dummy) Sta. 1, 2, 3, 4, 5, 6	MER: MK-20 (Launch) Sta. 6
13R	MK-20	300-gal Tank	MER: MK-20 (Launch) Sta. 6	TER
13L	MK-20	300-gal Tank	MER: MK-20 (Dummy) Sta. 1, 2, 3, 4	TER: MK-20 (Dummy). Sta. 2, 3 MK-20 (Launch) Sta. 1

TABLE IV (Concluded)

Configuration	Launch Store Model	Inboard Pylon	Center Pylon	Outboard Pylon
14R	MK-20	300-gal Tank	MER: MK-20 (Dummy) Sta. 6 MK-20 (Launch) Sta. 5	TER
14L	MK-20	300-gal Tank	MER: MK-20 (Dummy) Sta. 1, 2, 3, 4	TER: MK-20 (Dummy) Sta. 3 MK-20 (Launch) Sta. 2
15R	MK-20	300-gal Tank	MER: MK-20 (Dummy) Sta. 5, 6 MK-20 (Launch) Sta. 2	TER
15L	MK-20	300-gal Tank	MER: MK-20 (Dummy) Sta. 1, 2, 3, 4	TER: MK-20 (Launch) Sta. 3
16R	MK-20	300-gal Tank	MER: MK-20 (Dummy) Sta. 2, 5, 6 MK-20 (Launch) Sta. 1	TER
16L	MK-20	300-gal Tank	MER. MK-20 (Dummy) Sta. 1, 2, 3, 4	TER: MK-20 (Launch) Sta. 2
17R	300-gal Tank	300-gal Tank (Launch)	MER	TER
17L	300-gal Tank	300-gal Tank (Launch)	MER: MK-20 (Dummy) Sta. 1, 2, 3, 4	TER: MK-20 (Dummy) Sta. 1, 2, 3
18R	CBU-52B/B	CBU-52B/B (Dummy)	CBU-52B/B (Launch)	Empty
18L	CBU-52B/B	CBU-52B/B (Dummy)	CBU-52B/B (Dummy)	CBU-52B/B (Launch)
19R	BLU-52A/B	BLU-52A/B (Dummy)	BLU-52A/B (Launch)	Empty
19L	BLU-52A/B	BLU-52A/B (Dummy)	BLU-52A/B (Dummy)	BLU-52A/B (Launch)
20R	CBU-52B/B	CBU-52B/B (Launch)	Empty	Empty
21R	BLU-52A/B	BLU-52A/B (Launch)	Empty	Empty

UNCLASSIFIED

Security Classification

DOCUMENT CONTROL DATA - R & D

(Security classification of title, body of abstract and indexing annotation must be entered when the overall report is classified)

1. ORIGINATING ACTIVITY (Corporate author) Arnold Engineering Development Center Arnold Air Force Station, Tennessee	2a. REPORT SECURITY CLASSIFICATION UNCLASSIFIED 2b. GROUP N/A

3. REPORT TITLE

SEPARATION CHARACTERISTICS OF SEVERAL EXTERNAL STORES FROM THE A-7D AIRCRAFT AT MACH NUMBERS FROM 0.325 TO 0.95

4. DESCRIPTIVE NOTES (Type of report and inclusive dates)

April 5 to 12, 1972 - Final Report

This document has been approved for public release its distribution is unlimited. Per TAB 76-7 26 March 1976

5. AUTHOR(S) (First name, middle initial, last name)

Robert H. Roberts, ARO, Inc.

6. REPORT DATE	7a. TOTAL NO. OF PAGES	7b. NO. OF REFS
July 1972	104	1

8a. CONTRACT OR GRANT NO. b. PROJECT NO c. Program Element 27121F d. System 337A	9a. ORIGINATOR'S REPORT NUMBER(S) AEDC-TR-72-95 AFATL-TR-72-120 9b. OTHER REPORT NO(S) (Any other numbers that may be assigned this report) ARO-PWT-TR-72-70

10. DISTRIBUTION STATEMENT Distribution limited to U.S. Government agencies only; this report contains information on test and evaluation of military hardware; July 1972; other requests for this document must be referred to Air Force Armament Laboratory (DLGC), Eglin AFB, Florida 32542.

11. SUPPLEMENTARY NOTES	12. SPONSORING MILITARY ACTIVITY
Available in DDC	AFATL (DLGC), Eglin AFB, Florida 32542

13. ABSTRACT

Tests were conducted in the Aerodynamic Wind Tunnel (4T) using 0.05-scale models to investigate the separation characteristics of the SUU-25C/A and CBU-52B/B dispensers, MK-20 and BLU-52A/B bombs, and the 300-gal fuel tank when released from the Multiple Ejection Rack (MER), the Triple Ejection Rack (TER), and wing-pylon locations on the left and right wing of the A-7D aircraft. Captive trajectory data were obtained at Mach numbers from 0.325 to 0.95 at simulated pressure altitudes from 4000 to 7000 ft. The parent-aircraft angle of attack was varied from 2.0 to 10.6 deg, depending on Mach number, climb angle, and simulated altitude. At selected test conditions, parent climb (dive) angles of -50 and -70 deg were simulated.

Distribution limited to U.S. Government agencies only; this report contains information on test and evaluation of military hardware; July 1972; other requests for this document must be referred to Air Force Armament Laboratory (DLGC), Eglin AFB, Florida 32542.

DD FORM 1 NOV 65 1473

UNCLASSIFIED

Security Classification

14. KEY WORDS	LINK A		LINK B		LINK C	
	ROLE	WT	ROLE	WT	ROLE	WT
separation						
characteristics						
SUU-25C/A dispenser						
CBU-52B/B dispenser						
MK-20 bomb						
BLU-52A/B bomb						
fuel tank						
A-7D aircraft						
Mach numbers						

AFSC
Arnold AFS Tenn